King's Research Portal

DOI:
10.1093/imrn/rnu239

Document Version
Peer reviewed version

Link to publication record in King's Research Portal

Citation for published version (APA):
Bertola, M., & Bothner, T. J. (2015). Zeros of Large Degree Vorob'ev–Yablonski Polynomials via a Hankel Determinant Identity. *International Mathematics Research Notices*, *2015*(19). https://doi.org/10.1093/imrn/rnu239

Citing this paper
Please note that where the full-text provided on King's Research Portal is the Author Accepted Manuscript or Post-Print version this may differ from the final Published version. If citing, it is advised that you check and use the publisher's definitive version for pagination, volume/issue, and date of publication details. And where the final published version is provided on the Research Portal, if citing you are again advised to check the publisher's website for any subsequent corrections.

General rights
Copyright and moral rights for the publications made accessible in the Research Portal are retained by the authors and/or other copyright owners and it is a condition of accessing publications that users recognize and abide by the legal requirements associated with these rights.

•Users may download and print one copy of any publication from the Research Portal for the purpose of private study or research.
•You may not further distribute the material or use it for any profit-making activity or commercial gain
•You may freely distribute the URL identifying the publication in the Research Portal

Take down policy
If you believe that this document breaches copyright please contact librarypure@kcl.ac.uk providing details, and we will remove access to the work immediately and investigate your claim.

Download date: 12. Jan. 2025

ZEROS OF LARGE DEGREE VOROB'EV-YABLONSKI POLYNOMIALS VIA A HANKEL DETERMINANT IDENTITY

MARCO BERTOLA AND THOMAS BOTHNER

ABSTRACT. In the present paper we derive a new Hankel determinant representation for the square of the Vorob'ev-Yablonski polynomial $\mathcal{Q}_n(x), x \in \mathbb{C}$. These polynomials are the major ingredients in the construction of rational solutions to the second Painlevé equation $u_{xx} = xu + 2u^3 + \alpha$. As an application of the new identity, we study the zero distribution of $\mathcal{Q}_n(x)$ as $n \to \infty$ by asymptotically analyzing a certain collection of (pseudo) orthogonal polynomials connected to the aforementioned Hankel determinant. Our approach reproduces recently obtained results in the same context by Buckingham and Miller [3], which used the Jimbo-Miwa Lax representation of PII equation and the asymptotic analysis thereof.

1. Introduction and statement of results

Rational solutions of the second Painlevé equation

$$u_{xx} = xu + 2u^3 + \alpha, \qquad \alpha \in \mathbb{C}, \tag{1.1}$$

were introduced in [16, 17] in terms of a certain sequence of monic polynomials $\{\mathcal{Q}_n(x)\}_{n\geq 0}$, henceforth generally named Vorob'ev-Yablonski polynomials. These polynomials are defined via the differential-difference equation

$$\mathcal{Q}_{n+1}(x)\mathcal{Q}_{n-1}(x) = x\mathcal{Q}_n^2(x) - 4\Big[\mathcal{Q}_n''(x)\mathcal{Q}_n(x) - \big(\mathcal{Q}_n'(x)\big)^2\Big], \qquad n \geq 1,\ x \in \mathbb{C}$$

with $\mathcal{Q}_0(x) = 1, \mathcal{Q}_1(x) = x$. It was found that rational solutions of (1.1) exist if and only if $\alpha = n \in \mathbb{Z}$. For each value $n \geq 1$ they are uniquely given by

$$u(x) \equiv u(x;n) = \frac{\mathrm{d}}{\mathrm{d}x}\left\{\ln\left[\frac{\mathcal{Q}_{n-1}(x)}{\mathcal{Q}_n(x)}\right]\right\}, \quad u(x;0) = 0, \qquad u(x;-n) = -u(x;n). \tag{1.2}$$

The Vorob'ev-Yablonski polynomial $\mathcal{Q}_n(x)$ for $n \geq 0$ is a monic polynomials of degree $\frac{n}{2}(n+1)$ with integer coefficients. In the literature it is known [13] that $\mathcal{Q}_n(x)$ admits two determinantal representations; our first result will be a third representation.

Of the pre-existing formulæ we first state a formula of Jacobi-Trudi type: let $\{q_k(x)\}_{k\geq 0}$ be the polynomials defined by the generating function

$$F_1(t;x) = \exp\left[-\frac{4t^3}{3} + tx\right] = \sum_{k=0}^{\infty} q_k(x)t^k \tag{1.3}$$

and set in addition $q_k(x) \equiv 0$ for $k < 0$. Then

$$\mathcal{Q}_n(x) = \prod_{k=1}^{n}(2k+1)^{n-k}\ \det\Big[q_{n-2\ell+j}(x)\Big]_{\ell,j=0}^{n-1}, \qquad n \geq 1. \tag{1.4}$$

Date: October 31, 2014.

2000 *Mathematics Subject Classification.* Primary 33E17; Secondary 34E05, 34M50.

Key words and phrases. Vorob'ev-Yablonski polynomials, Hankel determinant representation, asymptotic behavior of (pseudo) orthogonal polynomials, Riemann-Hilbert problem, Deift-Zhou nonlinear steepest descent method.

The first author is supported in part by the Natural Sciences and Engineering Research Council of Canada. The second author acknowledges support by Concordia University through a postdoctoral fellow top-up award.

Secondly one can compute $\mathcal{Q}_n(x)$ from a Hankel determinant: let $\{p_k(x)\}_{k\geq 0}$ be the polynomials defined recursively via

$$p_0(x) = x, \qquad p_1(x) = 1, \qquad p_{k+1}(x) = p_k'(x) + \sum_{m=0}^{k-1} p_m(x)p_{k-1-m}(x), \tag{1.5}$$

in particular

$$p_2(x) = x^2, \qquad p_3(x) = 4x, \qquad p_4(x) = 2x^3 + 5, \qquad p_5(x) = 16x^2, \qquad p_6(x) = 5x\left(x^3 + 10\right).$$

Then

$$\mathcal{Q}_n(x) = \kappa^{-\frac{n}{2}(n+1)} \det\left[p_{\ell+j-2}\left(\kappa x\right)\right]_{\ell,j=1}^{n}, \quad n \geq 1; \qquad \kappa = -2^{-\frac{2}{3}}. \tag{1.6}$$

Although this identity expresses $\mathcal{Q}_n(x)$ as an exact Hankel determinant, the polynomials $\{p_k(x)\}_{k\geq 0}$ cannot be derived from an elementary generating function as it was the case for $\{q_k(x)\}_{k\geq 0}$ in (1.3).

Our first major result is a seemingly new Hankel determinant representation for the squares of $\mathcal{Q}_n(x)$, which indeed results from an elementary generating function. Let $\{\mu_k(x)\}_{k\geq 0}$ be the collection of polynomials defined by the generating function

$$F_2(t;x) = \exp\left[-\frac{t^3}{3} + tx\right] = \sum_{k=0}^{\infty} \mu_k(x)t^k. \tag{1.7}$$

These polynomials satisfy the four-term recurrence

$$\mu_{k+3}(x) = \frac{x\mu_{k+2}(x)}{k+3} - \frac{\mu_k(x)}{k+3}, \qquad k \geq 0 \tag{1.8}$$

with $\mu_0(x) = 1, \mu_1(x) = x$ and $\mu_2(x) = \frac{1}{2}x^2$. Moreover

$$\mu_3(x) = \frac{x^3-2}{3!}, \qquad \mu_4(x) = \frac{x(x^3-8)}{4!}, \qquad \mu_5(x) = \frac{x^2(x^3-20)}{5!}, \qquad \mu_6(x) = \frac{x^6 - 40x^3 + 40}{6!},$$

and in general

$$\mu_k(-\kappa x) = q_k(x)(-\kappa)^k, \qquad k \geq 0.$$

The relation to the Vorob'ev-Yablonski polynomials is as follows

Theorem 1.1. *For any $n \geq 1$, we have*

$$\mathcal{Q}_{n-1}^2(x) = (-)^{\lfloor \frac{n}{2} \rfloor} \frac{1}{2^{n-1}} \prod_{k=1}^{n-1} \left[\frac{(2k)!}{k!}\right]^2 \det\left[\mu_{\ell+j-2}(x)\right]_{\ell,j=1}^{n}. \tag{1.9}$$

where $\lfloor y \rfloor$ denotes the floor function of a real number y.

The proof of Theorem 1.1 is found in Section 2. Theorem 1.1 can be put to practical use in the analysis of the distributions of the zeros of $\mathcal{Q}_n(x)$ when $n \to \infty$. This very same asymptotic problem was very recently addressed in [3] where Buckingham and Miller have analyzed the large degree asymptotics of $\mathcal{Q}_n(x)$ in different regions of the complex x-plane. Their approach uses a specific Lax representation of (1.1) and corresponding Riemann–Hilbert problem, which is completely different than the one we derive here (Sec. 3), and then they proceed to an asymptotic resolution of the RHP as $n \to \infty$.

Indeed, a direct consequence of Theorem 1.1 is that we can frame the same analysis in the relatively familiar context of large-degree asymptotics of orthogonal polynomials with respect to a varying weight in the spirit of [8]; recall that

$$\mu_k(x) = \frac{1}{k!}\frac{\mathrm{d}^k}{\mathrm{d}t^k}F_2(t;x)\Big|_{t=0} = -\frac{1}{2\pi i}\oint F_2(w;x)\frac{\mathrm{d}w}{w^{k+1}} = -\oint \zeta^k \,\mathrm{d}\nu(\zeta;x) \tag{1.10}$$

where the line integrals are taken along the unit circle $S^1 = \{\zeta \in \mathbb{C} : |\zeta| = 1\}$ in clockwise orientation and

$$\mathrm{d}\nu(\zeta;x) = \frac{1}{2\pi i}e^{-\theta(\zeta;x)}\frac{\mathrm{d}\zeta}{\zeta}, \qquad \theta(\zeta;x) = \frac{1}{3\zeta^3} - \frac{x}{\zeta}. \tag{1.11}$$

In this setting we now introduce (pseudo) orthogonal polynomials

Definition 1.2. *The monic orthogonal polynomials $\{\psi_n(\zeta;x)\}_{n\geq 0}$ of exact degree n are defined by the requirements*

$$\oint \psi_n(\zeta;x)\zeta^m \mathrm{d}\nu(\zeta;x) = \begin{cases} h_n(x), & m=n \\ 0, & m\leq n-1 \end{cases} \tag{1.12}$$

$$\psi_n(\zeta;x) = \zeta^n + \mathcal{O}\left(\zeta^{n-1}\right), \qquad \zeta\to\infty. \tag{1.13}$$

Also here, the line integral is taken along the unit circle S^1 in clockwise orientation.

For any fixed $n\in\mathbb{N}$, the existence of $\psi_n(\zeta;x)$ amounts to a problem of Linear Algebra and rests upon the nonvanishing of the Hankel determinant of the moments (1.10) of the measure $\mathrm{d}\nu(\zeta;x)$

$$\det\Big[\mu_{\ell+j-2}(x)\Big]_{\ell,j=1}^{n} \neq 0.$$

Recall also that the normalizing constants are related to the Hankel determinants by

$$h_n(x) = -\frac{\det[\mu_{\ell+k-2}(x)]_{\ell,k=1}^{n+1}}{\det[\mu_{\ell+k-2}(x)]_{\ell,k=1}^{n}}. \tag{1.14}$$

Now combining (1.14) with (1.9) and (1.2), we obtain for $n\geq 1$

$$h_n(x) = 2(-)^{n-1}\left[\frac{n!}{(2n)!}\right]^2\left(\frac{\mathcal{Q}_n(x)}{\mathcal{Q}_{n-1}(x)}\right)^2, \qquad u(x;n) = -\frac{1}{2}\frac{h_n'(x)}{h_n(x)}. \tag{1.15}$$

Hence zeros of the n-th Vorob'ev-Yablonski polynomial $\mathcal{Q}_n(x)$, respectively poles of the n-th rational solutions $u(x;n)$ to (1.1), are in one-to-one correspondence with the exceptional values of the parameter x for which the n-th orthogonal polynomial $\psi_n(\zeta;x)$ (1.12),(1.13) ceases to exist.

In this perspective, our second result confirms an analog one in [3], namely it shows that the Vorob'ev-Yablonski polynomials of large degree (after a rescaling) are zero-free outside a star shaped region $\overline{\Delta}\subset\mathbb{C}$ defined as follows

Definition 1.3. *Let $a=a(x)$ denote the (unique) solution of the cubic equation*

$$1+2xa^2-4a^3=0 \tag{1.16}$$

subject to boundary condition

$$a = \frac{x}{2}+\mathcal{O}\left(x^{-2}\right), \qquad x\to\infty. \tag{1.17}$$

The three branch points $x_k=-\frac{3}{\sqrt[3]{2}}e^{\frac{2\pi i}{3}k}, k=0,1,2$ of equation (1.16) form the vertices of the star shaped region $\overline{\Delta}=\Delta\cup\partial\Delta$ depicted in Figure 1 below which contains the origin and whose boundary $\partial\Delta$ consists of three edges defined implicitly via the requirement

$$\Re\left\{-2\ln\left(\frac{1-\sqrt{1+2a^3}}{ia\sqrt{2a}}\right)-\sqrt{1+2a^3}\left(\frac{4a^3-1}{3a^3}\right)\right\}=0. \tag{1.18}$$

Here, all branches of fractional exponents and logarithms are chosen to be principal ones.

The topology of Δ is discussed in Section 3.2. In terms of the latter definition, our second main result shows that the region $\mathbb{C}\backslash\overline{\Delta}$ does not contain any zeros of $\mathcal{Q}_n(n^{\frac{2}{3}}x)$, provided n is large enough. We have

Theorem 1.4 (see [3], Theorem 1)**.** *Let $x\in\mathbb{C}:\mathrm{dist}(x,\overline{\Delta})\geq\delta>0$, then the orthogonal polynomials $\psi_n(\zeta;n^{\frac{2}{3}}x),\zeta\in S^1$ defined by (1.12) and (1.13) exist if n is sufficiently large. Equivalently, the (rescaled) Vorob'ev-Yablonski polynomials $\widehat{Q}_n(x)=\mathcal{Q}_n(n^{\frac{2}{3}}x)$ for large n have no zeros in the same region of the complex x-plane.*

We point out that while the final result overlaps (see Remark 6.2) with the result of [3], the method is substantially different since we start from the new determinantal expression of $\mathcal{Q}_n(x)$ obtained in Theorem 1.1.

At this point we decided to perform asymptotic analysis only in the interior and exterior of the region Δ; hence we shall not address issues related to the asymptotic behavior when x is on the boundary (or vicinity)

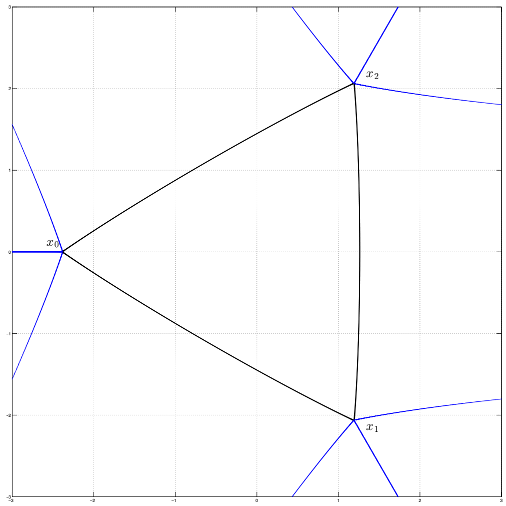

FIGURE 1. The star shaped region $\overline{\Delta} = \Delta \cup \partial\Delta$. The boundary $\partial\Delta$ is given as the union of the three black solid curves.

of Δ, presumably the result would only confirm those of the forthcoming paper [4]. We are also focusing on the location of the zeroes of $\widehat{Q}_n(x) = \mathcal{Q}_n(n^{\frac{2}{3}}x)$ inside of Δ (hence, location of the poles of $u(x;n)$) rather than the asymptotic behavior of the rational solution $u(x;n)$ itself, not to unnecessarily duplicate the results.

There are interesting differences in the methods of our analysis inside Δ, compared to the one in [3][1] although the end result is the same. In [3] the author need to introduce an elliptic curve (of genus 1) dependent on the value of x in Δ; in contrast, we need to introduce a *hyperelliptic curve* of genus 2 of the form

$$X = \left\{(z,w): \ w^2 = P_3\left(z^2\right)\right\} \tag{1.19}$$

where $P_3(\zeta) = (\zeta + a^2)(\zeta + b^2)(\zeta + c^2)$ is a polynomial of degree 3 with distinct roots given implicitly in (3.34) and (3.36). In [3], the authors introduce an exceptional set of discrete points in order to complete the Riemann-Hilbert analysis inside the star shaped region Δ, compare equations (4-96) and (4-97) in the aforementioned text. In our case the corresponding exceptional set is first defined in terms of the vanishing of a Riemann Theta function of genus 2 (see App. (B)); however, given the high symmetry of our curve X, we will eventually reduce the appearance of $\Theta(z|\boldsymbol{\tau})$ in the definition of the corresponding exceptional set (4.34) to a condition which involves only a theta function $\vartheta(\rho) = \vartheta(\rho|\varkappa)$ associated to an elliptic curve. In order to explain in detail the condition, let us set

$$\mathrm{d}\phi(z) = \frac{\sqrt{P_3(z^2)}}{z^4}\,\mathrm{d}z \tag{1.20}$$

and recall that the parameters a, b, c (i.e. the branch points of X) all depend on x implicitly via (3.34) and (3.36). Our analog to (4-96), (4-97) in [3] reads as follows.

Theorem 1.5. *Let $\mathcal{Z}_n \subset \Delta$ be the discrete collection of points $\{x_{n,k}\}$ defined via*

$$\vartheta\left(\frac{n}{2\pi i}\left[\oint_{\mathcal{B}_1}\mathrm{d}\phi + \varkappa_2\oint_{\mathcal{A}_1}\mathrm{d}\phi\right] + \frac{1}{2}\left[\int_{a_1}^{0}\frac{\eta_2}{\mathbb{A}_{22}} + \frac{\varkappa_2}{2}\right]\right) = 0 \tag{1.21}$$

where $\vartheta(\rho) = \vartheta_3(\rho|\,\varkappa_2) = \sum_{m\in\mathbb{Z}}\exp[i\pi m^2\varkappa_2 + 2\pi i m\rho]$ is the Jacobi theta function and we put

$$\eta_2 = \frac{z\,\mathrm{d}z}{w}\ , \quad \mathbb{A}_{22} = \oint_{\mathcal{A}_2}\eta_2\ , \qquad \varkappa_2 = \frac{\oint_{\mathcal{B}_2}\eta_2}{\oint_{\mathcal{A}_2}\eta_2} \tag{1.22}$$

[1]In loc. cit. the region Δ is termed the "elliptic region".

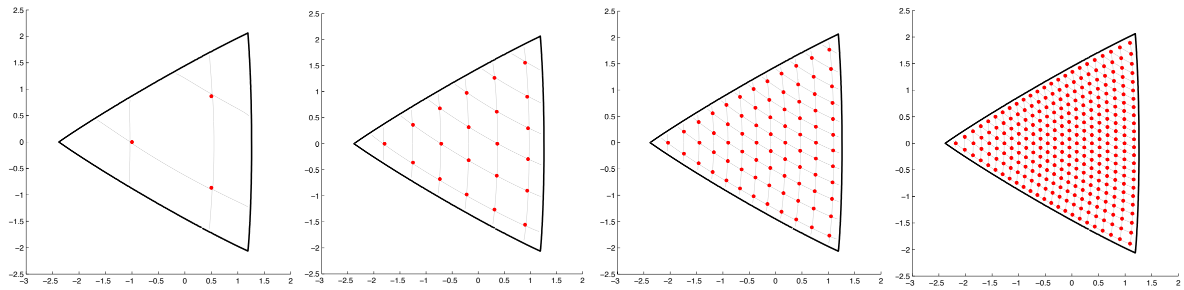

FIGURE 2. The lines expressing the quantization conditions (1.24) and the zeros of the polynomial $\widehat{Q}_n(x)$ computed numerically, for $n = 2, 6, 12, 24$ (from left to right). As can be seen, the zeros of $\widehat{Q}_n(x)$ form a regular pattern, a feature which was first observed in [5].

for a specific choice of homology basis $\{\mathcal{A}_j, \mathcal{B}_j\}_{j=1}^2$ shown in Figure 13. Uniformly for x belonging to any compact subset of $\Delta \setminus \mathcal{Z}_n$ the polynomial $\psi_n(\zeta; n^{\frac{2}{3}}x), \zeta \in S^1$ exists for n sufficiently large. Moreover, for x in the same compact set, $\widehat{Q}_n(x) \neq 0$ for n large enough.

The condition (1.21) is equivalently formulated as

$$\frac{n}{2\pi i}\left[\oint_{\mathcal{B}_1} \mathrm{d}\phi + \varkappa_2 \oint_{\mathcal{A}_1} \mathrm{d}\phi\right] + \frac{1}{2}\left[\int_{a_1}^{0} \frac{\eta_2}{\mathbb{A}_{22}} + \frac{\varkappa_2}{2}\right] = \frac{1+\varkappa_2}{2} + k + \ell\varkappa_2, \quad k, \ell \in \mathbb{Z} \tag{1.23}$$

The integrals $\oint_{\mathcal{B}_1, \mathcal{A}_1} \mathrm{d}\phi$ are purely imaginary (see (3.36)) and since $\Im \varkappa_2 > 0$, any complex number ρ can be uniquely expressed as $\sigma + \varkappa_2 \xi \quad \sigma, \xi \in \mathbb{R}$. Thus the condition (1.23) can be expressed as the pair of quantization conditions

$$\frac{n}{2\pi i} \oint_{\mathcal{B}_1} \mathrm{d}\phi = \frac{1}{2} + k + \sigma \ , \qquad \frac{n}{2\pi i} \oint_{\mathcal{A}_1} \mathrm{d}\phi = \frac{1}{4} + \ell + \xi \ , \tag{1.24}$$

where $k, \ell \in \mathbb{Z}$ and $\sigma + \varkappa_2 \xi = \frac{1}{2}\int_{a_1}^{0} \frac{\eta_2}{\mathbb{A}_{22}}$. The lines of the quantization conditions (1.24) are shown in Figure 2 for different values of n. We note that the agreement is remarkably much better - even for very small values of n - than what Theorem 1.6 below leads to expect.

The outlined reduction of the appearing Riemann theta function to a Jacobi theta function combined with an application of the argument principle to smooth functions yields the following Theorem that localizes the zeros of $\widehat{Q}_n(x)$ within disks of radius $\mathcal{O}(n^{-1})$.

Theorem 1.6. *For each compact subset K of the interior of Δ, and for any arbitrarily small $r_0 > 0$ there exists $n_0 = n_0(K, r_0)$ such that the zeros of $\widehat{Q}_n(x) = \mathcal{Q}_n(n^{\frac{2}{3}}x), n \geq n_0$ that fall within K are inside disks of radius r_0/n centered around the points of the exceptional set $\mathcal{Z}_n$.*

The paper is organised as follows: we first prove Theorem 1.1 in Section 2 by applying identity (1.4). After that preliminary steps for the Riemann-Hilbert analysis of the (pseudo) orthogonal polynomials $\{\psi_n(\zeta; x)\}$ are taken in Section 3. This includes a rescaling of the weight and the construction of the relevant g-functions which are used outside and inside the star. The g-functions reduce the initial RHP to the solution of model problems and we state their explicit construction in Section 4. Section 5 completes the proofs of Theorems 1.4 and 1.5. In the end we compare our results obtained outside and inside the star to [3], this is done in Section 6 which also gives the proof of Theorem 1.6.

2. Proof of Theorem 1.1

The identity (1.9) follows from several equivalence transformations. First we go back to (1.4) and notice that $q_0(x) = 1$, the convention $q_k(x) \equiv 0$ for $k < 0$ as well as the empty product imply

$$\mathcal{Q}_n(x) = \prod_{k=1}^{n} (2k+1)^{n-k} \det\left[q_{n-2\ell+j}(x)\right]_{\ell,j=0}^{n}, \qquad n \geq 0.$$

Thus (1.9) is in fact equivalent to the identity

$$\left\{\det\left[q_{n-2\ell+j}(x)\right]_{\ell,j=1}^{n}\right\}^2=(-)^{\lfloor\frac{n}{2}\rfloor}2^{(n-1)^2}\det\left[\mu_{\ell+j-2}(x)\right]_{\ell,j=1}^{n},\qquad n\geq 1. \tag{2.1}$$

Since

$$F_1(t;x)\big(F_1(t;x)\pm F_1(-t;x)\big)=F_2(2t;x)\pm 1$$

holds identically in t and x, we have from comparison

$$2^{k-1}\mu_k(x)+\frac{\delta_{k0}}{2} = \sum_{m=0}^{k}q_{k-2m}(x)q_{2m}(x),\qquad k\geq 0, \tag{2.2}$$

$$2^{k-1}\mu_k(x)-\frac{\delta_{k0}}{2} = \sum_{m=0}^{k}q_{k-2m-1}(x)q_{2m+1}(x),\qquad k\geq 0. \tag{2.3}$$

Now back to the left hand side of (2.1) with $n\geq 1$. We first shift indices, then permute columns and rows in the second factor, transpose the first matrix and then evaluate the product

$$\left\{\det\left[q_{n-2\ell+j}(x)\right]_{\ell,j=1}^{n}\right\}^2=\left\{\det\left[q_{n-1-2\ell+j}(x)\right]_{\ell,j=0}^{n-1}\right\}^2=\det\left[q_{n-1-2\ell+j}(x)\right]_{\ell,j=0}^{n-1}\det\left[q_{2\ell-j}(x)\right]_{\ell,j=0}^{n-1}$$
$$=\det\left[q_{n-1-2j+\ell}(x)\right]_{\ell,j=0}^{n-1}\det\left[q_{2\ell-j}(x)\right]_{\ell,j=0}^{n-1}=\det\left[\sum_{m=0}^{n-1}q_{n-1-2m+\ell}(x)q_{2m-j}(x)\right]_{\ell,j=0}^{n-1}.$$

Now use (2.2) and (2.3) to evaluate the entries. In the first row

$$\sum_{m=0}^{n-1}q_{n-1-2m}(x)q_{2m-j}(x) = 2^{n-2-j}\mu_{n-1-j}(x),\qquad j=0,\ldots,n-2$$
$$\sum_{m=0}^{n-1}q_{n-1-2m}(x)q_{2m-(n-1)}(x)=\begin{cases}\frac{\mu_0(x)}{2}-\frac{1}{2}, & n\equiv 0 \bmod 2\\ \frac{\mu_0(x)}{2}+\frac{1}{2}, & n\equiv 1\bmod 2.\end{cases}$$

For the second and subsequent rows

$$\sum_{m=0}^{n-1}q_{n-1-2m+\ell}(x)q_{2m-j}(x)=2^{n-2-j+\ell}\mu_{n-1-j+\ell}(x),\qquad j=0,\ldots,n-1,\quad \ell=1,\ldots,n-1$$

which shows that

$$\left\{\det\left[q_{n-2\ell+j}(x)\right]_{\ell,j=1}^{n}\right\}^2=\det\left[2^{n-2-j+l}\tilde{\mu}_{n-1-j+\ell}(x)\right]_{\ell,j=0}^{n-1}=(-)^{\lfloor\frac{n}{2}\rfloor}\det\left[2^{\ell+j-1}\tilde{\mu}_{\ell+j}(x)\right]_{\ell,j=0}^{n-1}$$

where we permuted only the columns ($j\mapsto n-1-j$) in the last step and introduced

$$\tilde{\mu}_k(x)=\mu_k(x),\quad k\geq 1;\qquad \tilde{\mu}_0(x)=\begin{cases}0, & n\equiv 0\bmod 2,\\ 2, & n\equiv 1\bmod 2.\end{cases}$$

Notice that we have suppressed the dependency on n in the notation of $\tilde{\mu}_k(x)$. Factoring out common factors we continue

$$\left\{\det\left[q_{n-2\ell+j}(x)\right]_{\ell,j=1}^{n}\right\}^2=(-)^{\lfloor\frac{n}{2}\rfloor}2^{(n-1)^2}\frac{1}{2}\det\left[\tilde{\mu}_{\ell+j}(x)\right]_{\ell,j=0}^{n-1}=(-)^{\lfloor\frac{n}{2}\rfloor}2^{(n-1)^2}\frac{1}{2}\det\left[\tilde{\mu}_{\ell+j-2}(x)\right]_{\ell,j=1}^{n}$$

and therefore, compare (2.1), are left to show that

$$\det\left[\tilde{\mu}_{\ell+j-2}(x)\right]_{\ell,j=1}^{n}=2\det\left[\mu_{\ell+j-2}(x)\right]_{\ell,j=1}^{n},\qquad n\geq 1. \tag{2.4}$$

This identity is definitely satisfied for $n=1$, hence let us assume that $n\geq 2$. By multilinearity

$$\det\left[\tilde{\mu}_{\ell+j-2}(x)\right]_{\ell,j=1}^{n}=\det\left[\mu_{\ell+j-2}(x)\right]_{\ell,j=1}^{n}+(-)^{n-1}\det\left[\mu_{\ell+j}(x)\right]_{\ell,j=1}^{n-1},$$

thus we need to verify that

$$(-)^{n-1}\det\Big[\mu_{\ell+j}(x)\Big]_{\ell,j=1}^{n-1}=\det\Big[\mu_{\ell+j-2}(x)\Big]_{\ell,j=1}^{n},\qquad n\geq 2. \tag{2.5}$$

Both sides in the latter equation are polynomials in $x\in\mathbb{C}$, hence if we manage to establish equality in (2.5) outside a set $E\subset\mathbb{C}$ of measure zero, it follows by continuation for all $x\in\mathbb{C}$. In our case, we will verify (2.5) for $x\in\mathbb{C}\backslash E$ with

$$E=\left\{x\in\mathbb{C}:\ \det\Big[\mu_{j+k}(x)\Big]_{j,k=1}^{m}=0,\quad m=1,\ldots,n-2\right\}$$

using the following algorithm: we start (1) on the right hand side of (2.5) and add appropriate combinations of rows to subsequent rows, starting from row n and continuing with row $n-1$, etc. Formally with $\mu_k(x)\equiv 0$ for $k<0$

$$\mu_{\ell+j-2}\ \mapsto\ \mu_{\ell,j}^{(1)}=\mu_{\ell+j-2}-\left\{\frac{x\mu_{(\ell-1)+j-2}}{\ell-1}-\frac{\mu_{(\ell-3)+j-2}}{\ell-1}\right\},\qquad \ell=4,\ldots,n$$

$$\mu_{\ell+j-2}\ \mapsto\ \mu_{\ell,j}^{(1)}=\mu_{\ell+j-2}-\left\{\frac{x\mu_{(\ell-1)+j-2}}{\ell-1}\right\},\qquad \ell=2,3$$

for any $j\in\{1,\ldots,n\}$. Recalling (1.8) this step implies

$$\mu_{\ell,1}^{(1)}=\mu_{1,\ell}^{(1)}=0,\ \ \ell=2,\ldots,n;\qquad \mu_{\ell,\ell}^{(1)}=-\mu_{2\ell-2},\ \ \ell=2,\ldots,n,\ \ell\neq 3;\qquad \mu_{3,3}^{(1)}=-\mu_4-\frac{\mu_1}{2}.$$

In the next step (2) we add an α_1-multiple of the second row to the third row and then an α_2-multiple of the second column to the third column, where

$$\alpha_1=\frac{\mu_{23}^{(1)}+\mu_3}{\mu_2},\qquad \alpha_2=\frac{\mu_{32}^{(1)}+\mu_3}{\mu_2},$$

provided $\mu_2\neq 0$, which is satisfied for $x\in\mathbb{C}\backslash E$. Using again the recursion (1.8), this move leads to the replacement

$$\mu_{\ell,j}^{(1)}\mapsto\mu_{\ell,j}^{(2)}=\mu_{\ell,j}^{(1)};\quad \mu_{2,j}^{(1)}\mapsto\mu_{2,j}^{(2)}=\mu_{2,j}^{(1)};\quad \mu_{\ell,2}^{(1)}\ \mapsto\ \mu_{\ell,2}^{(2)}=\mu_{\ell,2}^{(1)};\quad \ell,j=4,\ldots,n$$

as well as

$$\mu_{3,j}^{(1)}\mapsto\mu_{3,j}^{(2)}=\mu_{3,j}^{(1)}+\alpha_1\mu_{2,j}^{(1)};\quad \mu_{\ell,3}^{(1)}\mapsto\mu_{\ell,3}^{(2)}=\mu_{\ell,3}^{(1)}+\alpha_2\mu_{\ell,2}^{(1)},\quad \ell,j=4,\ldots,n$$

and most importantly

$$\mu_{2,2}^{(1)}\mapsto\mu_{2,2}^{(2)}=-\mu_2,\qquad \mu_{2,3}^{(1)}\mapsto\mu_{2,3}^{(2)}=-\mu_3,\qquad \mu_{3,2}^{(1)}\mapsto\mu_{3,2}^{(2)}=-\mu_3,\qquad \mu_{3,3}^{(1)}\mapsto\mu_{3,3}^{(2)}=-\mu_4. \tag{2.6}$$

Hence step (2) shows that

$$\det\Big[\mu_{\ell+j-2}(x)\Big]_{\ell,j=1}^{n}=\det\begin{bmatrix}\mu_0 & 0 & 0 & 0 & \cdots & 0\\ 0 & -\mu_2 & -\mu_3 & \mu_{24}^{(2)} & \cdots & \mu_{2n}^{(2)}\\ 0 & -\mu_3 & -\mu_4 & \mu_{34}^{(2)} & \cdots & \mu_{3n}^{(2)}\\ 0 & \mu_{42}^{(2)} & \mu_{43}^{(2)} & -\mu_6 & & \vdots\\ \vdots & \vdots & \vdots & & \ddots & \\ 0 & \mu_{n2}^{(2)} & \mu_{n3}^{(2)} & \cdots & & -\mu_{2n-2}\end{bmatrix},\qquad \mu_2\neq 0.$$

In step (3) we add a β_{11}-multiple of the second column and a β_{21}-multiple of the third column to the fourth column, followed by then adding a β_{12}-multiple of the second row and a β_{22}-multiple of the third row to the fourth row. Here $\{\beta_{jk}\}$ are determined from the linear system

$$\begin{bmatrix}\mu_2 & \mu_3\\ \mu_3 & \mu_4\end{bmatrix}\begin{bmatrix}\beta_{11} & \beta_{12}\\ \beta_{21} & \beta_{22}\end{bmatrix}=\begin{bmatrix}\mu_{24}^{(2)}+\mu_4 & \mu_{42}^{(2)}+\mu_4\\ \mu_{34}^{(2)}+\mu_5 & \mu_{43}^{(2)}+\mu_5\end{bmatrix}.$$

provided the determinant of its coefficients matrix, i.e. $\det\left[\mu_{j+k}\right]_{j,k=1}^{2}$ does not vanish, which again is guaranteed for $x\in\mathbb{C}\backslash E$. In terms of the recursion (1.8), this leads us to

$$\det\Big[\mu_{\ell+j-2}(x)\Big]_{\ell,j=1}^{n}=\det\begin{bmatrix}\mu_0 & 0 & 0 & 0 & 0 & \cdots & 0\\ 0 & -\mu_2 & -\mu_3 & -\mu_4 & \mu_{25}^{(3)} & \cdots & \mu_{2n}^{(3)}\\ 0 & -\mu_3 & -\mu_4 & -\mu_5 & \mu_{35}^{(3)} & \cdots & \mu_{3n}^{(3)}\\ 0 & -\mu_4 & -\mu_5 & -\mu_6 & \mu_{45}^{(3)} & \cdots & \mu_{4n}^{(3)}\\ 0 & \mu_{52}^{(3)} & \mu_{53}^{(3)} & \mu_{54}^{(3)} & -\mu_8 & & \vdots\\ \vdots & \vdots & \vdots & \vdots & & \ddots & \\ 0 & \mu_{n2}^{(3)} & \mu_{n3}^{(3)} & \mu_{n4}^{(3)} & \cdots & & -\mu_{2n-2}\end{bmatrix},\qquad \det\left[\mu_{j+k}\right]_{j,k=1}^{2}\neq0.$$

Step (3) is then followed by step (4) in which we add appropriate combinations of the second, third and fourth column/row to the fifth column/row, and so forth. After $(n-1)$ steps in this algorithm, we end up with the identity

$$\det\Big[\mu_{\ell+j-2}(x)\Big]_{\ell,j=1}^{n}=\det\begin{bmatrix}\mu_0 & 0 & 0 & \cdots & 0 & 0\\ 0 & -\mu_2 & -\mu_3 & \cdots & -\mu_{n-1} & \mu_{2n}^{(n-1)}\\ 0 & -\mu_3 & -\mu_4 & \cdots & -\mu_n & \mu_{3n}^{(n-1)}\\ \vdots & \vdots & \vdots & \ddots & & \vdots\\ 0 & -\mu_{n-1} & -\mu_n & & -\mu_{2n-4} & \mu_{n-1,n}^{(n-1)}\\ 0 & \mu_{n2}^{(n-1)} & \mu_{n3}^{(n-1)} & \cdots & \mu_{n,n-1}^{(n-1)} & -\mu_{2n-2}\end{bmatrix},\qquad \det\left[\mu_{j+k}\right]_{j,k=1}^{n-3}\neq0.$$

In the final step (n) we add combinations of the second, third, fourth,…,$(n-1)^{\text{st}}$ row/column to the n^{th} row/column according to the system

$$\begin{bmatrix}\mu_2 & \mu_3 & \cdots & \mu_{n-1}\\ \vdots & & & \vdots\\ \mu_{n-1} & \mu_n & \cdots & \mu_{2n-4}\end{bmatrix}\begin{bmatrix}\gamma_{11} & \gamma_{12}\\ \vdots & \vdots\\ \gamma_{n-2,1} & \gamma_{n-2,2}\end{bmatrix}=\begin{bmatrix}\mu_{2n}^{(n-1)}+\mu_n & \mu_{n2}^{(n-1)}+\mu_n\\ \vdots & \vdots\\ \mu_{n-1,n}^{(n-1)}+\mu_{2n-3} & \mu_{n,n-1}^{(n-1)}+\mu_{2n-3}\end{bmatrix}$$

and establish (2.5) from the recursion (1.8) after extracting $(n-1)$ signs, provided that $\det\left[\mu_{j+k}\right]_{j,k=1}^{n-2}\neq0$, which holds for $x\in\mathbb{C}\backslash E$. This verifies (2.5) by analytic continuation and tracing back all equivalence transformations completes therefore the proof of Theorem 1.1.

3. Riemann-Hilbert analysis - preliminary steps

It is well known that orthogonal polynomials can be characterized in terms of the solution of a Riemann-Hilbert problem (RHP), first introduced by Fokas, Its and Kitaev [11]. In present context of (1.11), the relevant RHP is defined as follows:

Definition 3.1. *Let γ be a simple, smooth Jordan curve encircling the origin in clockwise orientation. Determine the 2×2 matrix-valued piecewise analytic function $\Gamma(z)\equiv\Gamma(z;x,n)$ such that*

- *$\Gamma(z)$ is analytic for $z\in\mathbb{C}\backslash\gamma$*
- *The boundary values on γ are related via*

$$\Gamma_+(z)=\Gamma_-(z)\begin{bmatrix}1 & w(z;x)\\ 0 & 1\end{bmatrix},\qquad z\in\gamma;\qquad w(z;x)=\frac{1}{2\pi i}e^{-\theta(z;x)}\frac{1}{z}\tag{3.1}$$

  with θ as in (1.11).
- *As $z\to\infty$, we have*

$$\Gamma(z)=\left(I+\frac{\Gamma_1(x,n)}{z}+\mathcal{O}\left(z^{-2}\right)\right)z^{n\sigma_3}\tag{3.2}$$

The solvability of the Γ-RHP is equivalent to the existence of the orthogonal polynomial $\psi_n(\zeta;x)$, in fact [6]

$$\psi_n(\zeta;x) = \Gamma_{11}(\zeta;x,n), \tag{3.3}$$

and in addition

$$h_n(x) = -2\pi i \lim_{z\to\infty} z\Big(\Gamma(z;x,n)z^{-n\sigma_3} - I\Big)_{12}, \qquad \big(h_{n-1}(x)\big)^{-1} = \frac{i}{2\pi}\lim_{z\to\infty} z\Big(\Gamma(z;x,n)z^{-n\sigma_3} - I\Big)_{21}. \tag{3.4}$$

We will solve the latter RHP as $n\to\infty$ for rescaled $x\in\mathbb{C}$ outside and inside (there subject to an additional constraint) the star shaped region described in Definition (1.3). Our approach uses standard methods from the Deift-Zhou nonlinear steepest descent framework (cf. [9],[7],[8]) and consists of a series of explicit and invertible transformations. In terms of the solution of the RHP 3.1 the solution of the Painlevé equation $u(x;n)$ is obtained as specified below.

Proposition 3.2. *The rational solution $u(x;n)$ of the Painlevé II equation (1.1) given by (1.15) is also expressible as*

$$u(x;n) = -\frac{1}{2}\frac{h_n'(x)}{h_n(x)} = \frac{1}{2}\frac{\Gamma_{11}(0;x,n)\Gamma_{12}(0;x,n)}{\Gamma_{1;12}(x,n)} \tag{3.5}$$

where $\Gamma_1(x,n)$ is the matrix appearing in the expansion at $z=\infty$ (3.2).

The expression is an immediate application of the following Lemma

Lemma 3.3. *We have*

$$\partial_x h_n(x) = 2\pi i\,\Gamma_{12}(0;x,n)\Gamma_{11}(0;x,n) \tag{3.6}$$

Proof. The matrix valued function $\Psi(z;x,n)\equiv\Gamma(z;x,n)\mathrm{e}^{-\frac{1}{2}\theta(z;x)\sigma_3}z^{-\frac{1}{2}\sigma_3}$, $z\in\mathbb{C}\backslash\gamma$ solves a RHP with jumps that are independent of z and, most importantly, of x. Thus the matrix $W(z;x,n)\equiv\partial_x\Psi(z;x,n)\Psi^{-1}(z;x,n)$ is analytic in $\mathbb{C}\backslash\{0\}$, in fact

$$W(z;x,n) = \partial_x\Gamma(z;x,n)\Gamma^{-1}(z;x,n) + \frac{1}{2z}\Gamma(z;x,n)\sigma_3\Gamma^{-1}(z;x,n).$$

From this, a local analysis near $z=\infty$ and $z=0$ shows that $W(z;x,n)=\mathcal{O}\left(z^{-1}\right)$, hence by Liouville's theorem we have that $W(z;x,n)=\frac{C}{z}$ for a matrix C that is constant in z. In order to compute C explicitly we notice that the first term in the sum above is bounded at $z=0$, thus

$$W(z;x,n) = \frac{1}{2z}\Gamma(0;x,n)\sigma_3\Gamma^{-1}(0;x,n).$$

On the other hand, by the same argument, looking at the expansion near $z=\infty$, we have that

$$W(z;x,n) = \frac{1}{z}\partial_x\Gamma_1(x,n) + \frac{\sigma_3}{2z}.$$

Choosing the $(1,2)$ entry yields with unimodularity of $\Gamma(z)$,

$$\partial_x\Gamma_{1;12}(x,n) = -\Gamma_{11}(0;x,n)\Gamma_{12}(0;x,n). \tag{3.7}$$

□

3.1. **Rescaling and the abstract g-function.** In order to study the polynomials $\widehat{Q}_n(x)=\mathcal{Q}_n(n^{\frac{2}{3}}x)$ we consider the following change of variables

$$\psi_n^o(z;x) = N^{\frac{n}{3}}\psi_n\left(N^{-\frac{1}{3}}z;N^{\frac{2}{3}}x\right), \qquad h_n^o(x) = N^{\frac{2n}{3}}h_n\left(N^{\frac{2}{3}}x\right). \tag{3.8}$$

Consequently, the measure of orthogonality of these new orthogonal polynomials is

$$\mathrm{d}\nu(z;x)\mapsto\mathrm{d}\nu^o(z;x) = \frac{1}{2\pi i}e^{-N\theta(z;x)}\frac{\mathrm{d}z}{z}, \qquad N\in\mathbb{N} \tag{3.9}$$

Under the scaling (3.9), the initial Γ-RHP is replaced by a RHP for the function $\Gamma^o(z)\equiv\Gamma^o(z;x,n,N)$ with jump

$$\Gamma_+^o(z) = \Gamma_-^o(z)\begin{bmatrix}1 & w^o(z;x)\\ 0 & 1\end{bmatrix}, \qquad z\in\gamma; \qquad w^o(z;x) = \frac{1}{2\pi i}e^{-N\theta(z;x)}\frac{1}{z}$$

and asymptotic behavior (3.2). As we are interested in the large n asymptotics of the normalizing coefficients $h_n(x)$, we will solve the Γ^o-RHP for $\Gamma^o(z) = \Gamma^o(z;x,n,n)$.

Construction of the g-function. The purpose of the so–called g-function is to normalize the RHP at infinity. This function is analytic off $\mathcal{B} \subset \mathbb{C}$ which consists of a finite union of oriented smooth arcs, whose endpoints and shape depend on $x \in \mathbb{C}$. We shall present the requirements here and then prove the existence.

Suppose that there is a *positive* density $\rho(z)\mathrm{d}z$ on $\mathcal{B}$ of total mass 1 such that (the parametric dependence on x is understood):

$$g(z) = \int_{\mathcal{B}} \ln(z-w)\rho(w)|\mathrm{d}w|, \quad z \in \mathbb{C}\backslash\mathcal{B} \qquad g_+(z) + g_-(z) = \theta(z;x) + \ell + i\alpha_j, \quad z \in \mathcal{B}_j \tag{3.10}$$

where $\mathcal{B}_j$ denote the connected components of $\mathcal{B}$ and $\ell \in \mathbb{C}, \alpha_j \in \mathbb{R}$ can only depend on x. At infinity we have thus (since the total mass of ρ is unity)

$$g(z) = \ln z + \mathcal{O}\left(z^{-1}\right), \quad z \to \infty. \tag{3.11}$$

and $g(z)$ has a jump $g_+(z) - g_-(z) = 2\pi i$ on a contour that extends to infinity. Assuming temporarily the existence of $g(z)$, differentiating in (3.10) with respect to z and applying the Plemelj formula, we have

$$\left(g'(z)\right)_+^2 = \left(g'(z)\right)_-^2 + 2\pi i \theta_z(z;x)\rho(z), \quad z \in \mathcal{B}, \qquad (') = \frac{\partial}{\partial z}$$

which is solved as

$$\left(g'(z)\right)^2 = \int_{\mathcal{B}} \frac{\theta_w(w;x)\rho(w)}{w-z}\mathrm{d}w = \theta_z(z;x)g'(z) + \int_{\mathcal{B}} \frac{\theta_w(w;x) - \theta_z(z;x)}{w-z}\rho(w)\mathrm{d}w. \tag{3.12}$$

The last integral defines a meromorphic function in $z \in \mathbb{C}$ with its only singularity being a fourth order pole at the origin, thus (3.12) implies for $y(z) = g'(z) - \frac{1}{2}\theta_z(z;x)$ that

$$y^2 = \left(\frac{\theta_z}{2}\right)^2 + \int_{\mathcal{B}} \frac{\theta_w(w;x) - \theta_z(z;x)}{w-z}\rho(w)\mathrm{d}w = \frac{P_6(z;x)}{z^8} \tag{3.13}$$

with a polynomial $P_6(z;x) = z^6 + \mathcal{O}\left(z^5\right), z \to \infty$. All together

$$g(z) = \frac{1}{2}\theta(z;x) + \int_{ia}^{z} y(\lambda)\mathrm{d}\lambda + \frac{\ell}{2}, \quad z \in \mathbb{C}\backslash\mathcal{B} \tag{3.14}$$

where ia is one of the endpoints of one of the smooth arcs of which $\mathcal{B}$ consists.

The complex effective potential and its characterization. It is convenient to introduce the *complex effective potential*

$$\varphi(z) = \theta(z;x) - 2g(z) + \ell = -2\int_{ia}^{z} y(\lambda)\mathrm{d}\lambda, \quad z \in \mathbb{C}\backslash\mathcal{B} \tag{3.15}$$

The following properties of φ are equivalent to the existence of the g-function and characterize φ (the proof of these statements is simple if not already obvious)

- Near $z=0$ the effective potential has the behavior

  $$\varphi(z) = \theta(z;x) + \mathcal{O}(1) \quad \Rightarrow \quad y(z) = -\frac{1}{2}\theta_z(z;x) + \mathcal{O}(1), \qquad \theta(z;x) = \frac{1}{3z^3} - \frac{x}{z}. \tag{3.16}$$

  while near $z=\infty$ it behaves as

  $$\varphi(z) = -2\ln z + \mathcal{O}(1) \tag{3.17}$$

- Analytic continuation of $\varphi(z)$ in the domain $\mathbb{C}\backslash\mathcal{B}$ yields the same function up to addition of *imaginary* constants; in particular, the analytic continuation of $\varphi(z)$ around a large circle yields $\varphi(z) + 2\pi i$;
- For each component $\mathcal{B}_j$ of $\mathcal{B}$ we have that (compare (3.10)),

  $$\varphi_+(z) + \varphi_-(z) = -2i\alpha_j, \quad z \in \mathcal{B}_j, \quad \alpha_j \in \mathbb{R}$$

- The effective potential $\Phi(z;x) \equiv \Re\varphi(z;x)$ is a harmonic function in $\mathbb{C}\backslash\mathcal{B}$ (one verifies from (3.15) that all possible jumps of $\varphi(z)$ are purely imaginary) and $\Phi(z)\big|_{\mathcal{B}} \equiv 0$.

- **Inequality 1.** The fact that the density $\rho(z)$ is a positive density is equivalent (via the Cauchy Riemann equations) to the statement that $\Phi(z)$ *decreases* as we move from a point of $\mathcal{B}$ in the transversal direction. To put it differently, the sign of $\Phi(z)$ on the left and right of $\mathcal{B}$ is *negative.*
- **Inequality 2.** We can continuously deform the contour of integration γ to a simple Jordan curve (still denoted by γ) such that $\mathcal{B} \subset \gamma$ and such that $\Phi(z)\big|_{\gamma\setminus\mathcal{B}} > 0$.

From (3.13) we observe that $\varphi(z)$ and $g(z)$ are related to the antiderivative of the differential $y(z)\mathrm{d}z$ which is defined on a Riemann surface X of genus between 0 and 2 and given by the equation $w^2 = P_6(z)$. Since $\Phi(z) = \Re\varphi(z)$ is zero on $\mathcal{B}$, it also follows that $\mathcal{B}$ is a (subset of) its zero level set; therefore, $\mathcal{B}$ consists of an union of arcs defined locally by the differential equation $\Re(y\mathrm{d}z) = 0$. In the following, we shall prove that for any value of $x \in \mathbb{C}$, the polynomial $P_6(z;x)$ is *even* and that it has only one of two possible forms below

$$y(z) = \frac{1}{z^4}\sqrt{P_6(z;x)}\ , \qquad P_6(z;x) = \begin{cases} \left(z^2+a^2\right)\left(z^2-z_0^2\right)^2, & x \in \mathbb{C}\setminus\Delta \\ \left(z^2+a^2\right)\left(z^2+b^2\right)\left(z^2+c^2\right), & x \in \Delta \end{cases} \tag{3.18}$$

where Δ is a simply connected region containing $x = 0$ that will be described *en route*, it is depicted in Figure 1. The parameters appearing in (3.18) are completely (for $x \in \mathbb{C}\setminus\Delta$) or partially ($x \in \Delta$) specified by the requirement (3.16), see Sections 3.3 and 3.4.

The overall logic is to show that there exists a differential $\omega(z) = -\frac{2}{z^4}\sqrt{P_6(z)}\,\mathrm{d}z$ whose integral defines a function $\varphi(z)$ with the required properties. Clearly, ω is a differential defined on the Riemann surface

$$X = \{(w,z) \in \mathbb{C}^2: \quad w^2 = P_6(z)\}.$$

which is of genus between zero and two. The first necessary condition is that

$$\oint_\gamma \omega \in i\mathbb{R} \tag{3.19}$$

for all closed loops γ on the Riemann surface X (i.e. a loop in the z–plane containing an even number of zeros of P_6, counted with multiplicity). The following lemma is of immediate proof, which is left to the reader

Lemma 3.4. *Suppose that condition (3.19) holds and let ia be one of the odd-multiplicity zeros of P_6; then the expression $\mathbf{F}(p) = \Re\int_{ia}^{p}\omega$ yields a harmonic function of $p = (w,z) \in X$ minus the two points above $z = 0$. The values of $\mathbf{F}(p)$ at two points $(\pm w, z)$ differ only by a sign and the zero level set of $\mathbf{F}$ is well defined on the z–plane. Moreover all branch points of X belong to the zero level set of $\mathbf{F}$.*

We can realize X as a two–sheeted cover of the z–plane by placing cuts (here denoted by $\mathcal{B}$) between the branch points (i.e. the zeros of $P_6(z)$), and this can be done in infinitely many ways. Then $\sqrt{P_6(z)}$ becomes a single-valued analytic function on $\mathbb{C}\setminus\mathcal{B}$ and the evaluation of $\mathbf{F}$ at the two points above $z \in \mathbb{C}\setminus\mathcal{B}$ yields two harmonic functions on $\mathbb{C}\setminus\big(\mathcal{B}\cup\{0\}\big)$ differing by a sign; assuming that $\mathcal{B}$ is chosen not to extend to ∞ we denote by $\Phi(z)$ the determination that behaves like $-2\ln|z|$ near $z = \infty$. For a general placement of $\mathcal{B}$ the function $\Phi(z)$ is *discontinuous* across $\mathcal{B}$. Since the zero level set of $\mathbf{F}(p)$ is well defined in the z-plane (given that the two determinations differ only by sign), *if we can place $\mathcal{B}$ so that $\Phi(z)\big|_{\mathcal{B}} \equiv 0$, then the resulting $\Phi(z)$ is also continuous across $\mathcal{B}$* and thus defines a function which is **continuous** on $\mathbb{C}\setminus\{0\}$ and **harmonic** on $\mathbb{C}\setminus\big(\mathcal{B}\cup\{0\}\big)$; as a result, for any $z_0 \in \dot{\mathcal{B}}$ there[2] is a small disk $\mathbb{D}_{z_0}$ on which $\Phi(z)$ is either nonnegative or nonpositive. In order to fulfill **Inequality 1** we must see under which circumstances it is possible to place $\mathcal{B} \subseteq \{\Phi(z) = 0\}$ so that Φ is *nonpositive* when restricted to small disks mentioned above. Then we must also verify also **Inequality 2**.

3.2. **The inequalities of the effective potential $\Phi(z)$ and shape of Δ.** We shall use a deformation argument by first proving that the required **Inequality 1,2** for $\Phi(z)$ (and thus the g-function itself) exists for $x > 0$ and large, and then "propagate" the result to all values of x. It is very helpful if the reader keeps Figure 4 in front while following the description.

Preliminaries. The quadratic differential $(\omega)^2 = \frac{4}{z^8}P_6(z;x)\mathrm{d}z^2$ is precisely of the type studied by Jenkins and Spencer [12], that is, of the form $R(z)\mathrm{d}z^2$ with $R(z)$ a rational function; the following statements are

[2]For a topological space Z, $\dot{Z}$ is the set of interior points. Thus $\dot{\mathcal{B}}$ is the subset of all points that are not endpoints.

proved ibidem. Let the set $\mathfrak{H}_x$ consist of the union of the second order poles on the Riemann sphere and all "critical trajectories": these are all solutions of $\Re\omega = -2\Re y(z)\mathrm{d}z = 0$ that issue from each of the zeros (and simple poles of $R(z)$, but in our case there is none). In the little vignettes of Figure 4, these are marked in red, blue and green. In our case the zeros are $\pm ia$ and $\pm z_0 \equiv \pm\frac{1}{\sqrt{2a}}$, see (3.22) for genus 0 or (3.33), (3.34), (3.45) for genus 2. Also [14], there are $2k+1$ branches of $\mathfrak{H}_x$ issuing from each of the points of order k of $R(z)$, $k = -1, 0, 1, \ldots$ (the case $k = -1$ corresponds to simple poles, and all others to zeros). Consider now the connected components of $\mathbb{C}\setminus\mathfrak{H}_x = \sqcup_j K_j$; it is a simple argument in analytic functions (see [12]) that each *simply* connected component K_j is conformally mapped by $\varphi(z)$ into a half-plane or a vertical strip $\alpha < \Phi < \beta$; each *doubly* connected component K_j is mapped to an annulus (or a punctured disk) $\mathcal{A}_{r_+,r_-} \equiv \{r_- < |w| < r_+\}$ by $w = \mathrm{e}^{\frac{2i\pi}{p}\varphi(z)}$ where $p = \oint_\gamma \mathrm{d}\varphi$ and γ is a closed simple contour separating the two boundary components of K_j. It is also shown in [12] that these are in fact the only possibilities for the topology of the connected components K_j. Moreover, there is a one-to-one correspondence between annular domains (including the degenerate case of a punctured disk) and free homotopy classes of simple closed contours $\gamma \subset \mathbb{C}\setminus\mathfrak{H}_x$ for which $\oint_\gamma \omega \neq 0$. Furthermore each double pole with positive bi-residue of the quadratic differential corresponds to domains conformally equivalent to a punctured disk (with the pole at its center); in our case $z = \infty$ is a second order pole of ω^2 (i.e. a simple pole of ω) with positive residue and thus there is one disk domain which we denote by K_∞ with $z = \infty$ at its (conformal) center.

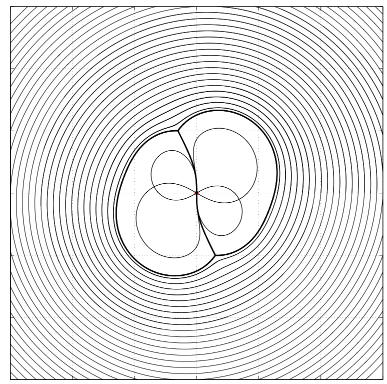

FIGURE 3
Illustration of the conformal punctured disk K_∞, foliated by the trajectories C_r. The complement D_0 contains the other critical trajectories.

General properties for arbitrary x. The equation (3.17) shows that $z = \infty$ is at the center of a conformal punctured disk via the conformal map $w = \mathrm{e}^{\frac{1}{2}\varphi(z)}$; the level sets $C_r \equiv \{z : \Phi(z; x) = -2\ln r\}$ thus are foliating a region around $z = \infty$ in topological circles if r is sufficiently large. Thus none of the hyperelliptic trajectories issuing from $\pm ia, \pm z_0$ (genus 0) or the branch points $a_1, \ldots, a_6$ (genus 2) can "escape" to infinity; they either connect to $z = 0$ or amongst each other. Let r_0 be the infimum of the $r > 0$ for which C_r is smooth; this means that C_{r_0} contains at least one zero of $\mathrm{d}_z\varphi$ (in our case, given the symmetry, it contains then two zeros). The annular (punctured disk) domain K_∞ is then (see Figure 3)

$$K_\infty = \overline{\bigcup_{r>r_0} C_r}. \tag{3.20}$$

We denote also $D_0 \equiv \overline{\mathbb{C}\setminus K_\infty}$, which is thus a simply connected, symmetric region containing the origin.

Sufficient condition for the correct inequalities in genus zero. We now argue that $r_0 = 0$ is a sufficient condition. To put it differently, the "first encounter" of the level sets C_r as r decreases must be with the two branch points $\pm ia$ rather than $\pm z_0$. We shall then verify that this occurs for $x > 0$ large enough. Thus suppose now that $r_0 = 0$ and thus $\pm ia \in K_\infty$ and $\pm z_0 \in Int(D_0)$; in particular $\Phi(z)$ is *negative* in K_∞ and zero on its boundary. Then the simple, closed loop ∂K_∞ is separated into two components by $\pm ia$ and each of them is a hyperelliptic trajectory. We know that there must be three trajectories from each $\pm ia$ and two of them are already accounted for and form the boundary of D_0 (these are the red curve and its reflection around the origin (thin, black) in Figure 7, for example); thus the third trajectory is entirely contained in D_0, which is compact.

Now let us turn our attention to D_0; the points $\pm z_0 \in D_0$. In D_0 each branch of $y(z)$ (3.22) is single valued (the branch points are on the boundary of D_0). Only one of the two branches of $y(z)$ has the behavior $y(z) \sim -\frac{1}{2}\theta_z(z; x), z \to 0$; integrating this branch from ia coincides with $\varphi(z; x)$ in D_0. The value of the sign of $\Phi(z)$ in the interior of D_0 close to the boundary D_0 determines which of the two parts of $\partial D_0\setminus\{\pm ia\}$ is the branch cut $\mathcal{B}$: this is the part which has $\Phi(z) < 0$ on *both* sides (i.e. in D_0 and K_∞). At this point we have a candidate for Φ that already fulfills **Inequality 1**. Now, on $\mathcal{B}$ we have that $\Phi(z)$ is continuous but not harmonic, while on $\partial D_0\setminus\mathcal{B}$ it is continuous and harmonic. We now need to show that there is a path connecting $\pm ia$ and lying within $\Phi(z) > 0$, i.e. **Inequality 2**. This follows from the topological description of the possible regions K_j discussed in the previous part "Preliminaries". Indeed let K_1 be the region in D_0 and adjacent to the arc $\partial D_0 \backslash \mathcal{B}$ where $\varphi(z)$ is conformally one-to-one. Since Φ is *negative* on K_∞, zero on $\partial D_0 \backslash \mathcal{B}$ and harmonic across it, then Φ must be positive in K_1 and from the discussion of signs thus far, this is either a half-plane $\Re w = \Phi(z) > 0$ or a strip $0 < \Phi(z) < \epsilon$ (the only annular domain is K_∞). The two points $\pm ia$ are mapped on the imaginary axis $\Re w = \Phi(z) = 0$; thus there is a path connecting $\varphi(ia)$ to $\varphi(-ia)$ in the w-plane lying in the right half plane. The preimage of this path $\mathcal{L}$ in the z-plane connects thus $\pm ia$ and $\Phi(z)$ restricted to the interior points of this path is strictly positive. Note also that $\mathcal{L}$ is homotopic (at fixed endpoints) to $\partial D_0 \backslash \mathcal{B}$ in $\mathbb{C} \setminus \{0\}$ and hence the concatenation of $\gamma = \mathcal{B} \cup \mathcal{L}$ is (freely) homotopic to ∂D_0 which is a simple loop around the origin. Thus both, **Inequality 1,2** for $\Phi(z)$ are fulfilled.

Sufficient condition for the correct inequalities in (symmetric) genus two. With the same general setup as in the previous case, we claim that a sufficient condition is that **all** branch points a_j lie on $\partial D_0 = \partial K_\infty$. In this case ∂K_∞ is broken into 6 arcs (see for example the vignette for $x = 0$ in Figure 5). There is only one branch of $y(z)$ that behaves as $y(z) \sim -\frac{1}{2}\theta_z(z; x)$ near $z = 0$; the integral of this branch with base point a_1 is single–valued in $D_0 = \mathbb{C} \backslash K_\infty$ because the region contains no branch points and the residue of $y(z)$ at $z = 0$ vanishes; this integral then defines φ (and Φ) within D_0. The level curves of $\Phi(z)$ that issue from a_j and do not connect to other branch points must connect to the origin because $\Phi(z)$ changes sign exactly six times when going around the origin. The regions where $\varphi(z)$ is now one-to-one within D_0 are six half-planes because their boundary has only one connected component. Necessarily in three of them $\Phi(z) < 0$ and three of them $\Phi(z) > 0$. The arcs of $\partial K_\infty \backslash \{a_1, \dots, a_6\}$ bounding the three regions where $\Phi(z) < 0$ are the cuts and the other are simply zero level sets separating regions where Φ has opposite signs. The possibility of connecting two branch points that are connected by an arc of these level sets follows exactly by the same argument used in the previous paragraph.

Occurrence of the sufficient conditions. See Proposition 3.5 for genus zero and Proposition 3.9 for genus two.

Continuation from genus zero to (symmetric) genus two. These types of transitions are analyzed extensively in [1, 15] but we repeat here the essential points. The condition for the validity of the genus-zero assumption fails when $\pm z_0 \in \partial K_\infty$ (recall that ∂K_∞ is part of the zero level set of $\Phi(z)$ and it is made of trajectories from $\pm ia$). Let us say that $-z_0$ falls on $\mathcal{B}$ and z_0 on the other branch of the zero level set; in Figure 6 the point $-z_0$ (pane 1) is sinking ($\Phi(z_0) \searrow 0$) and at the critical point the shaded region is pinched, leaving no room to the contour of integration: it is necessary then to split the double zero of $(\mathrm{d}\varphi)^2$ into two simple zeros, thus creating a new branch cut. The details of this transition are analyzed in Section 3.4.1. Symmetrically for $-z_0$. This forces to open a new cut near z_0 and break the cut at $-z_0$, thus "generating" four new branch points; their dependence on x is then dictated implicitly by the equations (3.34), (3.45), both of which are symmetric under $z \mapsto -z$ and thus the symmetry $z \to -z$ is preserved. Now we need to argue that, as x moves in the genus two region, no further transitions can occur. But this is simple (see again [1, 15]) because there are no other saddle points of $\Phi(z)$ that can interfere with the topology of the zero-level set. Thus the only other transitions are when two (or more) branch points coalesce; but these occurrences are already described above. Thus we conclude that in the phase-diagram we only find the genus zero and the (symmetric) genus two regions.

Topology of the discriminant locus. By discriminant locus we refer to the locus in the x–plane where the inequalities fail for the genus zero ansatz; from the discussion above it follows that this can occur for x within certain branches of the locus (3.28), which expresses the fact that $\Phi(z_0; x) = 0$, i.e., the saddle point of $\Phi(z)$ lies on the zero level set. However the locus described by (3.28) contains "spurious" solutions, as we now explain (these are the solid blue rays and the two thin blue arcs from each $x_{0,1,2}$ in Figure 1).

We have discussed that in the genus zero region, two of the three trajectories from each branch point $\pm ia$ connect to the other branch point, and the third connects (generically in x) to the origin. The condition

(3.28) states that $\pm z_0$ are connected by one of the three trajectories connecting to one, or both, $\pm ia$. Given the $\mathbb{Z}_2$ symmetry, there are thus two, qualitatively distinct situations:

(1) Each of the point $\pm z_0$ are connected to both $\pm ia$, i.e., they belong to ∂K_∞ and thus the required inequalities are violated for certain perturbations of x.
(2) The points $\pm z_0$ belong to the zero level set and are connected to $\pm ia$ by one trajectory (each) and to 0 by another trajectory.

We can use the parameter $\sigma = \Im\varphi(z_0)$ to parametrize the position of z_0 along the trajectory connecting to $\pm ia$; note that σ is the distance from ia measured in the (flat) metric $|\mathrm{d}\varphi|^2$. It is a simple consequence of the explicit form that the coincidence of z_0 with ia corresponds to $\sigma = 0$ while the coincidence of z_0 with $-ia$ corresponds to $\sigma = \pi$. For these two extremes, we have the degenerate situations corresponding to the three vertices of the region Δ and $x^3 = -\frac{3}{\sqrt[3]{2}}$ (3.30).

Summarizing we have just proved that there is a branch of (3.28) that connects the three critical points $x_{0,1,2}$ and can be parametrized by $\sigma = \Im\varphi(z_0) \in [0, \pi]$. We now show that the union of these is topologically a circle. Indeed, it follows from the discussion that points on $\partial\Delta$ must parametrize the position of z_0 on the boundary ∂K_∞. The latter is topologically a circle and thus so is $\partial\Delta$. A local analysis (left to the reader) of (3.28) near $a_k = -\mathrm{e}^{i\frac{2\pi k}{3}}/\sqrt[3]{2},\ k = 0, 1, 2$ (corresponding to the points $x_{0,1,2}$) will also show that there are *five* branches of the locus that issue from each $x_{0,1,2}$ at angular separation $\frac{2\pi}{5}$, as shown in Figure 1. Two of them have just been described. A third one corresponds to the situation (2) above. These configurations too can be parametrized by $\sigma = \Im\varphi(z_0)$. Since z_0 is connected to one of $\pm ia$ and zero, the distance σ from the branch point can be arbitrarily large: indeed the point $z = 0$ is at infinity in the metric $|\mathrm{d}\varphi|^2$. On this branch of the locus (3.28) the parameter a tends to infinity because $\pm z_0 \to 0$ and thus $x \to \infty$; therefore these branches fall outside of Δ, exactly as the numerical picture in Figure 1 shows; in fact they are the straight rays (solid blue in Figure 1). This is proven by considering the situation $a < a_0$: in this case the saddle points $\pm z_0$ belong to the segment $[-ia, ia] \subset i\mathbb{R}$ and it is simple to verify that (3.28) holds. The other two rays issuing from $a_{1,2}$ (or $x_{1,2}$) follow from the $\mathbb{Z}_3$ symmetry, which is an easy consequence of the explicit equation (3.28) together with (1.16).

The remaining two branches of (3.28) issuing from the vertices of Δ do not correspond to any particular configuration that can be achieved within the genus-zero assumption. Now, of the 5 branches at x_0 we know that the ray extending to $-\infty$ corresponds to the configuration (2); the two branches that correspond to (1) are those forming an angle $\frac{4\pi}{5}$ (and not $\frac{2\pi}{5}$) with said ray. This is proved as follows: for $a \sim a_0$ (setting $\delta a = a - a_0$) a direct computation (left to the reader) shows that (with $z - ia = \frac{i}{2}\zeta$)

$$\varphi(z; a) = (1 + \mathcal{O}(\delta a)) \left(-\frac{2}{5} 2^{\frac{5}{6}} \zeta^{\frac{5}{2}} + 2 2^{\frac{5}{6}} \delta a\, \zeta^{\frac{3}{2}} + \mathcal{O}\big(\zeta^{\frac{7}{2}}\big) \right). \tag{3.21}$$

Thus the saddle point is approximately $\zeta_{\text{saddle}} \simeq 3\,\delta a$ and $\Re\varphi(z_0; a) \sim \frac{12}{5}\sqrt{3}\, 2^{\frac{5}{6}} \Re((\delta a)^{\frac{5}{2}})$; this vanishes for $\delta a < 0$ (corresponding to the branch of (3.28) giving the straight ray) and then the closest trajectories are $\delta a \in \mathrm{e}^{i\frac{2\pi}{5}}\mathbb{R}$. Since the map $x = x(a) = \frac{4a^3-1}{2a^2}$ given by (1.16) behaves like $x - x_0 \sim -3\sqrt[3]{2}(\delta a)^2$, this means that the angular separation is doubled and our statement is proved. The $\mathbb{Z}_3$ symmetry allows to use this result also for the other vertices $x_{1,2}$.

To complete we have still to rule out the possibility of other (disconnected) branches of (3.28); this could conceivably happen if $\pm z_0$ are on the zero level set of $\Phi(z)$, *but* on a different connected component than the one $\pm ia$ belonging to. However, an easy argument shows that this is impossible; if it were the case there would be two connected components of $\Phi(z) = 0$. On one we find $\pm ia$ and on the other we find $\pm z_0$. But then there should be at least one saddle point in the region separating the two connected components (because $\Phi(z)$ is harmonic and there cannot be a maximum). However the only saddle points of $\Phi(z)$ are precisely $\pm z_0$. This concludes the discussion.

3.3. **The concrete g-function for genus zero.** Using the top expression in (3.18) for $P_6(z; x)$, and imposing (3.16), after simple algebra we obtain

$$y(z) = g'(z) = \frac{1}{z^4}\left(z^2 - \frac{1}{2a}\right)\left(z^2 + a^2\right)^{\frac{1}{2}}, \qquad z \in \mathbb{C}\backslash\mathcal{B}, \qquad \mathcal{B} = [-ia, ia]. \tag{3.22}$$

where the parameter $a = a(x)$ is determined in terms of x by the condition (3.16) and translates to the cubic equation (1.16). It is however more expedient to think of x as a function of a and discuss the properties of $\varphi(z)$ in terms of a directly. An elementary integration yields the following expressions for $g(z)$ and $\varphi(z)$,

$$g(z) = \frac{1}{2}\theta(z;x) + \ln\left(z + \sqrt{z^2+a^2}\right) + \sqrt{z^2+a^2}\left(\frac{z^2(1-6a^3)+a^2}{6a^3z^3}\right) - \ln(ia) + \frac{\ell}{2}, \tag{3.23}$$

with the Lagrange multiplier equal to

$$\ell = 2 - \frac{1}{3a^3} + \ln\left(\frac{-a^2}{4}\right), \tag{3.24}$$

and the complex effective potential

$$\varphi(z) = -2\int_{ia}^{z} y(\lambda)\mathrm{d}\lambda = -2\ln\left(\frac{z+\sqrt{z^2+a^2}}{ia}\right) + \sqrt{z^2+a^2}\left(\frac{z^2(6a^3-1)-a^2}{3a^3z^3}\right). \tag{3.25}$$

Here, the branch cut $\mathcal{B}$ is an arc extending from ia to $-ia$ to be discussed shortly and the branch for $\sqrt{z^2+a^2}$ is such that $\sqrt{z^2+a^2} \sim z$ for large z.

Proposition 3.5. *The effective potential $\Phi(z;a) \equiv \Re\varphi(z;a)$ from (3.25) has the following properties:*

- **(1)** *The function $\Phi(z;a)$ is defined up to a sign depending on the choice of determination of $\sqrt{z^2+a^2}$ (provided the same choice is made in the whole expression).*
- **(2)** *The level sets $\{z \in \mathbb{C} : \Phi(z;a) = 0\}$ are well defined independently of the choice of determination and they are invariant under the reflection $z \mapsto -z$.*
- **(3)** *As $a \to \infty$ (i.e. $x \to \infty$) there are two smooth branches of the level set $\{z : \Phi(z;a) = 0\}$ that connect $\pm ia$, symmetric under $z \mapsto -z$.*

Proof. **(1)** Changing sign in front of $\sqrt{z^2+a^2}$ and taking then the real part gives the opposite sign overall; for this one must notice that

$$\left(\frac{z+\sqrt{z^2+a^2}}{ia}\right)\left(\frac{z-\sqrt{z^2+a^2}}{ia}\right) = \frac{z^2-z^2-a^2}{-a^2} = 1. \tag{3.26}$$

(2) This follows immediately from **(1)** and inspection for the symmetry.
(3) From the expression (3.25) it is clear that $\Phi(ia;a) = 0$ and so ia belongs to the zero level set. To show that there is a smooth branch as claimed for large a rescale $z \mapsto a\,z$ and send $a \to \infty$; this maps $\pm ia$ to $\pm i$ (and of course $\infty \to \infty$). The claim thus reduces to verifying that $\pm i$ belong to the boundary of a punctured disk domain with ∞ at its center. We obtain

$$\varphi(az;a) \underset{a\to+\infty}{\longrightarrow} Q(z) \equiv -2\ln\left(\frac{z+\sqrt{1+z^2}}{i}\right) + \frac{2}{z}\sqrt{z^2+1} = -2\int_i^z \sqrt{1+\lambda^2}\,\frac{\mathrm{d}\lambda}{\lambda^2} \tag{3.27}$$

and the limit is easily seen to be uniform in any compact set of the Riemann sphere not containing $z = 0$ (which is sufficient for us because we want to discuss the topology of level sets that avoid zero). It is straightforward to verify that the sign of $\Re Q(z)$ behaves like that of $\Re z^{-1}$ near $z = 0$ and hence changes only twice around a loop. Thus at most one trajectory from each $\pm i$ connects to zero. The other two must connect the two branch points together (they cannot escape to infinity and do not connect to zero). This proves that, for $x \to +\infty$, there is a connecting trajectory (in fact, two by symmetry) between $\pm ia$. Thus $\pm ia$ belong to ∂K_∞ and the condition is verified. □

We now address the position of $\mathcal{B} = \mathcal{B}(a)$; let $a > 0$ and sufficiently large so that Proposition 3.5 applies. We claim that the correct choice is the branch of $\Phi(z) = 0$ that intersects $\mathbb{R}_+$ (whose existence is guaranteed by point **(3)** of Proposition 3.5); then this choice fixes, by deformation, the cut for all $x \notin \Delta$. To see this, consider the behavior of $y(z)$ on $z \in \mathbb{R}_+$: the behavior near $z = 0$ must be $y(z) \sim -\frac{1}{2}\theta_z(z;x) \sim \frac{1}{2z^4}$ and thus must tend to $+\infty$ for $z \downarrow 0$, which requires that $\sqrt{z^2+a^2} \sim -a$ for $z \to 0$. On the other hand near $z = \infty$ we must have $y(z) \sim \frac{1}{z}$ which means that $\sqrt{z^2+a^2} \sim z$. Therefore the determination of the root in (3.22) must change as we move from $z = +\infty$ to $z = 0_+$ and thus the proper placement of the cut must be the one that intersects $\mathbb{R}_+$.

Remark 3.6. *As a consequence of this choice for the cut we have that* $\sqrt{z^2+a^2} \sim -a$ *in the region* $D_0 = Int(\mathcal{B} \cup -\mathcal{B})$ *(the interior of the Jordan curve* $\mathcal{B} \cup (-\mathcal{B})$*). Thus, in particular the evaluation of* $\sqrt{z^2+a^2}$ *at* $z = \pm z_0$ *gives* $-\sqrt{\frac{1}{2a}+a^2}$ *where this last expression is meant to behave as* $-a$ *for large* a*, i.e. the root is principal and positive for* $a > 0$*. The cuts of this last expression are chosen as three segments that run from each of the roots of* $2a^3 = -1$ *to* $a = 0$*.*

Equation for the boundary of Δ. Following the discussion of Sect. 3.2 the boundary $\partial\Delta$ of the star shaped region $\overline{\Delta}$ as introduced in Definition 1.3 are determined by the condition that the real part $\Phi(z)$ of $\varphi(z)$ at one of the saddle-points vanishes, i.e.

$$\Phi(z)\Big|_{z=\pm\frac{1}{\sqrt{2a}}} = \pm\Re\left\{-2\ln\left(\frac{\frac{1}{\sqrt{2a}} - \sqrt{\frac{1}{2a}+a^2}}{ia}\right) - \sqrt{2a}\sqrt{\frac{1}{2a}+a^2}\left(\frac{4a^3-1}{3a^3}\right)\right\} = 0. \tag{3.28}$$

Here[3] the determination of signs in front of the roots follows from Remark 3.6. In particular, if x_{cr} belongs to the set (3.28), then the normal direction in the x–plane is

$$\nabla_x\Phi(z_0) = -\overline{\frac{2\sqrt{\frac{1}{2a}+a^2}}{\sqrt{2a}}} = -2\overline{z_0\sqrt{z_0^2+a^2}} \tag{3.29}$$

where the complex number on the right side is to be interpreted as a 2D vector as usual. Notice that the only branch points of the cubic equation (1.16) are given by the three points

$$x_k = -\left(\frac{3}{\sqrt[3]{2}}\right)e^{\frac{2\pi i}{3}k}, \qquad k = 0,1,2 \tag{3.30}$$

or equivalently, these points (in the complex x-plane) correspond (via (1.16)) to the critical situation (in the complex z-plane) when the branch points $z = \pm ia$ collide with one of the saddle points $z = \pm\frac{1}{\sqrt{2a}}$.

Remark 3.7. *At the saddle point* $-z_0 = -\frac{1}{\sqrt{2a}}$ *of* $\Phi(z)$ *the directions of ascent in the* z*–plane are given by*

$$\sqrt{\varphi_{zz}(-z_0)} = \pm 2i\overline{\left(\frac{1}{z_0^3}\sqrt{z_0^2+a^2}\right)}^{\frac{1}{2}} = \pm 2i\overline{\left((2a)^{\frac{3}{2}}\sqrt{\frac{1}{2a}+a^2}\right)}^{\frac{1}{2}} \tag{3.31}$$

with the root $\sqrt{\frac{1}{2a}+a^2}$ *to be intended as principal for* $a > 0$ *(and continuation thereof for other values of* a*). In particular, for* $a > 0$ *and large we have* $\Phi(-z_0) > 0$ *and the directions of ascent are in the imaginary direction. This remains true also at the boundary of* Δ*, which is where* $\Phi(-z_0) = 0$*.*

Remark 3.8. *In* [3] *(equations (3-3),(3-5) and (3-22)), the conditions for the boundary edges in the complex* ξ*-plane are stated as*

$$\begin{aligned}\Re\left\{-\ln\left(-S+\sqrt{\frac{3S^3-4}{3S}}\right)+\sqrt{\frac{3S^3-4}{3S}}\frac{\xi}{3}+\ln\left(\frac{2}{\sqrt{3S}}\right)\right\} &= 0\\ 3S^3+4\xi S+8 &= 0\end{aligned}$$

and the latter system, under the identifications

$$\xi = \left(\frac{3}{2}\right)^{\frac{1}{3}}x, \qquad S = -\left(\frac{2}{3}\right)^{\frac{1}{3}}\frac{1}{a},$$

is identical to (3.28),(1.16). Hence the star shaped region of Figure 1 is, up to a rescaling, identical to the one shown in Figure 16 in [3].

[3] We use that $\frac{1}{a}\left(\frac{1}{\sqrt{2a}} - \sqrt{\frac{1}{2a}+a^2}\right) = \left(\frac{1}{a}\left(-\frac{1}{\sqrt{2a}} - \sqrt{\frac{1}{2a}+a^2}\right)\right)^{-1}$, which explains the $\pm$ in front of the $\Re$.

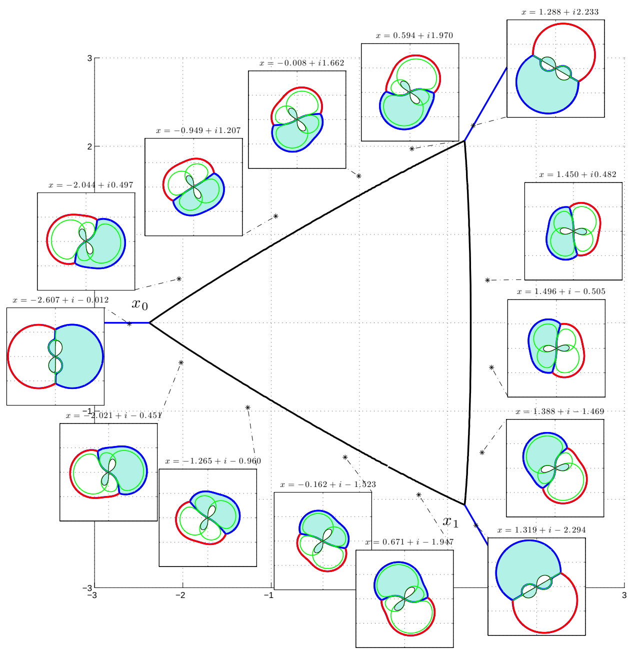

FIGURE 4. We plot the branch cut $\mathcal{B}$ in red for several choices $x \in \mathbb{C} : \mathrm{dist}(x, \overline{\Delta}) \geq \delta > 0$. The level sets $\Phi(z) = \Re\varphi(z) = 0$ are shown as solid blue lines and the shaded regions indicate were $\Phi(z) > 0$. In the white regions we have $\Phi(z) < 0$ and along the green lines $\Phi(z) \equiv \Phi(\pm(2a)^{-\frac{1}{2}})$.

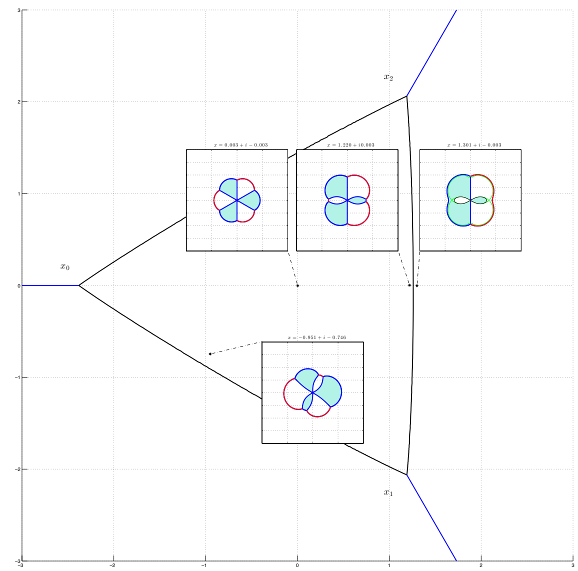

FIGURE 5. We plot the branch cut $\mathcal{B}$ in red for several choices $x \in \mathbb{C} : \mathrm{dist}(x, \mathbb{C}\backslash\overline{\Delta}) \geq \delta > 0$. The level sets $\Phi(z) = 0$ are shown as solid blue lines and the shaded regions indicate were $\Phi(z) > 0$. In the white regions we have $\Phi(z) < 0$.

We finish our discussion of the genus zero case by depicting the branch cut $\mathcal{B}$ and various sign properties of $\varphi(z)$: To this end assume that $x \in \mathbb{C} : \mathrm{dist}(x, \overline{\Delta} = \Delta \cup \partial\Delta) \geq \delta > 0$, i.e. x is chosen from the unbounded domain and we stay away from the edges and vertices. In Figure 4 the branch cut $\mathcal{B}$ is indicated in red for several choices $x \in \mathbb{C} : \mathrm{dist}(x, \overline{\Delta}) \geq \delta > 0$ in the complex z-plane. The orientation is such that the $(-)$ side extends to the unbounded component.

3.4. **The concrete g-function for genus two.** In this case we have $P_6(z; x) \equiv R(z) = \prod_{k=1}^{6}(z - a_k)$ where $a_j \neq a_k$ for $j \neq k$. This means we are working with the hyperelliptic curve

$$X = \big\{(z, w) : \; w^2 = R(z)\big\}; \qquad \mathcal{B} = \bigcup_{k=1}^{3}[a_{2k-1}, a_{2k}] \tag{3.32}$$

for which we use the representation as two-sheeted covering of the Riemann sphere $\mathbb{CP}^1$, obtained by gluing together two copies of $\mathbb{C}\backslash\mathcal{B}$ along $\mathcal{B}$ in the standard way. For future purposes, we let $\sqrt{R(z)} \sim z^3$ as $z \to \infty^+$ on the first sheet, and $\sqrt{R(z)} \sim -z^3$ as $z \to \infty^-$ on the second sheet. As our subsequent analysis shows, we can consider the symmetric choice

$$y(z) = \frac{\sqrt{R(z)}}{z^4}, \qquad z \in \mathbb{C}\backslash\mathcal{B} \qquad a_1 = ia, \quad a_2 = ib, \quad a_3 = ic; \qquad a_{k+3} = -a_k, \quad k = 1, 2, 3. \tag{3.33}$$

Here, the points $a = a(x), b = b(x), c = c(x) \in \mathbb{C}$ are partially determined from (3.16), i.e. they satisfy

$$J_3 \equiv a^2b^2c^2 = \frac{1}{4}, \qquad J_2 \equiv a^2b^2 + a^2c^2 + b^2c^2 = -\frac{x}{2} \tag{3.34}$$

so that

$$R(z) = z^6 + z^4 J_1 - z^2 \left(\frac{x}{2}\right) + \frac{1}{4}\,, \qquad J_1 \equiv a^2 + b^2 + c^2. \tag{3.35}$$

Together with the algebraic equations (3.34) we require that

$$\Re\left(\oint_{\mathcal{A}_1} \mathrm{d}\varphi\right) = 0, \qquad \Re\left(\oint_{\mathcal{B}_1} \mathrm{d}\varphi\right) = 0. \tag{3.36}$$

which provides two additional (real) equations which, together with (3.34), determine implicitly J_1. These conditions guarantee one of the requirements for $\varphi(z)$, that is, that analytic continuation along a closed curve in $\mathbb{C}\backslash\mathcal{B}$ yields the same function up to imaginary additive constant. The corresponding g function is then given by

$$g(z) = \frac{1}{2}\theta(z;x) + \int_{a_1}^{z} y(\lambda)\mathrm{d}\lambda + \frac{\ell}{2}, \qquad z \in \mathbb{C}\backslash\mathcal{B} \tag{3.37}$$

with the Lagrange multiplier equal to

$$\ell = 2\ln a_1 - 2\int_{a_1}^{\infty^+} \left(y(\lambda) - \frac{1}{\lambda}\right)\mathrm{d}\lambda. \tag{3.38}$$

Proposition 3.9. *For $x = 0$ the solution to the system (3.34),(3.36) is given by*

$$a_{1,0} = ia_0 = \frac{1}{\sqrt[3]{2}}e^{-i\frac{5\pi}{6}}, \qquad a_{2,0} = ib_0 = \frac{1}{\sqrt[3]{2}}e^{i\frac{5\pi}{6}}, \qquad a_{3,0} = ic_0 = \frac{1}{\sqrt[3]{2}}e^{i\frac{\pi}{2}},$$

namely the vertices of a hexagon and we have that $R(z) = z^6 + \frac{1}{4}$.

Proof. **Boutroux condition.** The integral between branch points is computed explicitly

$$\Re\left(\int_{a_{j,0}}^{a_{j+1,0}} \sqrt{R(z)}\,\frac{\mathrm{d}z}{z^4}\right) = \Re\left(-\frac{\sqrt{R(z)}}{3z^3} + \frac{1}{3}\ln\left(2z^3 + 2\sqrt{R(z)}\right)\right)\Bigg|_{z=a_{j,0}}^{a_{j+1,0}} = \Re\left(\ln z\Big|_{z=a_{j,0}}^{a_{j+1,0}}\right) = 0\ .$$

Connectedness of the level curves. First of all, the set $\{z \in \mathbb{C}\backslash\{0\} :\ \Phi(z) = 0\}$ consists of one connected component alone; this is so because there are no saddle points and if there were two or more connected components, there would have to be a saddle point in the region bounded by them. We shall now verify that the level curves satisfy the conditions specified in Section 3.2. The critical trajectories must

(1) connect all six branch points
(2) obey the $\mathbb{Z}_6$ symmetry because of obvious symmetry.

A simple counting then shows that the only possibility is that exactly one trajectory from each branch point (in fact a straight segment) connects the branch points to 0 because the sign of $\Phi(z)$ changes six times around a small circle surrounding the origin. The other two trajectories must then connect the branch points. This is depicted in the center of Figure 5. Then, the discussion on the condition for the correct inequalities of $\Phi(z)$ in genus two applies. ∎

The determination of the square root that we use has the property that $\sqrt{R(z)} \sim z^3$ for $z \to \infty$ and $\sqrt{R(z)} \sim \sqrt{a^2b^2c^2} = \frac{1}{2}$ for $z \to 0$.

3.4.1. *Modulation equations.* We use the terminology of [15]; the same idea was also used in [1]. Consider the derivative of $y(z;x)$ w.r.t. x; here we need to be careful because the dependence on x is not analytic (i.e. $y(z;x)$ depends on both x and $\bar{x}$). To be explicit, let $x = x(t)$ be a smooth curve parametrized by the parameter $t \in \mathbb{R}$; then

$$\dot{y}(z;x(t)) = \frac{\mathrm{d}}{\mathrm{d}t}y(z;x(t)) = \frac{z^2\gamma - \mathbf{n}}{4z^2\sqrt{R(z)}}\ , \quad \gamma \equiv 2\frac{\mathrm{d}}{\mathrm{d}t}J_1(a,b,c), \quad \mathbf{n} \equiv \frac{\mathrm{d}}{\mathrm{d}t}x(t). \tag{3.39}$$

We see that $\dot y(z;x)\mathrm{d}z$ must have zero residue at $z=\infty$, and, given the Boutroux condition (3.36), purely imaginary periods. The constant $\gamma(x)$ is thus completely determined by this requirement; it boils down to

$$\gamma(a,b,c) = \frac{\det\begin{bmatrix} 2\Re\oint_{\mathcal{A}_1}\frac{\mathbf{n}\,\mathrm{d}z}{z^2\sqrt{R(z)}} & \overline{\oint_{\mathcal{A}_1}\eta_1} \\ 2\Re\oint_{\mathcal{B}_1}\frac{\mathbf{n}\,\mathrm{d}z}{z^2\sqrt{R(z)}} & \overline{\oint_{\mathcal{B}_1}\eta_1}\end{bmatrix}}{2i\Im\left(\oint_{\mathcal{A}_1}\eta_1\overline{\oint_{\mathcal{B}_1}\eta_1}\right)}\ , \qquad \eta_1 \equiv \frac{\mathrm{d}z}{\sqrt{R(z)}}. \tag{3.40}$$

We now study the behavior of $\gamma(a,b,c)$ when two of its parameter collide, say $b,c\to iz_0$ with $z_0^2=\frac{1}{2a}$.

Lemma 3.10. *As $b^2\to -z_0^2$ and $c^2\to -z_0^2$ we have*

$$\gamma = \frac{\mathbf{n}}{z_0^2} - \rho_\epsilon \frac{8\epsilon z_0\sqrt{z_0^2+a^2}}{\ln|b-c|}(1+o(1)), \qquad \rho_\epsilon \equiv \Re\int_{ia}^{\epsilon z_0}\frac{\mathbf{n}\mathrm{d}z}{4z_0^2z^2\sqrt{z^2+a^2}}. \tag{3.41}$$

where[4] $\epsilon=\pm 1$.

Proof. We leave it to the reader to verify that ($\mathcal{A}_1$ is the contour surrounding ia, ib and being "pinched", and $\mathcal{B}_1$ is the contour surrounding $ib, ic\sim z_0$)

$$\oint_{A_1}\frac{\mathbf{n}\mathrm{d}z}{z^2\sqrt{R(z)}} = \frac{\mathbf{n}\ln(b-c)}{z_0^3\sqrt{z_0^2+a^2}} + C_1 + o(1)\ , \quad \oint_{A_1}\eta_1 = \frac{\ln(b-c)}{z_0\sqrt{z_0^2+a^2}} + C_2 + o(1),$$

and

$$\oint_{B_1}\frac{\mathbf{n}\mathrm{d}z}{z^2\sqrt{R(z)}} = \frac{2\pi i\,\mathbf{n}}{2z_0^3\sqrt{z_0^2+a^2}} + \mathcal{O}(b-c), \qquad \oint_{B_1}\eta_1 = \frac{2\pi i}{2z_0\sqrt{z_0^2+a^2}} + \mathcal{O}(b-c),$$

where the constants C_1, C_2 are not immediately important, although they could be computed. Plugging the latter expansions into the determinant formula (3.40) immediately yields

$$\gamma = \frac{\mathbf{n}}{z_0^2} + \frac{C_3}{\ln|b-c|}\big(1+o(1)\big), \quad b,c\to iz_0. \tag{3.42}$$

We now compute the constant C_3 by the following argument; the expression $\dot y(z,x(t))$ must have purely imaginary periods; inserting (3.42) yields

$$\dot y(z,x(t)) = \mathbf{n}\frac{z^2-z_0^2}{4z_0^2z^2\sqrt{R(z)}} + \frac{C_3}{4\ln|b-c|}\frac{1}{\sqrt{R(z)}}\big(1+o(1)\big).$$

Then we have, for $b-c\to 0$,

$$\begin{aligned}\int_{ia}^{z_0}\dot y(z,x(t))\mathrm{d}z &= \frac{\mathbf{n}}{4z_0^2}\int_{ia}^{z_0}\frac{\mathrm{d}z}{z^2\sqrt{z^2+a^2}} + \frac{C_3}{4\ln|b-c|}\frac{\ln(b-c)}{2z_0\sqrt{z_0^2+a^2}}\big(1+o(1)\big)\\ &= \frac{\mathbf{n}}{4z_0^2}\int_{ia}^{z_0}\frac{\mathrm{d}z}{z^2\sqrt{z^2+a^2}} + \frac{C_3}{8z_0\sqrt{z_0^2+a^2}} + o(1).\end{aligned}$$

The real part of this integral must be identically zero and thus

$$\Re\frac{C_3}{8z_0\sqrt{z_0^2+a^2}} = -\Re\frac{\mathbf{n}}{4z_0^2}\int_{ia}^{z_0}\frac{\mathrm{d}z}{z^2\sqrt{z^2+a^2}}.$$

On the other hand, taking a small loop around z_0 that includes ib, ic in the limit, we obtain

$$\oint\dot y(z,x(t))\mathrm{d}z = \frac{2\pi i\,C_3}{\ln|b-c|\,2z_0\sqrt{z_0^2+a^2}}\big(1+o(1)\big) + \mathcal{O}(b-c) \tag{3.43}$$

and since this must be purely imaginary as well, we conclude that $\frac{C_3}{2z_0\sqrt{z_0^2+a^2}}\in\mathbb{R}$. In other words we have

$$\gamma = \frac{\mathbf{n}}{z_0^2} - \frac{8z_0\sqrt{z_0^2+a^2}}{\ln|b-c|}\Re\int_{ia}^{z_0}\frac{\mathbf{n}\mathrm{d}z}{4z_0^2z^2\sqrt{z^2+a^2}}\big(1+o(1)\big). \tag{3.44}$$

[4] Although the writing (3.41) may seem to depend on ϵ, in fact it does not since the value of ρ_ϵ changes sign as well with ϵ.

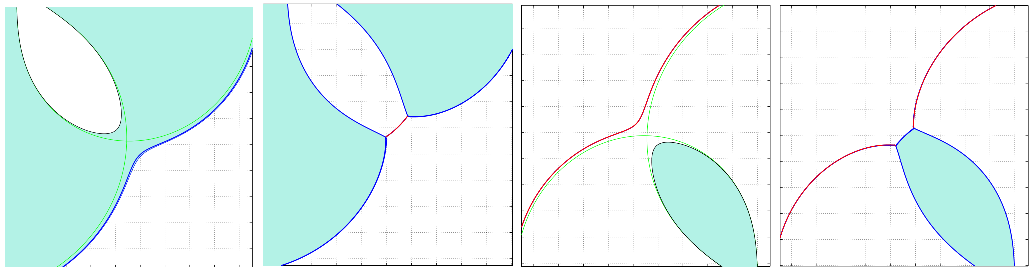

FIGURE 6. The transition as x traverses the discriminant from genus zero (pane 1) to genus two (pane 2). The direction of the split of the two branch points is along the direction of steepest ascent of $\Phi(z)$ at the saddle point $-z_0 = -\frac{1}{\sqrt{2a}}$ (panes 1-2) and z_0 (panes 3-4). The value of $\Phi(z)$ at the saddle point $-z_0$ decreases from the top left to the top right pane and symmetrically decreases from pane 3 to pane 4. As before, in the white region we have $\Phi(z) < 0$, opposed to that in the shaded ones, $\Phi(z) > 0$. Also we depict the branch cut $\mathcal{B}$ in red and along the green lines $\Phi(z) \equiv \Phi(\pm(2a)^{-\frac{1}{2}})$.

□

At this point we have the system of differential equations for the symmetric polynomials J_1, J_2, J_3 (3.34) in a^2, b^2, c^2

$$\begin{cases} \frac{\mathrm{d}}{\mathrm{d}t} J_1 = \frac{1}{2}\gamma(a^2, b^2, c^2) \\ \frac{\mathrm{d}}{\mathrm{d}t} J_2 = -\frac{\mathbf{n}}{2} \\ \frac{\mathrm{d}}{\mathrm{d}t} J_3 = 0 \end{cases} . \tag{3.45}$$

The integration of this system from an initial condition that satisfies the Boutroux condition (3.36), will preserve (by construction) that condition. The topology of the critical trajectories cannot change except when two or more of a, b, c coalesce and the properties of the effective potentials remain valid under deformation if they are obeyed at the initial point.

Direction of splitting of branch points. Let $x_{cr} \in \partial\Delta$ and $x = x(t) = x_{cr} + \mathbf{n}t$, for $t \in \mathbb{R}$ in a neighborhood of 0, with $|\mathbf{n}| = 1$. In [1] it was shown that the double roots $\pm z_0$ split each into two roots that behave as

$$z_{\pm}^{(+)} = z_0 \pm K^{(+)} \sqrt{\frac{t}{\ln|t|}} \big(1 + o(1)\big) \qquad z_{\pm}^{(-)} = -z_0 \pm K^{(-)} \sqrt{\frac{t}{\ln|t|}} \big(1 + o(1)\big) , \tag{3.46}$$

with $K^{(\pm)}$ a constant that we are going to compute now (giving us the direction of splitting): Using (3.45) we have by Taylor expansion that

$$\begin{aligned} R(z; x(t)) &= z^6 + z^4 \left(a_0^2 - 2z_0^2 + \frac{\mathbf{n}t}{2z_0^2} - t\rho_\epsilon \frac{4z_0\sqrt{z_0^2 + a_0^2}}{\ln|t|} + o\left(\frac{t}{\ln t}\right) \right) - \frac{z^2}{2}(x + \mathbf{n}t) + \frac{1}{4} \\ &= \left(z^2 + a_0^2 + \frac{\mathbf{n}ta_0^2}{2z_0^2(z_0^2 + a_0^2)} \right) \left(z^2 - z_0^2 - \frac{\mathbf{n}t}{4(z_0^2 + a_0^2)} \right)^2 - t\rho_\epsilon z^4 \frac{4z_0\sqrt{z_0^2 + a_0^2}}{\ln|t|} + \mathcal{O}(t^2). \end{aligned}$$

From this, we find that, the roots near ϵz_0 with $\epsilon = \pm 1$ behave as follows:

$$R(z; x(t)) = 0 \quad \Rightarrow \quad (z - \epsilon z_0)^2 4z_0^2(z_0^2 + a_0^2) = \epsilon t\rho_\epsilon \frac{4z_0^5\sqrt{z_0^2 + a_0^2}}{\ln|t|} \big(1 + o(1)\big),$$

$$z_{\pm} \sim \epsilon z_0 \pm \overbrace{\left(\rho_\epsilon \frac{\epsilon z_0^3}{\sqrt{z_0^2 + a_0^2}} \right)^{\frac{1}{2}}}^{K^{(\epsilon)}} \sqrt{\frac{t}{\ln|t|}} \tag{3.47}$$

Now note that with Lemma 3.10,

$$\rho_\epsilon = \Re \int_{ia}^{\epsilon z_0} \frac{\mathbf{n} \mathrm{d}z}{4z_0^2 z^2 \sqrt{z^2+a^2}} = -\frac{1}{2}\dot{\Phi}(z;x(t))\Big|_{z=\epsilon z_0} \tag{3.48}$$

where we used that

$$\dot{y}(z;x(t)) = \frac{\mathbf{n}}{4z_0^2 z^2 \sqrt{z^2+a^2}}.$$

Note that $K^{(+)} = K^{(-)}$ from their explicit expressions and the symmetry of Φ (which implies $\rho_- = -\rho_+$). We now focus on the saddle $-z_0 = -\frac{1}{\sqrt{2a}}$ which, according to our convention, is the saddle point that intersects the zero-level set of $\Phi(z)$ not on the branch cut (while z_0, by symmetry, is on $\mathcal{B}$). Thus, with $\epsilon = -1$, $\rho_- > 0$ means that the value of $\Phi(z)$ at $-z_0$ is *decreasing* and hence we are moving towards the genus two region, i.e. $\mathbf{n}$ points towards the inside of Δ. Hence, for $t > 0$ the two roots in (3.47) move in the direction of steepest ascent (3.31) as expected and depicted in panes 1-2 of Figure 6 , and the required properties for the effective potentials are preserved across the transition. Symmetrically, when $z_0 \in \mathcal{B}$ the first inequality for $\Phi(z)$ (see (3.16) and following) fails; a small gap must be created by allowing the saddle point z_0 to split into two new branch points (see panes 3-4 of Figure 6).

At this point we have enough information to move on to the next transformation in the nonlinear steepest descent analysis.

4. Riemann-Hilbert analysis - construction of parametrices

The g-functions derived in Subsections 3.3 and 3.4 are used to normalize the RHP for $\Gamma^o(z;x,n,n)$ in the spectral variable z at infinity, depending on whether x lies outside the star shaped region or inside. This eventually reduces the global solution of the RHPs to the construction of local model functions (parametrices) which are standard near the branch points.

4.1. Genus zero parametrices.

Let $x \in \mathbb{C} : \mathrm{dist}(x, \overline{\Delta}) \geq \delta > 0$, i.e. away from the edges and vertices of the star shaped region. Before we employ the g-function transformation, we first deform the original jump contour γ to a contour which passes through the branch points $\pm ia$, which on one side follows $\mathcal{B}$ and on the other side lies inside the shaded region and again connects the two branch points. We denote the latter part of the jump contour with $\mathcal{L}$, see Figure 7 below for one possible choice. Such a contour deformation is always possible since $w^o(z;x)$ is analytic away from the origin.

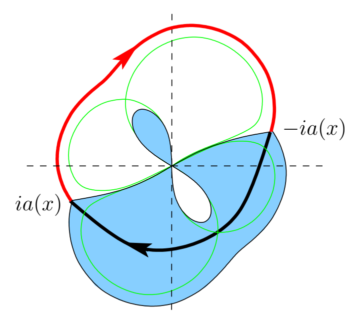

Figure 7. Deformation of the jump contour γ to the union of $\mathcal{B} \cup \mathcal{L}$. The branch cut $\mathcal{B}$ is indicated in red and $\mathcal{L}$ in black. The picture corresponds to one possible choice of $x \in \mathbb{C}$: $\mathrm{dist}(x, \overline{\Delta}) \geq \delta > 0$ with $\Re x < 0$ and $\Im x > 0$.

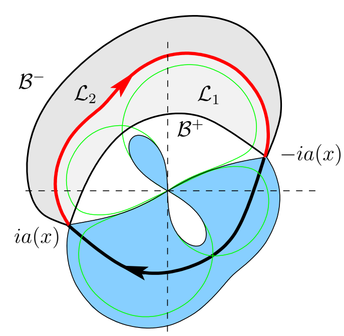

Figure 8. Opening of lenses in genus zero. The contours $\mathcal{B}^\pm$ are given the same orientation as $\mathcal{B}$.

Now introduce

$$Y(z)=\exp\left[-\frac{n\ell}{2}\sigma_3\right]\Gamma^o(z)\exp\left[-n\left(g(z)-\frac{\ell}{2}\right)\sigma_3\right],\qquad z\in\mathbb{C}\backslash\mathcal{B} \tag{4.1}$$

where $g(z)$ is given in (3.23) and the Lagrange multiplier in (3.24). Recalling (3.10) (here in genus zero case with $\alpha=0$) we are lead to the following RHP

- $Y(z)$ is analytic for $z\in\mathbb{C}\backslash(\mathcal{B}\cup\mathcal{L})$
- On the clockwise oriented contour $\mathcal{L}\cup\mathcal{B}$ as shown in Figure 7

$$\begin{aligned}Y_+(z)&=Y_-(z)\begin{bmatrix}e^{-n(g_+(z)-g_-(z))} & (2\pi iz)^{-1}\\ 0 & e^{n(g_+(z)-g_-(z))}\end{bmatrix},\qquad z\in\mathcal{B}\\ Y_+(z)&=Y_-(z)\begin{bmatrix}1 & (2\pi iz)^{-1}e^{-n\varphi(z)}\\ 0 & 1\end{bmatrix},\qquad z\in\mathcal{L}\end{aligned}$$

- As $z\to\infty$, we see from (3.11) that

$$Y(z)=I+\mathcal{O}\left(z^{-1}\right)$$

As we have $\Re\varphi(z)>0$ in the shaded regions around $\mathcal{B}$ (Figure 8, i.e. $\Re\varphi>0$ in the whole white region in Figure 7), one concludes

$$\begin{bmatrix}1 & (2\pi iz)^{-1}e^{-n\varphi(z)}\\ 0 & 1\end{bmatrix}\longrightarrow I,\qquad n\to\infty \tag{4.2}$$

where the convergence is exponentially fast for $z\in\mathcal{L}$ away from the branch points $z=\pm ia$. On the other hand

$$G(z)=g_+(z)-g_-(z),\qquad z\in\mathcal{B} \tag{4.3}$$

admits local analytical continuation into the bounded and unbounded white regions (compare Figure 7). In fact with (3.10) on the $(\mp)$ side

$$G(z)=\pm\left(\theta(z;x)-2g_{\mp}(z)+\ell\right)=\pm\varphi_{\mp}(z),\qquad z\in\mathcal{B}$$

These continuations allow us to factorize the jump on $\mathcal{B}$

$$\begin{aligned}\begin{bmatrix}e^{-nG(z)} & (2\pi iz)^{-1}\\ 0 & e^{nG(z)}\end{bmatrix}&=\begin{bmatrix}1 & 0\\ 2\pi ize^{n\varphi_-(z)} & 1\end{bmatrix}\begin{bmatrix}0 & (2\pi iz)^{-1}\\ -2\pi iz & 0\end{bmatrix}\begin{bmatrix}1 & 0\\ 2\pi ize^{n\varphi_+(z)} & 1\end{bmatrix}\\ &=S_{L_1}(z)S_P(z)S_{L_2}(z)\end{aligned}$$

and open lenses: We depicted the contours $\mathcal{B}^{\pm}$ in Figure 8 and introduce

$$S(z)=\begin{cases}Y(z)S_{L_1}(z), & z\in\mathcal{L}_1\\ Y(z)S_{L_2}^{-1}(z), & z\in\mathcal{L}_2\\ Y(z), & \text{else.}\end{cases} \tag{4.4}$$

This opening leads to jumps on the lens boundaries $\mathcal{B}^{\pm}$

$$S_+(z)=S_-(z)\begin{bmatrix}1 & 0\\ 2\pi ize^{n\varphi(z)} & 1\end{bmatrix},\qquad z\in\mathcal{B}^{\pm}$$

as well as on the contours $\mathcal{B}\cup\mathcal{L}$

$$S_+(z)=S_-(z)\begin{bmatrix}0 & (2\pi iz)^{-1}\\ -2\pi iz & 0\end{bmatrix},\quad z\in\mathcal{B};\qquad S_+(z)=S_-(z)\begin{bmatrix}1 & (2\pi iz)^{-1}e^{-n\varphi(z)}\\ 0 & 1\end{bmatrix},\quad z\in\mathcal{L}.$$

However $\Re\varphi(z)<0$ in the white regions, thus

$$\begin{bmatrix}1 & 0\\ 2\pi ize^{n\varphi(z)} & 1\end{bmatrix}\longrightarrow I,\qquad n\to\infty \tag{4.5}$$

again exponentially fast for $z\in\mathcal{B}^{\pm}$ away from the branch points $z=\pm ia$. The latter (4.5) combined with (4.2), we therefore have to focus on the local contributions arising from the contour $\mathcal{B}$ and the neighborhood of the branch points $z=\pm ia$.

Define the outer parametrix $M = M(z;x)$ as

$$M(z) = (2\pi i)^{-\frac{1}{2}\sigma_3}\left(\frac{a}{2}\right)^{-\frac{1}{2}\sigma_3}\big(\delta(z)\big)^{-\sigma_2}\mathcal{D}(z)^{\sigma_3}(2\pi i)^{\frac{1}{2}\sigma_3}, \qquad z\in\mathbb{C}\backslash\mathcal{B} \tag{4.6}$$

where the scalar Szegö function is given by

$$\mathcal{D}(z) = \exp\left[\frac{\sqrt{z^2+a^2}}{2\pi i}\int_{ia}^{-ia}\frac{\ln(w)}{\sqrt{w^2+a^2}_+}\frac{dw}{w-z}\right] = \sqrt{a}\left(\frac{\sqrt{z^2+a^2}-a}{\sqrt{z^2+a^2}+z}\right)^{\frac{1}{2}}$$

with principal branches for all fractional power functions and

$$\delta(z) = \left(\frac{z-ia}{z+ia}\right)^{\frac{1}{4}} \longrightarrow 1, \qquad z\to\infty$$

is analytic on $\mathbb{C}\backslash\mathcal{B}$. One checks readily that (4.6) is analytic on $\mathbb{C}\backslash\mathcal{B}$, square integrable up to the boundary and

$$M_+(z) = M_-(z)\begin{bmatrix}0 & (2\pi i z)^{-1}\\ -2\pi i z & 0\end{bmatrix}, \quad z\in\mathcal{B}; \qquad M(z)\longrightarrow I, \quad z\to\infty.$$

Hence the outer parametrix $M = M(z;x), z\in\mathbb{C}\backslash\mathcal{B}$ exists for all $x\in\mathbb{C}:\mathrm{dist}(x,\overline{\Delta})\geq\delta>0$.

The inner parametrices near the branch points are standard objects in the Deift-Zhou framework since they are constructed out of Airy-functions, see e.g. [8]. We briefly state the final formulae in this subsection and summarize other necessary details in Appendix A. All constructions are motivated from the local expansions

$$\varphi(z) = c_0(z-ia)^{\frac{3}{2}}\big(1+\mathcal{O}(z-ia)\big), \qquad z\to ia, \quad z\in\mathcal{B}^+\cup\mathcal{B}^- \tag{4.7}$$

$$\varphi(z) = -2\pi i + \hat{c}_0(z+ia)^{\frac{3}{2}}\big(1+\mathcal{O}(z+ia)\big), \qquad z\to -ia, \quad z\in\mathcal{B}^+\cup\mathcal{B}^- \tag{4.8}$$

where the function $(z+ia)^{\frac{3}{2}}$ is defined for $z\in\mathbb{C}\backslash(-\infty,-ia]$, i.e. with a branch cut to the left of $-ia$ and $(z-ia)^{\frac{3}{2}}$ for $z\in\mathbb{C}\backslash[ia,\infty)$, i.e. with a branch cut to the right of ia. Specifically the parametrix $U(z)$ near $z=-ia$ is given as

$$U(z) = B_U(z)\big(-i\sqrt{\pi}\big)A^{RH}\big(\zeta(z)\big)e^{\frac{2}{3}\zeta^{3/2}(z)\sigma_3}(2\pi i z)^{\frac{1}{2}\sigma_3}, \qquad |z+ia|<r \tag{4.9}$$

where $A^{RH}(\zeta)$ is defined in (A.2), we use the locally analytic (compare (4.8)) change of variables

$$\zeta(z) = \left(\frac{3N}{4}\right)^{\frac{2}{3}}\Big(-2g(z)+\theta(z;x)+\ell+2\pi i\Big)^{\frac{2}{3}}, \qquad |z+ia|<r$$

and the multiplier $B_U(z)$ equals

$$B_U(z) = M(z)(2\pi i z)^{-\frac{1}{2}\sigma_3}\begin{bmatrix}-i & i\\ 1 & 1\end{bmatrix}\zeta^{-\frac{1}{4}\sigma_3}(z).$$

By construction, $B_U(z)$ can have at worst a singularity of square root type at $z=-ia$, however for $z\in\mathcal{B}$ close to $z=-ia$,

$$\big(B_U(z)\big)_+ = M_-(z)\begin{bmatrix}0 & (2\pi i z)^{-1}\\ -2\pi i z & 0\end{bmatrix}(2\pi i z)^{-\frac{1}{2}\sigma_3}\begin{bmatrix}-i & i\\ 1 & 1\end{bmatrix}\zeta_-^{-\frac{1}{4}\sigma_3}(z)e^{-i\frac{\pi}{2}\sigma_3} = \big(B_r(z)\big)_-.$$

Thus the singularity has to be removable and $B_U(z)$ is in fact analytic in a neighborhood of $z=-ia$. We now easily check that the behavior of $A^{RH}(\zeta)$, see Figure 19, implies jumps as depicted in Figure 9 for $U(z)$. Here the jump contours can always be locally deformed to match the local contours in the S-RHP near the branch points.

Also, as $n\to\infty$ (hence $|\zeta|\to\infty$), the two model functions $M(z)$ and $U(z)$ satisfy the desired matching condition, i.e.

$$\begin{aligned} U(z) &= M(z)(2\pi i z)^{-\frac{1}{2}\sigma_3}\left\{I+\frac{1}{48\zeta^{3/2}}\begin{bmatrix}1 & 6i\\ 6i & -1\end{bmatrix}+\mathcal{O}\left(\zeta^{-6/2}\right)\right\}(2\pi i z)^{\frac{1}{2}\sigma_3}\\ &= \big(I+\mathcal{O}\left(n^{-1}\right)\big)M(z), \qquad n\to\infty \end{aligned} \tag{4.10}$$

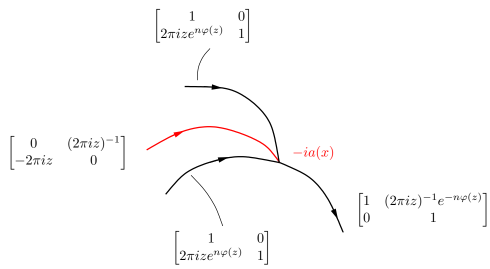

FIGURE 9. Jump behavior of $U(z)$ near $z = -ia$

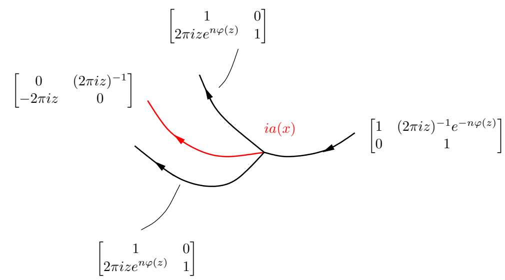

FIGURE 10. Jump behavior of $V(z)$ near $z = ia$

valid for $x \in \mathbb{C} : \operatorname{dist}(x, \overline{\Delta}) \geq \delta > 0$ and for all $z \in \mathbb{C}$ such that $0 < r_1 \leq |z + ia| \leq r_2 < \frac{\delta}{2}$.

The remaining parametrix near $z = ia$ is introduced along the same lines. We take

$$V(z) = B_V(z) i\sqrt{\pi}\tilde{A}^{RH}\big(\zeta(z)\big)e^{\frac{2}{3}i\zeta^{3/2}(z)\sigma_3}(2\pi i z)^{\frac{1}{2}\sigma_3}, \qquad |z - ia| < r \tag{4.11}$$

with the multiplier

$$B_V(z) = M(z)(2\pi i z)^{-\frac{1}{2}\sigma_3}\begin{bmatrix} -i & -i \\ 1 & -1 \end{bmatrix}\left(e^{-i\pi}\zeta(z)\right)^{\frac{1}{4}\sigma_3},$$

the change of variables

$$\zeta(z) = e^{i\pi}\left(\frac{3N}{4}\right)^{\frac{2}{3}}\Big(-2g(z) + \theta(z; x) + \ell\Big)^{\frac{2}{3}}, \qquad |z - ia| < r$$

and the function $\tilde{A}^{RH}$ is given in (A.4). Also here $B_V(z)$ is analytic near $z = ia$ since

$$\big(B_V(z)\big)_+ = M_-(z)\begin{bmatrix} 0 & (2\pi i z)^{-1} \\ -2\pi i z & 0 \end{bmatrix}(2\pi i z)^{-\frac{1}{2}\sigma_3}\begin{bmatrix} -i & -i \\ 1 & -1 \end{bmatrix}\left(e^{-i\pi}\zeta(z)\right)_-^{\frac{1}{4}\sigma_3}e^{-i\frac{\pi}{2}\sigma_3} = \big(B_V(z)\big)_-$$

but the singularity can be at worst of square root type. Thus $V(z)$ has jumps as in Figure 10 and we have the matching relation

$$\begin{aligned} V(z) &= M(z)(2\pi i z)^{-\frac{1}{2}\sigma_3}\left\{I + \frac{i}{48\zeta^{3/2}}\begin{bmatrix} -1 & 6i \\ 6i & 1 \end{bmatrix} + \mathcal{O}\left(\zeta^{-6/2}\right)\right\}(2\pi i z)^{\frac{1}{2}\sigma_3} \\ &= \left(I + \mathcal{O}\left(n^{-1}\right)\right)M(z), \qquad n \to \infty \end{aligned} \tag{4.12}$$

valid for $x \in \mathbb{C} : \operatorname{dist}(x, \overline{\Delta}) \geq \delta > 0$ and for all z such that $0 < r_1 \leq |z + ia| \leq r_2 < \frac{\delta}{2}$. This completes the construction of all relevant parametrices in the genus zero case.

4.2. **Genus two parametrices.** Let $x \in \mathbb{C} : \operatorname{dist}(x, \mathbb{C}\backslash\overline{\Delta}) \geq \delta > 0$ throughout, i.e. we are inside the star shaped region but stay away from the edges and vertices. Again, we first deform the original jump contour γ to a contour which passes through all branch points $z = a_j, j = 1, \ldots, 6$, which on one side follows along the branch cut $\mathcal{B}$ and on the other side lies inside the shaded region, see Figure 11 for a possible choice

We will denote the segments of the deformed contour as follows

1. The branch cuts $(a_{2j-1}, a_{2j}), j = 1, 2, 3$ whose union equals $\mathcal{B}$ are denoted by γ_j
2. The gaps $(a_{2j}, a_{2j+1}), j = 1, 2$ are denoted by ϵ_j
3. The gap (a_6, a_1) is denoted by ϵ_0

With these, the g-function transformation

$$Y(z) = \exp\left[-\frac{n\ell}{2}\sigma_3\right]\Gamma^o(z)\exp\left[-n\left(g(z) - \frac{\ell}{2}\right)\sigma_3\right], \qquad z \in \mathbb{C}\backslash\mathcal{B}$$

with (3.37) and (3.38) transforms the initial RHP to the following one

Riemann-Hilbert Problem 4.1. *Find a 2×2 matrix valued function $Y(z; x)$ such that*

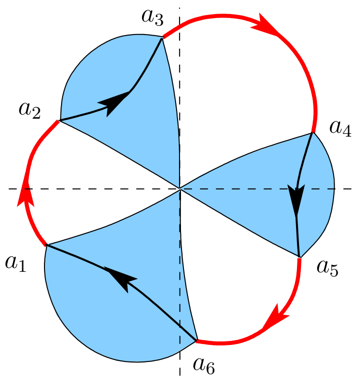

FIGURE 11. Deformation of the jump contour γ to the union of $\mathcal{B} \cup \mathcal{L}$. The branch cuts $\mathcal{B}$ are indicated in red and $\mathcal{L}$ in black. The picture corresponds to one possible choice of $x \in \mathbb{C} : \mathrm{dist}(x, \mathbb{C}\backslash\overline{\Delta}) \geq \delta > 0$ with $\Re x > 0, \Im x > 0$.

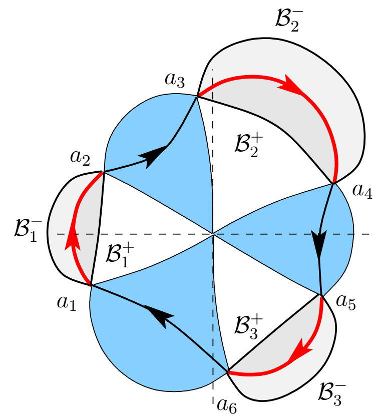

FIGURE 12. Opening of lenses in genus two. We give $\mathcal{B}_j^{\pm}$ the same orientation as γ_j.

- *$Y(z)$ is analytic for $z \in \mathbb{C}\backslash(\mathcal{B} \cup \mathcal{L})$*
- *We have jumps*

$$Y_+(z) = Y_-(z) \begin{bmatrix} e^{-nG(z)} & (2\pi i z)^{-1} e^{in\alpha_{j-1}} \\ 0 & e^{nG(z)} \end{bmatrix}, \qquad z \in \gamma_j,\ j = 1,2,3$$

$$Y_+(z) = Y_-(z) \begin{bmatrix} e^{-nG(z)} & (2\pi i z)^{-1} e^{-n\varphi(z)} \\ 0 & e^{nG(z)} \end{bmatrix}, \qquad z \in \epsilon_j,\ j = 0,1,2$$

where we use once more

$$G(z) = g_+(z) - g_-(z), \qquad z \in \mathcal{B} \cup \epsilon_0 \cup \epsilon_1 \cup \epsilon_2; \qquad G(z) = 0, \quad z \in \epsilon_0$$

and $\alpha_0 = 0, \alpha_1, \alpha_2 \in \mathbb{R}$
- *As $z \to \infty$,*

$$Y(z) = I + \mathcal{O}\left(z^{-1}\right)$$

Since in all shaded regions $\Re\varphi(z) > 0$, we obtain for the jump matrix $G_Y(z)$ in the latter problem

$$G_Y(z) e^{nG(z)\sigma_3} \longrightarrow I, \qquad z \in \epsilon_j,\ j = 1,2 \tag{4.13}$$

as $n \to \infty$ and the convergence is exponentially fast away from the branch points $z = a_j, j = 1, \ldots, 6$. In the white regions one uses again the analytical continuation of $G(z)$ combined with matrix factorizations. These techniques allow us to split the original contours $\gamma_1, \gamma_2, \gamma_3$ as shown in Figure 12. Without listing all formal steps, compare (4.4) in genus zero case, we are lead to a RHP for a function $S(z)$ with jumps

$$S_+(z) = S_-(z) \begin{bmatrix} 0 & (2\pi i z)^{-1} e^{in\alpha_{j-1}} \\ -2\pi i z e^{-in\alpha_{j-1}} & 0 \end{bmatrix}, \qquad z \in \gamma_j, \quad j = 1,2,3$$

on the branch cuts. The jumps on the corresponding lens boundaries are again exponentially close to the unit matrix in the limit $n \to \infty$, hence we need to focus on the construction of the parametrices.

In order to formulate the model RHP we neglect the entries in the jumps of $S(z)$ that are exponentially suppressed and use that $G(z) = g_+(z) - g_-(z)$ for $z \in \epsilon_j$ is piecewise constant

$$G(z) = -i\pi\Omega_j, \qquad j = 1,2.$$

We then are lead to the following model RHP

Riemann-Hilbert Problem 4.2. *Find a 2×2 matrix valued piecewise analytic function $M(z) = M(z;x)$ such that*

- *$M(z)$ is analytic for $z \in \mathbb{C}\backslash(\mathcal{B}\cup\epsilon_1\cup\epsilon_2)$*
- *The boundary values are connected via the jump relations*

$$\begin{aligned} M_+(z) &= M_-(z)\begin{bmatrix} 0 & (2\pi i z)^{-1}e^{in\alpha_{j-1}} \\ -2\pi i z e^{-in\alpha_{j-1}} & 0\end{bmatrix}, \qquad z\in\gamma_j, \quad j=1,2,3 \\ M_+(\lambda) &= M_-(\lambda)e^{in\pi\Omega_j\sigma_3}, \qquad z\in\epsilon_j, \quad j=1,2 \end{aligned}$$

- *$M(z)$ is square integrable at the branch points, more precisely for $j\in\{1,\dots,6\}$*

$$M(z) = \mathcal{O}\left(|z-a_j|^{-1/4}\right), \qquad z\to a_j,\ z\notin \mathcal{B}\cup\epsilon_1\cup\epsilon_2$$

- *We have the normalization*

$$M(z) = I + \mathcal{O}\left(z^{-1}\right), \qquad z\to\infty$$

In Figure 13 we depict schematically the jump matrices of the RHP 4.2. Next we introduce the cycles

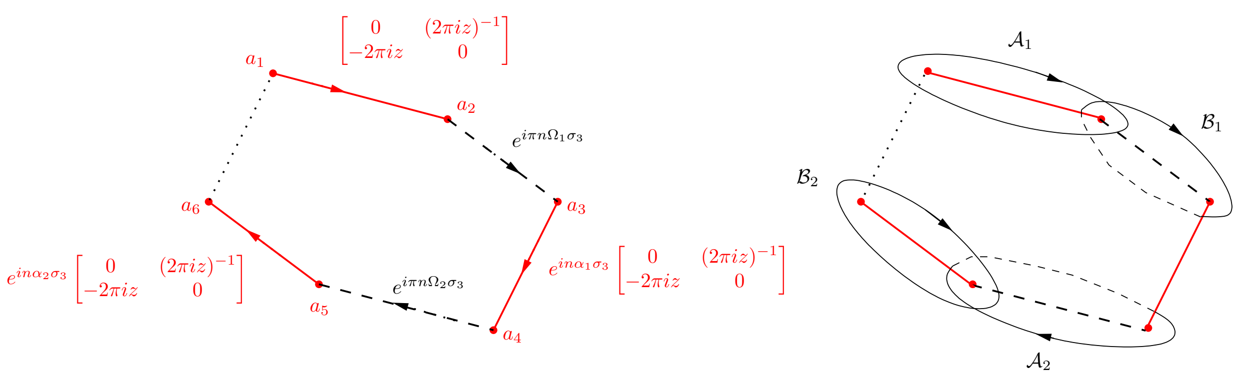

FIGURE 13. The jump contour for $M(z)$ on the left and on the right the homology basis for X

$\{\mathcal{A}_j,\mathcal{B}_j\}_{j=1}^2$ as indicated in the same Figure 13 on the right: these cycles form a homology basis for X (cf. [10]). The values of $\Omega_j = \frac{1}{i\pi}(g_+(z)-g_-(z)),\quad z\in\epsilon_j$ and $\alpha_{j-1} = \frac{1}{i}(g_+(z)+g_-(z)-\theta(z)-\ell),\quad z\in\gamma_j$ (cf. (3.10), (3.14)) can then be expressed in terms of the periods of the meromorphic differential $\mathrm{d}\phi = y(z)\mathrm{d}z$ as follows

$$\alpha_1 = \frac{1}{i}\oint_{\mathcal{B}_1}\mathrm{d}\phi,\quad \alpha_2 = \frac{1}{i}\left(\oint_{\mathcal{B}_1}\mathrm{d}\phi + \oint_{\mathcal{A}_2}\mathrm{d}\phi\right); \qquad \Omega_1 = \frac{1}{i\pi}\oint_{\mathcal{A}_1}\mathrm{d}\phi,\quad \Omega_2 = -\frac{1}{i\pi}\oint_{\mathcal{B}_2}\mathrm{d}\phi. \tag{4.14}$$

4.3. **Period matrices and normalized differentials.** We are now going to construct an explicit solution to the RHP 4.2 in terms of theta functions, however this requires some preparation. Recall the homology basis $\{\mathcal{A}_j,\mathcal{B}_j\}_{j=1}^2$ as shown in Figure 13 on the right. Introduce two holomorphic one forms on X and respective periods

$$\eta_1 = \frac{\mathrm{d}z}{\sqrt{R(z)}},\qquad \eta_2 = \frac{z\,\mathrm{d}z}{\sqrt{R(z)}}\ ;\qquad \mathbb{A}_{jk} = \oint_{\mathcal{A}_k}\eta_j,\qquad \mathbb{B}_{jk} = \oint_{\mathcal{B}_k}\eta_j. \tag{4.15}$$

Recalling the symmetry of the branch points $a_{k+3} = -a_k,\ k=1,2,3$ the reader verifies immediately that

$$\oint_{\mathcal{A}_1}\eta_1 = \oint_{\mathcal{A}_2}\eta_1,\qquad \oint_{\mathcal{B}_1}\eta_1 = \oint_{\mathcal{B}_2}\eta_1;\qquad \oint_{\mathcal{A}_1}\eta_2 = -\oint_{\mathcal{A}_2}\eta_2,\qquad \oint_{\mathcal{B}_1}\eta_2 = -\oint_{\mathcal{B}_2}\eta_2. \tag{4.16}$$

It is well-known (cf. [10]) that the A-period matrices $\mathbb{A} = [\mathbb{A}_{jk}]_{j,k=1}^2$, resp. B-period matrix $\mathbb{B} = [\mathbb{B}_{jk}]_{j,k=1}^2$ are non-singular, in particular from (4.16)

$$\mathbb{A} = \begin{bmatrix} \mathbb{A}_{11} & \mathbb{A}_{11} \\ -\mathbb{A}_{22} & \mathbb{A}_{22} \end{bmatrix}, \qquad \mathbb{A}_{jj} = \oint_{\mathcal{A}_j} \eta_j, \quad j = 1, 2.$$

This allows us to introduce the *normalized (first kind)* differentials $\{\omega_j\}_{j=1}^2$

$$\omega_1 = \frac{1}{2}\left(\frac{\eta_1}{\mathbb{A}_{11}} - \frac{\eta_2}{\mathbb{A}_{22}}\right), \qquad \omega_2 = \frac{1}{2}\left(\frac{\eta_1}{\mathbb{A}_{11}} + \frac{\eta_2}{\mathbb{A}_{22}}\right); \qquad \oint_{\mathcal{A}_k} \omega_j = \delta_{jk}, \qquad j, k = 1, 2. \tag{4.17}$$

The corresponding matrix of B-periods, $\boldsymbol{\tau} = [\tau_{jk}]_{j,k=1}^2$ with $\tau_{jk} = \oint_{\mathcal{B}_j} \omega_k$, is computed as

$$\boldsymbol{\tau} = \frac{1}{2}\begin{bmatrix} \varkappa_1 + \varkappa_2 & \varkappa_1 - \varkappa_2 \\ \varkappa_1 - \varkappa_2 & \varkappa_1 + \varkappa_2 \end{bmatrix}, \qquad \varkappa_j = \frac{1}{\mathbb{A}_{jj}} \oint_{\mathcal{B}_j} \eta_j = \frac{\mathbb{B}_{jj}}{\mathbb{A}_{jj}}, \quad j = 1, 2. \tag{4.18}$$

Finally we define the Abel map[5] by

$$\mathfrak{u} : \mathbb{CP}^1 \setminus (\mathcal{B} \cup \epsilon_1 \cup \epsilon_2) \to \mathbb{C}^2, \qquad z \mapsto \mathfrak{u}(z) = \int_{a_1}^{z} \vec{\omega}$$

where the integration contour is the same for both components and it is chosen in the simply connected domain $\mathbb{CP}^1 \setminus (\mathcal{B} \cup \epsilon_1 \cup \epsilon_2)$. We summarize the following properties

Proposition 4.3. *The Abelian integral* $\mathfrak{u}(z)$ *is single-valued and analytic in* $\mathbb{CP}^1 \setminus (\mathcal{B} \cup \epsilon_1 \cup \epsilon_2)$. *Moreover*

$$\mathfrak{u}_+(z) + \mathfrak{u}_-(z) = \begin{cases} 0, & z \in \gamma_1 \\ \boldsymbol{\tau}_1, & z \in \gamma_2 \\ \mathbf{e}_2 + \boldsymbol{\tau}_1, & z \in \gamma_3 \end{cases}, \qquad \mathfrak{u}_+(z) - \mathfrak{u}_-(z) = \begin{cases} 0, & z \in \epsilon_0 \\ \mathbf{e}_1, & z \in \epsilon_1 \\ -\boldsymbol{\tau}_2, & z \in \epsilon_2 \end{cases}$$

where $\mathbf{e}_j$ *denotes again the standard basis vector in* $\mathbb{C}^2$ *and* $\boldsymbol{\tau}_j = \boldsymbol{\tau}\mathbf{e}_j$. *Also* $\mathfrak{u}(a_1) = 0$ *and*

$$\mathfrak{u}(a_2) = \frac{1}{2}\mathbf{e}_1, \quad \mathfrak{u}(a_3) = \frac{1}{2}(\mathbf{e}_1 + \boldsymbol{\tau}_1), \quad \mathfrak{u}(a_4) = \frac{1}{2}(\boldsymbol{\tau}_1 - \boldsymbol{\tau}_2), \quad \mathfrak{u}(a_5) = \frac{1}{2}(\boldsymbol{\tau}_1 - \boldsymbol{\tau}_2 + \mathbf{e}_2), \quad \mathfrak{u}(a_6) = \frac{1}{2}(\boldsymbol{\tau}_1 + \mathbf{e}_2)$$

where all values are taken from the $(+)$ *side.*

4.4. **Szegö function.** Next we define a scalar Szegö function $\mathcal{D}(z)$ for $z \in \mathbb{CP}^1 \setminus (\mathcal{B} \cup \epsilon_1 \cup \epsilon_2)$

$$\mathcal{D}(z) = \exp\left[\frac{\sqrt{R(z)}}{2\pi i}\left\{\sum_{j=1}^{3} \int_{a_{2j-1}}^{a_{2j}} \frac{\ln w}{\sqrt{R(w)}_+} \frac{\mathrm{d}w}{w - z} - \sum_{j=1}^{2} \int_{a_{2j}}^{a_{2j+1}} \frac{i\pi\delta_j}{\sqrt{R(w)}_+} \frac{\mathrm{d}w}{w - z}\right\}\right] \tag{4.19}$$

where

$$\vec{\delta} = (\delta_1, \delta_2)^t = 2\big[\boldsymbol{\tau}_1, \mathbf{e}_2\big]^{-1}\big(\mathfrak{u}(\infty) - \mathfrak{u}(0)\big). \tag{4.20}$$

One checks directly that $\mathcal{D}(z)$ has the following analytical properties

- $\mathcal{D}(z)$ is analytic for $z \in \mathbb{C} \setminus ([a_1, a_2] \cup [a_2, a_3] \cup [a_3, a_4] \cup [a_4, a_5] \cup [a_5, a_6])$
- The following jumps hold, with orientation as indicated in Figure 13

$$\mathcal{D}_+(z)\mathcal{D}_-(z) = z, \qquad z \in \gamma_j, \quad j = 1, 2, 3$$
$$\mathcal{D}_+(z) = \mathcal{D}_-(z)e^{-i\pi\delta_j}, \qquad \lambda \in \epsilon_j, \quad j = 1, 2$$

- The function is bounded at infinity thanks to the following identities

$$\sum_{j=1}^{2} \int_{a_{2j}}^{a_{2j+1}} \frac{w^{k-1} i\delta_j}{\sqrt{R(w)}_+} \mathrm{d}w = \sum_{j=1}^{3} \int_{a_{2j-1}}^{a_{2j}} \frac{w^{k-1}}{\sqrt{R(w)}_+} \ln(w)\mathrm{d}w = i\pi \int_0^{\infty} \frac{w^{k-1}}{\sqrt{R(w)}} \mathrm{d}w, \quad k = 1, 2,$$

  which we can rewrite as a system

$$\left(\delta_1 \int_{a_2}^{a_3} + \delta_2 \int_{a_4}^{a_5}\right) \begin{bmatrix} 1 \\ w \end{bmatrix} \frac{\mathrm{d}w}{\sqrt{R(w)}_+} = \frac{1}{2}\left(\delta_1 \oint_{\mathcal{B}_1} + \delta_2 \oint_{\mathcal{A}_2}\right) \begin{bmatrix} 1 \\ w \end{bmatrix} \frac{\mathrm{d}w}{\sqrt{R(w)}} = \int_0^{\infty} \begin{bmatrix} 1 \\ w \end{bmatrix} \frac{\mathrm{d}w}{\sqrt{R(w)}}.$$

[5]To be precise, we are defining the Abel map only of one sheet of the Riemann surface. In the present setting, the Abel map of the other sheet is obtained by simply changing the overall sign $\mathfrak{u}(z) \mapsto -\mathfrak{u}(z)$.

Indeed, multiplying the above by $\mathbb{A}^{-1}$ we obtain

$$\delta_1 \oint_{\mathcal{B}_1} \vec{\omega} + \delta_2 \oint_{\mathcal{A}_2} \vec{\omega} = 2\int_0^{\infty} \vec{\omega} = 2\big(\mathfrak{u}(\infty) - \mathfrak{u}(0)\big)$$

and therefore

$$\delta_1 \boldsymbol{\tau}_1 + \delta_2 \mathbf{e}_2 = \big[\boldsymbol{\tau}_1, \mathbf{e}_2\big]\vec{\delta} = 2\big(\mathfrak{u}(\infty) - \mathfrak{u}(0)\big) \tag{4.21}$$

where $\mathbf{e}_j$ denotes the standard basis vector in $\mathbb{C}^2$ and $\boldsymbol{\tau}_j = \boldsymbol{\tau}\mathbf{e}_j$. Hence (4.20) ensures the required normalization $\mathcal{D}(\infty) < \infty$.

4.5. **Intermediate Step.** Keeping the properties of $\mathcal{D}(z)$ in mind, introduce

$$\Psi(z) = e^{i\frac{\pi}{4}\sigma_3}(2\pi i)^{\frac{1}{2}\sigma_3}\big(\mathcal{D}(\infty)\big)^{\sigma_3} M(z)\big(\mathcal{D}(z)\big)^{-\sigma_3}(2\pi i)^{-\frac{1}{2}\sigma_3} e^{-i\frac{\pi}{4}\sigma_3}, \qquad z \in \mathbb{C}\backslash(\mathcal{B}\cup\epsilon_1\cup\epsilon_2)$$

and obtain the following RHP with the jumps schematically depicted in Figure 14.

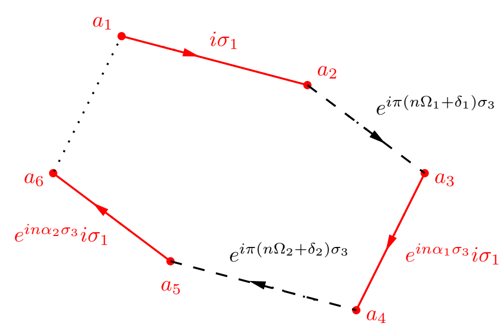

FIGURE 14. The jump contour for $\Psi(z)$.

Riemann-Hilbert Problem 4.4. *Find the 2×2 matrix valued function $\Psi(z)$ such that*

- $\Psi(z)$ *is analytic for* $z \in \mathbb{CP}^1\backslash(\mathcal{B}\cup\epsilon_1\cup\epsilon_2)$
- *The jumps are as follows*

$$\begin{aligned}\Psi_+(z) &= \Psi_-(z)e^{i\pi d_j\sigma_3} i\sigma_1, \qquad z\in\gamma_j, \quad j=0,1,2\\ \Psi_+(z) &= \Psi_-(z)e^{i\pi c_j\sigma_3}, \qquad z\in\epsilon_j, \quad j=1,2\end{aligned}$$

where we introduced the abbreviations

$$c_j = n\Omega_j + \delta_j, \quad j=1,2; \qquad d_j = \frac{n}{\pi}\alpha_j, \quad j=1,2; \qquad d_0 = 0 \tag{4.22}$$

- *As* $z\to\infty$,

$$\Psi(z) = I + \mathcal{O}\left(z^{-1}\right).$$

The construction of Ψ is the last step in the construction of $M(z)$. To this end we introduce the function

$$h(z) = \sqrt[4]{\frac{z-a_6}{\prod_1^5 (z-a_j)}}, \qquad z\in\mathbb{C}\backslash(\mathcal{B}\cup\epsilon_1\cup\epsilon_2)$$

with the branch fixed by the requirement $h(z) \sim \frac{1}{z}$ as $z\to\infty$. The boundary values of $h(z)$ satisfy

$$h_+(z) = h_-(z), \quad z\in\epsilon_0; \qquad h_+(z) = -h_-(z), \quad z\in\epsilon_1; \qquad h_+(z) = h_-(z), \quad z\in\epsilon_2 \tag{4.23}$$

$$h_+(z) = ih_-(z), \quad z\in\gamma_1; \qquad h_+(z) = -ih_-(z), \quad z\in\gamma_2; \qquad h_+(z) = ih_-(z), \quad z\in\gamma_3. \tag{4.24}$$

We now construct the solution to the model problem in terms of the Riemann theta function

$$\Theta(\vec{z}) \equiv \Theta(\vec{z}\,|\boldsymbol{\tau}) = \sum_{\vec{k}\in\mathbb{Z}^2} \exp\left[\pi\langle\vec{k}\boldsymbol{\tau},\vec{k}\rangle + 2\pi i\langle\vec{k},\vec{z}\rangle\right], \quad \vec{z}\in\mathbb{C}^2; \qquad \langle\vec{a},\vec{c}\rangle = \sum_{j=1}^{2} a_j c_j.$$

It is convenient also to introduce the *theta function with characteristics* $\vec{\boldsymbol{\alpha}},\vec{\boldsymbol{\beta}}\in\mathbb{C}^2$

$$\Theta\begin{bmatrix}\vec{\boldsymbol{\alpha}}\\ \vec{\boldsymbol{\beta}}\end{bmatrix}(\vec{z}\,|\boldsymbol{\tau})=\exp\left[2\pi i\left(\frac{1}{8}\langle\vec{\boldsymbol{\alpha}}\boldsymbol{\tau},\vec{\boldsymbol{\alpha}}\rangle+\frac{1}{2}\langle\vec{\boldsymbol{\alpha}},\vec{z}\,\rangle+\frac{1}{4}\langle\vec{\boldsymbol{\alpha}},\vec{\boldsymbol{\beta}}\,\rangle\right)\right]\Theta\left(\vec{z}+\frac{1}{2}\vec{\boldsymbol{\beta}}+\frac{1}{2}\boldsymbol{\tau}\vec{\boldsymbol{\alpha}}\,\middle|\,\boldsymbol{\tau}\right).$$

The reader will find in Appendix B all the main properties that are used below. Since we are dealing with a hyperelliptic Riemann surface X, the vector of Riemann constants $\mathcal{K}$ (cf. [10]) is given by

$$\mathcal{K}=\sum_{j=1}^{2}\mathfrak{u}(a_{2j+1})\equiv\frac{1}{2}(\mathbf{e}_1+\mathbf{e}_2-\boldsymbol{\tau}_2)\bmod\Lambda \tag{4.25}$$

where $\Lambda=\mathbb{Z}^2+\boldsymbol{\tau}\mathbb{Z}^2$ is the period lattice. Recall also (cf. [10]) that

$$\mathbf{f}^{(\pm)}(z)=\Theta\left(\mathfrak{u}(z)\mp\mathfrak{u}(\infty)-\mathfrak{u}(a_6)-\mathcal{K}\right) \tag{4.26}$$

does not vanish identically, since the divisor of the points $\infty^{\pm},a_6$ is nonspecial on the hyperelliptic Riemann surface X (compare again Appendix B for a short summary of the relevant theory). This observation allows us to introduce the functions $P^{(\pm)}(z)=P^{(\pm)}(z;\vec{\boldsymbol{\alpha}},\vec{\boldsymbol{\beta}})$ with

$$P^{(\pm)}(z)=\left(\frac{\Theta\begin{bmatrix}\vec{\boldsymbol{\alpha}}\\ \vec{\boldsymbol{\beta}}\end{bmatrix}\big(\mathfrak{u}(z)\mp\mathfrak{u}(\infty)-\mathcal{K}\big)}{\Theta\big(\mathfrak{u}(z)\mp\mathfrak{u}(\infty)-\mathfrak{u}(a_6)-\mathcal{K}\big)},\frac{\Theta\begin{bmatrix}\vec{\boldsymbol{\alpha}}\\ \vec{\boldsymbol{\beta}}\end{bmatrix}\big(-\mathfrak{u}(z)\mp\mathfrak{u}(\infty)-\mathcal{K}\big)}{\Theta\big(-\mathfrak{u}(z)\mp\mathfrak{u}(\infty)-\mathfrak{u}(a_6)-\mathcal{K}\big)}\right)h(z)e^{i\pi u_1(z)\sigma_3}.$$

where we use $\mathfrak{u}(z)=\big(u_1(z),u_2(z)\big)^t$. The following Proposition is crucial in the construction of the outer parametrix.

Proposition 4.5. *Both functions, $P^{(+)}(z)$ and $P^{(-)}(z)$, are single-valued and analytic in $\mathbb{C}\backslash(\mathcal{B}\cup\epsilon_1\cup\epsilon_2)$ with*

$$\begin{aligned}
P_+^{(\pm)}(z)&=P_-^{(\pm)}(z)(i\sigma_1),\quad z\in\gamma_1\\
P_+^{(\pm)}(z)&=P_-^{(\pm)}(z)\exp\Big[i\pi\langle\vec{\boldsymbol{\alpha}},\mathbf{e}_1\rangle\sigma_3\Big],\quad z\in\epsilon_1\\
P_+^{(\pm)}(z)&=P_-^{(\pm)}(z)\exp\Big[i\pi\langle\mathbf{e}_1,\vec{\boldsymbol{\beta}}\rangle\sigma_3\Big](-i\sigma_1),\quad z\in\gamma_2\\
P_+^{(\pm)}(z)&=P_-^{(\pm)}(z)\exp\Big[i\pi\big(1+\langle\mathbf{e}_2,\vec{\boldsymbol{\beta}}\,\rangle\big)\sigma_3\Big],\quad z\in\epsilon_2\\
P_+^{(\pm)}(z)&=P_-^{(\pm)}(z)\exp\Big[-i\pi\big(\langle\vec{\boldsymbol{\alpha}},\mathbf{e}_2\rangle-\langle\mathbf{e}_1,\vec{\boldsymbol{\beta}}\,\rangle\big)\sigma_3\Big](i\sigma_1),\quad z\in\gamma_3.
\end{aligned}$$

Proof. As the Abelian integral $\mathfrak{u}(z)$ is single-valued and analytic on $\mathbb{C}\backslash(\mathcal{B}\cup\epsilon_1\cup\epsilon_2)$ and $\mathbf{f}^{(\pm)}(z)$ does not vanish identically, we first obtain (cf. [10]) that $P^{(\pm)}(z)$ is single-valued and meromorphic on $\mathbb{C}\backslash(\mathcal{B}\cup\epsilon_1\cup\epsilon_2)$. Moreover, general theory (see Theorem B.3) asserts, that $\mathbf{f}^{(+)}(z)$ has precisely two zeros on X, both on the first sheet at $z=\infty^+$ and at $z=a_6$. However $h(z)$ has zeros at the same points and its local behavior matches the vanishing behavior of $\mathbf{f}^{(+)}(z)$, hence we obtain analyticity of the first column in $P^{(\pm)}(z)$ for $z\in\mathbb{C}\backslash(\mathcal{B}\cup\epsilon_1\cup\epsilon_2)$. The second column can be treated similarly using the parity of the theta-function. The stated jumps follow now directly from Proposition 4.3 and (4.23),(4.24) using that

$$F(\vec{z}\,)=\frac{\Theta\begin{bmatrix}\vec{\boldsymbol{\alpha}}\\ \vec{\boldsymbol{\beta}}\end{bmatrix}\big(\vec{z}\mp\mathfrak{u}(\infty)-\mathcal{K}\,|\boldsymbol{\tau}\big)}{\Theta(\vec{z}\mp\mathfrak{u}(\infty)-\mathfrak{u}(a_6)-\mathcal{K}\,|\boldsymbol{\tau})}e^{i\pi\langle\vec{z},\mathbf{e}_1\rangle}$$

formally satisfies

$$F(\vec{z}+\vec{\mu}+\boldsymbol{\tau}\vec{\lambda}\,|\boldsymbol{\tau})=\exp\Big[i\pi\left(\langle\vec{\mu},\mathbf{e}_1\rangle-\langle\vec{\lambda},\mathbf{e}_2\rangle+\langle\vec{\boldsymbol{\alpha}},\vec{\mu}\,\rangle-\langle\vec{\lambda},\vec{\boldsymbol{\beta}}\,\rangle\right)\Big]F(\vec{z}\,),\qquad\vec{\mu},\vec{\lambda}\in\mathbb{Z}^2.$$

□

We now compare the jumps of $P^{(\pm)}(z)$ to the ones stated in Figure 14 for $\Psi(z)$. This in turn leads to the following system in $\mathbb{Z}/2\mathbb{Z}$ for the yet unknowns $\vec{\boldsymbol{\alpha}}, \vec{\boldsymbol{\beta}}$

$$\langle \vec{\boldsymbol{\alpha}}, \mathbf{e}_1 \rangle \equiv c_1, \qquad \langle \mathbf{e}_1, \vec{\boldsymbol{\beta}} \rangle + 1 \equiv d_1, \qquad \langle \mathbf{e}_2, \vec{\boldsymbol{\beta}} \rangle + 1 \equiv c_2, \qquad \langle \mathbf{e}_1, \vec{\boldsymbol{\beta}} \rangle - \langle \mathbf{e}_2, \vec{\boldsymbol{\alpha}} \rangle \equiv d_2$$

and we take as solution in $\mathbb{C}^2$

$$\vec{\boldsymbol{\alpha}} = \begin{bmatrix} c_1 \\ d_1 - d_2 - 1 \end{bmatrix}, \qquad \vec{\boldsymbol{\beta}} = \begin{bmatrix} d_1 + 1 \\ c_2 + 1 \end{bmatrix}. \tag{4.27}$$

With the latter choice (4.27) and $P^{(\pm)}(z) = \big(P_1^{(\pm)}(z), P_2^{(\pm)}(z)\big)$

Proposition 4.6. (1) *The function*

$$Q(z) = Q(z; \vec{\boldsymbol{\alpha}}, \vec{\boldsymbol{\beta}}) = \begin{bmatrix} P_1^{(+)}(z) & P_2^{(+)}(z) \\ P_1^{(-)}(z) & P_2^{(-)}(z) \end{bmatrix}, \qquad z \in \mathbb{C} \backslash (\mathcal{B} \cup \epsilon_1 \cup \epsilon_2) \tag{4.28}$$

with $\vec{\boldsymbol{\alpha}}, \vec{\boldsymbol{\beta}}$ as in (4.27) is single-valued and analytic in $\mathbb{C}\backslash(\mathcal{B} \cup \epsilon_1 \cup \epsilon_2)$. Its jump behavior is depicted in Figure 14. Moreover, as $z \to \infty$,

$$Q(z) = C_0 \sigma_3 e^{i\pi u_1(\infty)\sigma_3} \Theta \begin{bmatrix} \vec{\boldsymbol{\alpha}} \\ \vec{\boldsymbol{\beta}} \end{bmatrix} \big(-\mathcal{K}\big) \left\{ I + \frac{Q_1}{z} + \mathcal{O}\left(z^{-2}\right) \right\}, \quad Q_1 = \big(Q_1^{jk}\big)_{j,k=1}^2 \tag{4.29}$$

where

$$C_0^{-1} = \langle \nabla \Theta(-\mathfrak{u}(a_6) - \mathcal{K}) \mathbb{A}^{-1}, \mathbf{e}_2 \rangle \neq 0$$

and

$$Q_1^{21} = -\frac{C_0^{-1} e^{2\pi i u_1(\infty)}}{\Theta\big(2\mathfrak{u}(\infty) - \mathfrak{u}(a_6) - \mathcal{K}\big)} \frac{\Theta \begin{bmatrix} \vec{\boldsymbol{\alpha}} \\ \vec{\boldsymbol{\beta}} \end{bmatrix} \big(2\mathfrak{u}(\infty) - \mathcal{K}\big)}{\Theta \begin{bmatrix} \vec{\boldsymbol{\alpha}} \\ \vec{\boldsymbol{\beta}} \end{bmatrix} \big(-\mathcal{K}\big)} \tag{4.30}$$

(2) *As a function of the characteristics $\vec{\boldsymbol{\alpha}}, \vec{\boldsymbol{\beta}}$, the matrix $Q(z)$ is periodic*

$$Q(z; \vec{\boldsymbol{\alpha}}, \vec{\boldsymbol{\beta}}) = Q(z; \vec{\boldsymbol{\alpha}} + 2\vec{\nu}, \vec{\boldsymbol{\beta}} + 2\vec{\nu}'), \quad \forall \vec{\nu}, \vec{\nu}' \in \mathbb{Z}^2. \tag{4.31}$$

The property **(2)** in Proposition 4.6 follows from Proposition B.2. Note that the dependency on n is only in the linear dependency of the characteristics $\vec{\boldsymbol{\alpha}}, \vec{\boldsymbol{\beta}}$ (4.22). Collecting the results we have completed the construction of Ψ which we summarize hereafter for reference.

Corollary 4.7. (1) *The solution of the RHP 4.4 is given by*

$$\Psi(z) := Q^{-1}(\infty) Q(z) \tag{4.32}$$

with $Q(z)$ as in Prop. 4.6 and

$$Q(\infty) = C_0 \sigma_3 e^{i\pi u_1(\infty)\sigma_3} \Theta \begin{bmatrix} \vec{\boldsymbol{\alpha}} \\ \vec{\boldsymbol{\beta}} \end{bmatrix} \big(-\mathcal{K}\big) \tag{4.33}$$

and the solution exists if and only if $\Theta \begin{bmatrix} \vec{\boldsymbol{\alpha}} \\ \vec{\boldsymbol{\beta}} \end{bmatrix} \big(-\mathcal{K}\big) \neq 0$.

(2) *For each compact subset of its domain of analyticity in z, the entries of $\Psi(z)$ are uniformly bounded with respect to the characteristics in any closed subset of the domain*

$$\vec{\boldsymbol{\alpha}}, \vec{\boldsymbol{\beta}} \in \mathbb{R}^2 : \quad \left| \Theta \begin{bmatrix} \vec{\boldsymbol{\alpha}} \\ \vec{\boldsymbol{\beta}} \end{bmatrix} \big(-\mathcal{K}\big) \right| > 0 \tag{4.34}$$

Note that the condition (4.34) is well defined because the absolute value of the Theta function involved is a periodic function of the characteristics (compare with the second property in Prop. B.2). The condition (4.34) can be made more transparent in terms of the data of our problem (we use (4.25))

$$\Theta \begin{bmatrix} \vec{\boldsymbol{\alpha}} \\ \vec{\boldsymbol{\beta}} \end{bmatrix} \big(-\mathcal{K}\big) \propto \Theta \left(\frac{1}{2} \vec{\boldsymbol{\beta}} + \frac{1}{2} \boldsymbol{\tau} \vec{\boldsymbol{\alpha}} - \mathcal{K} \right)$$

where the proportionality is by a never-vanishing term. Replacing the expressions (4.22), (4.14), (4.18), (4.21) in the above formula yields

$$\frac{1}{2}\vec{\boldsymbol{\beta}} + \frac{1}{2}\boldsymbol{\tau}\vec{\boldsymbol{\alpha}} - \mathcal{K} = \frac{1}{2}\begin{bmatrix} d_1 \\ c_2 \end{bmatrix} + \frac{\boldsymbol{\tau}}{2}\begin{bmatrix} c_1 \\ d_1 - d_2 \end{bmatrix} = \frac{n}{2\pi i}\begin{bmatrix} 1 \\ -1 \end{bmatrix}\left(\oint_{\mathcal{B}_1} \mathrm{d}\phi + \varkappa_2 \oint_{\mathcal{A}_1} \mathrm{d}\phi\right) + \mathfrak{u}(\infty) - \mathfrak{u}(0).$$

We can further simplify the expression (all values are taken from the $(+)$ side of the branch cuts):

$$\begin{aligned} \mathfrak{u}(0) &\overset{(4.17)}{=} \frac{1}{2}\begin{bmatrix} 1 \\ 1 \end{bmatrix}\int_{a_1}^{0} \frac{\eta_1}{\mathbb{A}_{11}} - \frac{1}{2}\begin{bmatrix} 1 \\ -1 \end{bmatrix}\int_{a_1}^{0} \frac{\eta_2}{\mathbb{A}_{22}} = \frac{1}{2}\begin{bmatrix} 1 \\ 1 \end{bmatrix}\frac{\varkappa_1}{2} - \frac{1}{2}\begin{bmatrix} 1 \\ -1 \end{bmatrix}\int_{a_1}^{0} \frac{\eta_2}{\mathbb{A}_{22}} \\ &= -\frac{1}{2}\left(\int_{a_1}^{0} \frac{\eta_2}{\mathbb{A}_{22}} - \frac{\varkappa_2}{2}\right)\begin{bmatrix} 1 \\ -1 \end{bmatrix} - \mathcal{K} + \frac{1}{2}\begin{bmatrix} 1 \\ 1 \end{bmatrix}. \end{aligned}$$

Thus we get

$$\mathfrak{u}(\infty) - \mathfrak{u}(0) = \frac{1}{2}\left(\int_{a_1}^{0} \frac{\eta_2}{\mathbb{A}_{22}} + \frac{\varkappa_2}{2}\right)\begin{bmatrix} 1 \\ -1 \end{bmatrix} + \mathfrak{u}(\infty) + \mathcal{K} - \frac{1}{2}(\varkappa_2 + 1)\begin{bmatrix} 1 \\ -1 \end{bmatrix} - \mathbf{e}_2$$

which implies all together

$$\begin{aligned} \frac{1}{2}\vec{\boldsymbol{\beta}} + \frac{1}{2}\boldsymbol{\tau}\vec{\boldsymbol{\alpha}} - \mathcal{K} &= \rho_n\begin{bmatrix} 1 \\ -1 \end{bmatrix} + \mathfrak{u}(\infty) + \mathcal{K} - \frac{1}{2}(\varkappa_2 + 1)\begin{bmatrix} 1 \\ -1 \end{bmatrix} - \mathbf{e}_2; \\ \rho_n &= \frac{n}{2\pi i}\left(\oint_{\mathcal{B}_1} \mathrm{d}\phi + \varkappa_2 \oint_{\mathcal{A}_1} \mathrm{d}\phi\right) + \frac{1}{2}\left(\int_{a_1}^{0} \frac{\eta_2}{\mathbb{A}_{22}} + \frac{\varkappa_2}{2}\right). \end{aligned} \tag{4.35}$$

Thus the non-solvability condition of the RHP 4.4 can be written in any of the following equivalent forms

$$\Theta\left(\frac{n}{2\pi i}\left(\oint_{\mathcal{B}_1} + \varkappa_2 \oint_{\mathcal{A}_1}\right)\mathrm{d}\phi\begin{bmatrix} 1 \\ -1 \end{bmatrix} + \mathfrak{u}(\infty) - \mathfrak{u}(0)\right) \overset{(4.35)}{=} \Theta\left(\left(\rho_n - \frac{\varkappa_2 + 1}{2}\right)\begin{bmatrix} 1 \\ -1 \end{bmatrix} + \mathfrak{u}(\infty) + \mathcal{K}\right) = 0. \tag{4.36}$$

This in turn defines implicitly a discrete set $\mathcal{Z}_n = \{x_{n,k}\}$ of points inside the star shaped region $\overline{\Delta}$ which eventually shall be identified with the zero set of the Vorob'ev-Yablonski polynomial $\mathcal{Q}_n(x)$ for sufficiently large n (compare Corollary 1 on page 65 in [3] in the setting of the poles of rational PII solutions). From now on we stipulate to stay away from the points of $\mathcal{Z}_n$ (4.36). Once this additional constraint on $x \in \mathbb{C} : \mathrm{dist}(x, \mathbb{C}\backslash\overline{\Delta}) \geq \delta > 0$ is in place we complete the construction of the outer parametrix.

Proposition 4.8. *Let $x \notin \mathcal{Z}_n$ and $x \in \mathbb{C}\backslash\overline{\Delta}$; then the model problem for the outer parametrix $M(z) = M(z;x)$ depicted in 13 is solvable. The solution is given explicitly by*

$$M(z) = e^{-i\frac{\pi}{4}\sigma_3}(2\pi i)^{-\frac{1}{2}\sigma_3}\big(\mathcal{D}(\infty)\big)^{-\sigma_3}\Psi(z)\big(\mathcal{D}(z)\big)^{\sigma_3}(2\pi i)^{\frac{1}{2}\sigma_3}e^{i\frac{\pi}{4}\sigma_3}, \qquad z \in \mathbb{C}\backslash(\mathcal{D} \cup \epsilon_1 \cup \epsilon_2).$$

with $\mathcal{D}(z)$ as in (4.19) and $\Psi(z)$ as in Cor. 4.7. For any closed subset of the domain of analyticity in z the entries of $M(z)$ are uniformly bounded in any compact subsets of $(n,x) \in \mathbb{R} \times \Delta$ where (4.34) holds.

The remaining six local parametrices near the branch points are defined in the disks

$$D(a_j, r) = \{z \in \mathbb{C} \,|\, |z - a_j| < r\}, \qquad j = 1, \ldots, 6$$

with $r > 0$ sufficiently small. The construction follows the standard lines using again Airy functions and we will not give details here. We only list the relevant matching relations between parametrices $P_j(z)$ and the outer model function $M(z)$, in fact

$$P_j(z) = \left(I + \mathcal{O}\left(n^{-1}\right)\right) M(z), \qquad n \to \infty \tag{4.37}$$

which holds for $x \in \mathbb{C} : \mathrm{dist}(x, \mathbb{C}\backslash\overline{\Delta}) \geq \delta > 0$ away from the zero set $\mathcal{Z}_n$ and uniformly for $z \in \bigcup_{j=1}^{6} \partial D(a_j, r)$. This completes the construction of the parametrices in the genus two situation.

4.6. **Reduction to Jacobi theta function of genus 1.** We now show that the expression on the left hand side of (4.36) is expressible as a square of the ordinary Jacobi theta function

$$\vartheta(z) \equiv \vartheta(z|\varkappa_2) = \sum_{k\in\mathbb{Z}} \exp\left[i\pi k^2 \varkappa_2 + 2\pi i k z\right], \qquad \varkappa_2 = \frac{\mathbb{B}_{22}}{\mathbb{A}_{22}} = \frac{\oint_{\mathcal{B}_2} \eta_2}{\oint_{\mathcal{A}_2} \eta_2}. \tag{4.38}$$

Lemma 4.9. **(1)** *Let $\mathcal{K} = \frac{1}{2}(\mathbf{e_1} + \mathbf{e_2} - \boldsymbol{\tau}_2)$ be the vector of Riemann constants (4.25) and $\boldsymbol{\tau}$ as in (4.18). Then we have*

$$\Theta\left(\lambda \begin{bmatrix} 1 \\ -1 \end{bmatrix} + \mathfrak{u}(z) + \mathcal{K} - \frac{1}{2}(\varkappa_2 + 1)\begin{bmatrix} 1 \\ -1 \end{bmatrix}\right) = C(z)\vartheta(\lambda)\vartheta\left(\lambda - \frac{1}{\mathbb{A}_{22}}\int_{a_1}^{z} \eta_2 - \frac{\varkappa_2}{2}\right) \tag{4.39}$$

identically for $\lambda \in \mathbb{C}$ and $z \in X$, where $C(z)$ is independent of λ and is a nowhere zero function of z on the universal cover of X. **(2)** *In particular if $z = \infty^{\pm}$, we obtain*

$$\Theta\left(\lambda \begin{bmatrix} 1 \\ -1 \end{bmatrix} + \mathfrak{u}(\infty^{\pm}) + \mathcal{K} - \frac{1}{2}(\varkappa_2 + 1)\begin{bmatrix} 1 \\ -1 \end{bmatrix}\right) = C(\infty^{\pm})e^{2\pi i\lambda}\vartheta^2(\lambda).$$

Proof. **(1)** Define for $\lambda \in \mathbb{C}$ and $z \in X$

$$f(\lambda) = f(\lambda; z|\varkappa_2) = \frac{\Theta\left(\lambda \begin{bmatrix} 1 \\ -1 \end{bmatrix} + \mathfrak{u}(z) + \mathcal{K} - \frac{1}{2}(\varkappa_2 + 1)\begin{bmatrix} 1 \\ -1 \end{bmatrix}\right)}{\vartheta(\lambda)\vartheta(\lambda + c(z))}.$$

Using the periodicity properties of the Theta functions involved the reader may verify that

$$f(\lambda + 1 + \varkappa_2) = f(\lambda)\exp\left[2\pi i\Big(c(z) + \frac{1}{\mathbb{A}_{22}}\int_{a_1}^{z}\eta_2 + \frac{\varkappa_2}{2}\Big)\right]$$

and therefore with $c(z) = -\frac{1}{\mathbb{A}_{22}}\int_{a_1}^{z}\eta_2 - \frac{\varkappa_2}{2}$ the function $f = f(\lambda)$ is elliptic. The Jacobi elliptic function $\vartheta(\lambda)$ as in (4.38) has a simple zero at $\lambda = \frac{1}{2}(1 + \varkappa_2)$, hence $f(\lambda)$ can have at most two simple poles in the fundamental region $\mathcal{R}$ of the quotient $\mathbb{C}/(\mathbb{Z} + \varkappa_2\mathbb{Z})$ If we substitute $\lambda = \frac{1}{2}(1 + \varkappa_2)$ then the numerator of

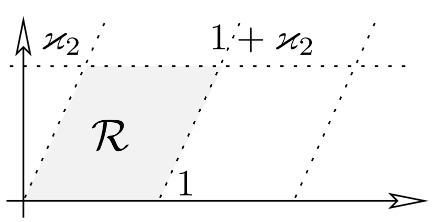

FIGURE 15. The fundamental region $\mathcal{R}$

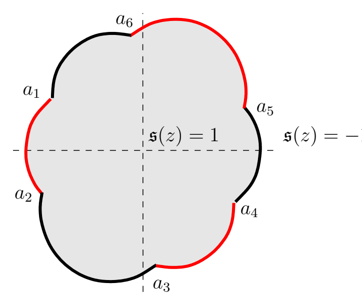

FIGURE 16. The signature function $\mathfrak{s}(z) = \frac{\sqrt{R(-z)}}{\sqrt{R(z)}}$

$f(\lambda)$ becomes $\Theta\big(\mathfrak{u}(z) + \mathcal{K}\big)$, which vanishes since the argument is the image of a divisor of degree $g - 1 = 1$ (see Corollary B.4). Hence $f(\lambda)$ can have at most one simple pole in $\mathcal{R}$, i.e. f is an elliptic function of order one, and therefore a constant. We have thus established (4.39) with a λ independent term $C = C(z)$. We now have to show that $C(z)$ does not vanish. To this end consider the behavior of

$$C(z) = \frac{\Theta\left(\lambda \begin{bmatrix} 1 \\ -1 \end{bmatrix} + \mathfrak{u}(z) + \mathcal{K} - \frac{1}{2}(\varkappa_2 + 1)\begin{bmatrix} 1 \\ -1 \end{bmatrix}\right)}{\vartheta(\lambda)\vartheta\left(\lambda - \frac{1}{\mathbb{A}_{22}}\int_{a_1}^{z}\eta_2 - \frac{\varkappa_2}{2}\right)}$$

as z varies over X. Once more, the periodicity properties of the Theta functions involved give the following behavior under analytic continuation along a closed contour γ:

$$z \mapsto z_\gamma \text{ along } \mathcal{A}_1: \ C(z_\gamma) = C(z); \qquad z \mapsto z_\gamma \text{ along } \mathcal{A}_2: \quad C(z_\gamma) = C(z)$$
$$z \mapsto z_\gamma \text{ along } \mathcal{B}_1: \ C(z_\gamma) = C(z)e^{-2\pi i u_2(z)}; \qquad z \mapsto z_\gamma \text{ along } \mathcal{B}_2: \quad C(z_\gamma) = C(z)e^{-2\pi i u_1(z) + i\pi\varkappa_2}.$$

If we assume that $C(z)$ is not identically zero (we shall prove this later), we can count the zeros of $C = C(P)$ on X by integrating $\mathrm{d}\ln C(P)$ along the boundary of the canonical dissection $\hat{X}$, i.e. we compute

$$\begin{aligned} \frac{1}{2\pi i}\oint_{\partial \hat{X}} \mathrm{d}\ln C(P) &= \frac{1}{2\pi i}\sum_{j=1}^{2}\left(\int_{P_0}^{P_0+\mathcal{A}_j} + \int_{P_0+\mathcal{A}_j}^{P_0+\mathcal{A}_j+\mathcal{B}_j} + \int_{P_0+\mathcal{A}_j+\mathcal{B}_j}^{P_0+\mathcal{B}_j} + \int_{P_0+\mathcal{B}_j}^{P_0}\right)\mathrm{d}\ln C(P) \\ &= \frac{1}{2\pi i}\sum_{j=1}^{2}\left(\int_{P_0}^{P_0+\mathcal{A}_j} - \int_{P_0+\mathcal{B}_j}^{P_0+\mathcal{A}_j+\mathcal{B}_j} + \int_{P_0+\mathcal{B}_j}^{P_0} - \int_{P_0+\mathcal{A}_j+\mathcal{B}_j}^{P_0+\mathcal{A}_j}\right)\mathrm{d}\ln C(P) \\ &= \int_{P_0}^{P_0+\mathcal{A}_1}\omega_2 + \int_{P_0}^{P_0+\mathcal{A}_2}\omega_1 = 0 \end{aligned}$$

and the last equality follows from the normalization $\oint_{\mathcal{A}_k}\omega_j = \delta_{jk}$ of the canonical differentials. Hence $C(z)$ is either identically zero or it has no zeros at all. We now show that it cannot be identically zero; if this were the case, we would have

$$\Theta\left(a\begin{bmatrix}1\\-1\end{bmatrix} + \mathfrak{u}(z) + \mathcal{K}\right) \equiv 0, \qquad \forall a \in \mathbb{C},\ \forall z \in X. \tag{4.40}$$

The Riemann surface under consideration has an involution $\mathfrak{j} : X \to X$ with

$$\mathfrak{j}(z,w) = \big(-z, \mathfrak{s}(z)w\big)$$

where $\mathfrak{s}(z) := \frac{\sqrt{R(z)}}{\sqrt{R(-z)}} \in \{\pm 1\}$; specifically $\mathfrak{s}(z) = -1$ on the outside of the region bounded by $\bigcup_{j=1}^{3}\gamma_j \cup \bigcup_{j=1}^{3}(-1)\gamma_j$, and $\mathfrak{s}(z) = 1$ inside (see Fig. 16). The function $\mathfrak{s}(z)$ accounts for the fact that $\sqrt{R(z)} : \mathbb{C}\backslash\mathcal{B} \to \mathbb{C}$, with $R(z)$ as in (3.35) and the cuts of the square root as stipulated, is neither an even nor odd function. For any point $P \in X$

$$\mathfrak{u}(P) = \int_{a_1}^{P}\vec{\omega} = \int_{\mathfrak{j}a_1}^{\mathfrak{j}P}\mathfrak{j}\vec{\omega} = -\sigma_1\int_{a_4}^{\mathfrak{j}P}\vec{\omega} = -\sigma_1\mathfrak{u}(\mathfrak{j}P) + \sigma_1\mathfrak{u}(a_4),$$

and therefore

$$\mathfrak{u}(P) + \mathfrak{u}(\mathfrak{j}P) = (I - \sigma_1)\mathfrak{u}(P) + \mathfrak{u}(a_4) \equiv b\begin{bmatrix}1\\-1\end{bmatrix}, \qquad b \in \mathbb{C}. \tag{4.41}$$

Now back to (4.40) choose $z = a_1$ so that $\mathfrak{u}(z) = 0$. Equation (4.41) shows that vectors of the form $[a,-a]^t$ are images of symmetric divisors of degree 2. However (compare Definition B.5) the special divisors of degree 2 on X are those that are invariant under the hyperelliptic involution and the only one that is also invariant under $\mathfrak{j}$ is the divisor of the two points above $z = 0$. Thus generically vectors of the form $[a,-a]^t$ are images of nonspecial divisors and the theta function therefore not identically zero. Combined with the previous argument principle computation this shows that $C(z) \neq 0$ for any $z \in X$. The second statement **[2]** follows from $-\frac{1}{\mathbb{A}_{22}}\int_{a_1}^{\infty}\eta_2 = -\frac{\varkappa_2}{2}$ and the periodicity of the Jacobi theta function. □

Now we go back to (4.36) and obtain with Lemma 4.9

$$\Theta\begin{bmatrix}\vec{\boldsymbol{\alpha}}\\\vec{\boldsymbol{\beta}}\end{bmatrix}(-\mathcal{K}) = C(\infty^+)e^{2\pi i(\rho_n + \frac{1}{8}\langle\vec{\boldsymbol{\alpha}}\boldsymbol{\tau},\vec{\boldsymbol{\alpha}}\rangle - \frac{1}{2}\langle\vec{\boldsymbol{\alpha}},\mathcal{K}\rangle + \frac{1}{4}\langle\vec{\boldsymbol{\alpha}},\vec{\boldsymbol{\beta}}\rangle)}\vartheta^2(\rho_n) \tag{4.42}$$

in other words the zeroset $\mathcal{Z}_n$ (4.36) is equivalently determined by the requirement

$$\vartheta\left(\frac{n}{2\pi i}\left[\oint_{\mathcal{B}_1}\mathrm{d}\phi + \varkappa_2\oint_{\mathcal{A}_1}\mathrm{d}\phi\right] + \frac{1}{2}\left[\int_{a_1}^{0}\frac{\eta_2}{\mathbb{A}_{22}} + \frac{\varkappa_2}{2}\right]\right) = 0 \tag{4.43}$$

which only involves a Jacobi theta function corresponding to a Riemann surface of genus one.

5. Completion of Riemann-Hilbert analysis - proof of theorems 1.4 and 1.5

We combine the local parametrices and move on to the ratio problems. These are solved by standard small norm arguments and Neumann series expansions.

5.1. **Proof of Theorem 1.4.** Recall the explicit construction of $M(z), U(z)$ and $V(z)$ in genus zero and define

$$\mathcal{E}(z) = S(z)\begin{cases}\big(U(z)\big)^{-1}, & |z+ia|<r\\ \big(V(z)\big)^{-1}, & |z-ia|<r\\ \big(M(z)\big)^{-1}, & |z\pm ia|>r.\end{cases} \tag{5.1}$$

This function has jumps on the contour $\Sigma_{\mathcal{E}}$ shown in Figure 17, jumps which are given as ratios of parametrices

$$\mathcal{E}_+(z) = \mathcal{E}_-(z)U(z)\big(M(z)\big)^{-1},\ \ z\in C_1; \qquad \mathcal{E}_+(z) = \mathcal{E}_-(z)V(z)\big(M(z)\big)^{-1},\ \ z\in C_2$$

as well as conjugations with the outer model function

$$\mathcal{E}_+(z) = \mathcal{E}_-(z)M(z)\begin{bmatrix}1 & 0\\ 2\pi i z e^{n\varphi(z)} & 1\end{bmatrix}\big(M(z)\big)^{-1},\ \ z\in\hat{\mathcal{B}}^{\pm};$$

$$\mathcal{E}_+(z) = \mathcal{E}_-(z)M(z)\begin{bmatrix}1 & (2\pi i z)^{-1}e^{-n\varphi(z)}\\ 0 & 1\end{bmatrix}\big(M(z)\big)^{-1},\ \ z\in\hat{\mathcal{L}}.$$

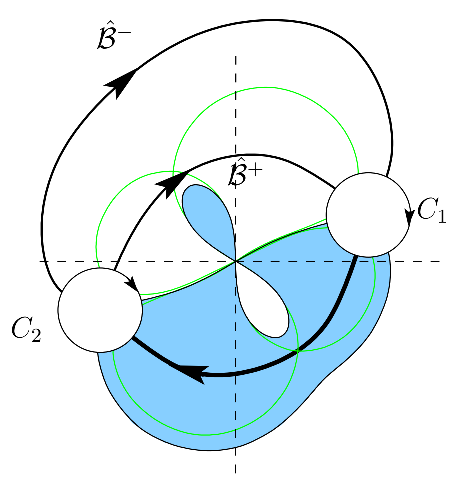

Figure 17. Jump contours in the ratio problem for $\mathcal{E}(z)$ as solid black lines - genus zero situation

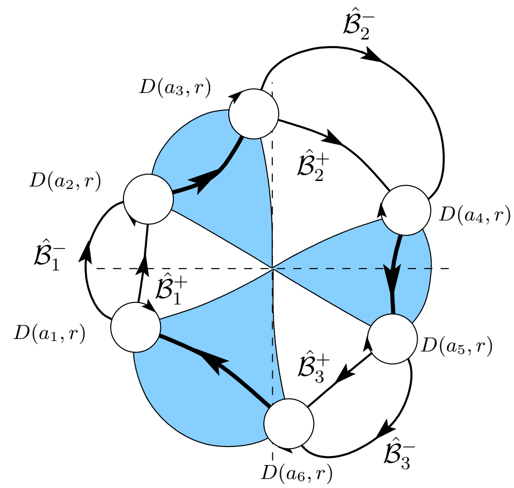

Figure 18. Jump contours in the ratio problem for $\mathcal{E}(z)$ as solid black lines - genus two situation

Also the function $\mathcal{E}(z)$ is normalized as

$$\mathcal{E}(z) = I + \mathcal{O}\left(z^{-1}\right), \qquad z\to\infty.$$

In terms of the previously derived estimates (4.2),(4.5),(4.10) and (4.12), we conclude for the jump matrix $G_{\mathcal{E}}(z)$ in the latter ratio problem,

$$\|G_{\mathcal{E}} - I\|_{L^2\cap L^\infty(\Sigma_{\mathcal{E}})} \le \frac{c}{n}, \qquad n\to\infty,\ c>0 \tag{5.2}$$

which is uniform with respect to $x\in\mathbb{C}: \mathrm{dist}(x,\overline{\Delta})\ge\delta>0$. Hence (cf. [9]) we can iteratively solve the singular integral equation

$$\mathcal{E}_-(z) = I + \frac{1}{2\pi i}\int_{\Sigma_{\mathcal{E}}}\mathcal{E}_-(w)\big(G_{\mathcal{E}}(w)-I\big)\frac{\mathrm{d}w}{w-z_-}, \qquad z\in\Sigma_{\mathcal{E}}$$

in $L^2(\Sigma_{\mathcal{E}})$ which is in fact equivalent to the $\mathcal{E}$-RHP. Moreover its unique solution satisfies

$$\|\mathcal{E}_- - I\|_{L^2(\Sigma_{\mathcal{E}})} \leq \frac{c}{n}, \qquad n\to\infty,\ c>0. \tag{5.3}$$

As we have employed a series of invertible transformations

$$\Gamma(z)\mapsto\Gamma^o(z)\mapsto Y(z)\mapsto S(z)\mapsto\mathcal{E}(z), \tag{5.4}$$

the unique solvability of the $\mathcal{E}$-RHP as $n\to\infty$ for $x\in\mathbb{C}:\mathrm{dist}(x,\overline{\Delta})\geq\delta>0$ implies Theorem 1.4 through (3.3).

5.2. **Proof of Theorem 1.5.** Fix $x\in\mathbb{C}:\mathrm{dist}(x,\mathbb{C}\backslash\overline{\Delta})\geq\delta>0$ away from the zeroset $\{x_k\}$ defined in (4.36). Now combine the outer parametrix $M(z)$ and the local ones $P_j(z)$ into the ratio function

$$\mathcal{E}(z) = S(z)\begin{cases}\big(P_j(z)\big)^{-1}, & z\in D(a_j,r),\ j=1,\ldots,6\\ \big(M(z)\big)^{-1}, & |z-a_j|>r.\end{cases}$$

with $r>0$ sufficiently small. The ratio solves a Riemann-Hilbert problem with jumps on a contour as shown in Figure 18 below and is normalized as

$$\mathcal{E}(z) = I+\mathcal{O}\left(z^{-1}\right), \qquad z\to\infty.$$

Since $M(z;x)$ is bounded on $\partial D(a_j,r)$ we use (4.13) and (4.37) to conclude

$$\|G_{\mathcal{E}}-I\|_{L^2\cap L^\infty(\Sigma_{\mathcal{E}})}\leq\frac{c}{n}, \qquad n\to\infty,\ c>0$$

which once more leads to the unique solvability of the ratio problem in the given situation. Tracing back the invertible transformations we get Theorem 1.5.

6. Asymptotics for normalizing coefficients: proof of Theorem 1.6

In this section we extract expansions for $h_n(x)$ as $n\to\infty$ and compare the results to [3].

6.1. **Expansions outside the star.** We go back to (3.8) and trace back the transformations

$$h_n^o(x) = -2\pi i\lim_{z\to\infty} z\Big(\Gamma^o(z)z^{-n\sigma_3}-I\Big)_{12}, \qquad \Gamma^o(z)z^{-n\sigma_3} = e^{\frac{n\ell}{2}\sigma_3}\mathcal{E}(z)M(z)e^{n(g(z)-\frac{\ell}{2}-\ln z)\sigma_3}, \qquad z\to\infty.$$

For $x\in\mathbb{C}:\mathrm{dist}(x,\overline{\Delta})\geq\delta>0$ we have

$$g(z) = \ln z-\frac{x}{2z}+\mathcal{O}\left(z^{-2}\right), \qquad M(z) = I+\frac{a}{2z}\begin{bmatrix}-1 & (a\pi i)^{-1}\\ -a\pi i & 1\end{bmatrix}+\mathcal{O}\left(z^{-2}\right)$$

as $z\to\infty$ and this combined with

$$\mathcal{E}(z) = I+\frac{i}{2\pi z}\int_{\Sigma_{\mathcal{E}}}\mathcal{E}_-(w)\big(G_{\mathcal{E}}(w)-I\big)\,\mathrm{d}w+\mathcal{O}\left(z^{-2}\right)$$

leads us to

$$\begin{aligned}\Gamma^o(z)z^{-n\sigma_3}-I \quad &= \quad \frac{e^{\frac{n\ell}{2}\sigma_3}}{z}\Bigg\{\frac{a}{2}\begin{bmatrix}-1 & (a\pi i)^{-1}\\ -a\pi i & 1\end{bmatrix}-\frac{x\sigma_3}{2}\\ &\qquad +\frac{i}{2\pi}\int_{\Sigma_{\mathcal{E}}}\mathcal{E}_-(w)\big(G_{\mathcal{E}}(w)-I\big)\,\mathrm{d}w+\mathcal{O}\left(z^{-1}\right)\Bigg\}e^{-\frac{n\ell}{2}\sigma_3}.\end{aligned}$$

Thus

$$\Gamma^o_{1;12}(x,n) = \frac{e^{n\ell}}{2\pi i}\left(1+\mathcal{O}\left(n^{-1}\right)\right), \quad n\to\infty \tag{6.1}$$

where we used (5.2) and (5.3) and which is uniform with respect to $x\in\mathbb{C}:\mathrm{dist}(x,\overline{\Delta})\geq\delta>0$. The latter expansion leads us to

Corollary 6.1. *Let $x \in \mathbb{C} : \mathrm{dist}(x, \overline{\Delta}) \geq \delta > 0$. Then for sufficiently large n the rational solutions $u(x;n)$ to PII equation (1.1) satisfy*

$$u(n^{\frac{2}{3}}x;n) = -\frac{n^{\frac{1}{3}}}{2a(x)}\left(1 + \mathcal{O}\left(n^{-1}\right)\right) \tag{6.2}$$

where $a = a(x)$ is the unique solution to the cubic equation (1.16) subject to the condition (1.17).

Proof. We use Proposition 3.2 and the scalings (3.8), (3.9), i.e.

$$u(n^{\frac{2}{3}}x;n) = \frac{n^{\frac{1}{3}}}{2}\frac{\Gamma^o_{11}(0;x,n,n)\Gamma^o_{12}(0;x,n,n)}{\Gamma^o_{1;12}(x,n)}. \tag{6.3}$$

In order to give an approximation of the right side of (6.3) we combine (4.1) and the expression (4.6),

$$\Gamma^o_{11}(0;x,n,n)\Gamma^o_{12}(0;x,n,n) = \frac{e^{n\ell}}{4\pi a}\left(\delta^2(0) - \delta^{-2}(0)\right)\left(1 + \mathcal{O}\left(n^{-1}\right)\right).$$

With $\delta(0) = e^{i\frac{\pi}{4}}$ and (6.1), this leads to

$$u(n^{\frac{2}{3}}x;n) = -\frac{n^{\frac{1}{3}}}{2a(x)}\left(1 + \mathcal{O}\left(n^{-1}\right)\right).$$

□

Remark 6.2. *The rational solutions $\mathcal{P}_m(\xi)$ (to a rescaled PII equation) in [3] are shown to satisfy the following large m-behavior (compare (3-61) in loc. cit.)*

$$\mathcal{P}_m\left(\left(m - \frac{1}{2}\right)^{\frac{2}{3}}\xi\right) = m^{\frac{1}{3}}\left\{\dot{\mathcal{P}}_m(\xi) + \mathcal{O}\left(m^{-1}\right)\right\}, \quad m \to \infty \tag{6.4}$$

outside the corresponding star shaped region in the complex ξ-plane, compare Remark 3.8. Here $\dot{\mathcal{P}}(\xi) = -\frac{1}{2}S(\xi)$, where $S = S(\xi)$ solves the cubic equation

$$3S^3 + 4\xi S + 8 = 0, \qquad S(\xi) = -\frac{2}{\xi} + \mathcal{O}\left(\xi^{-4}\right), \quad \xi \to \infty.$$

The relation between $\mathcal{P}_m(\xi)$ and $u(x;n)$ is as follows

$$u(x;n) = -\left(\frac{3}{2}\right)^{\frac{1}{3}}\mathcal{P}_n(\xi), \qquad \xi = \left(\frac{3}{2}\right)^{\frac{1}{3}}x.$$

Thus, using the previous identification $S = -(\frac{2}{3})^{\frac{1}{3}}\frac{1}{a}$, we get from (6.4) that

$$u\left(\left(n - \frac{1}{2}\right)^{\frac{2}{3}}x;n\right) = -\left(\frac{3}{2}\right)^{\frac{1}{3}}\mathcal{P}_n\left(\left(\frac{3}{2}\right)^{\frac{1}{3}}\left(n - \frac{1}{2}\right)^{\frac{2}{3}}x;n\right) = -\frac{n^{\frac{1}{3}}}{2a(\xi)}\left(1 + \mathcal{O}\left(n^{-1}\right)\right)$$

which should be compared to (6.2).

6.2. **Expansions inside the star.** For $x \in \mathbb{C} : \mathrm{dist}(x, \mathbb{C}\backslash\overline{\Delta}) \geq \delta > 0$ away from the zeroset $\mathcal{Z}_n$ (4.36) we have as $z \to \infty$

$$g(z) = \ln z - \frac{x}{2z} + \mathcal{O}\left(z^{-2}\right), \qquad M(z) = I + \frac{M_1}{z} + \mathcal{O}\left(z^{-2}\right)$$

involving

$$M_1 = e^{-i\frac{\pi}{4}\sigma_3}(2\pi i)^{-\frac{1}{2}\sigma_3}\big(\mathcal{D}(\infty)\big)^{-\sigma_3}Q_1\big(\mathcal{D}(\infty)\big)^{\sigma_3}(2\pi i)^{\frac{1}{2}\sigma_3}e^{i\frac{\pi}{4}\sigma_3}.$$

Since

$$\mathcal{D}(\infty) = \exp\left[-\frac{1}{2\pi i}\left(\sum_{j=1}^{3}\int_{a_{2j-1}}^{a_{2j}}\frac{w^2\ln w}{\sqrt{R(w)}_+}\mathrm{d}w - \sum_{j=1}^{2}\int_{a_{2j}}^{a_{2j+1}}\frac{i\pi\delta_j w^2}{\sqrt{R(w)}_+}\mathrm{d}w\right)\right] \neq 0$$

we can continue with

$$\Gamma^o(z)z^{-n\sigma_3} - I = \frac{e^{\frac{n\ell}{2}\sigma_3}}{z}\left\{M_1 - \frac{x\sigma_3}{2} + \frac{i}{2\pi}\int_{\Sigma_{\mathcal{E}}}\mathcal{E}_-(w)\big(G_{\mathcal{E}}(w) - I\big)\,\mathrm{d}w + \mathcal{O}\left(z^{-1}\right)\right\}e^{-\frac{n\ell}{2}\sigma_3}$$

and thus obtain the following analogue to (6.1) inside the star (recall the change of orientation in genus two)

$$\big(h_{n-1}^o(x)\big)^{-1} = ie^{-n\ell}\big(\mathcal{D}(\infty)\big)^2\Big\{Q_1^{21} + \mathcal{O}\left(n^{-1}\right)\Big\}, \qquad n \to \infty, \tag{6.5}$$

where Q_1^{21} is given in (4.30). Here the leading coefficient Q_1^{21} is written in terms of theta functions on a genus two hyperelliptic Riemann surface.

Using Lemma 4.9 and along the same lines as (4.42) we rewrite Q_1^{21} as

$$Q_1^{21} = \frac{C_0^{-1}e^{2\pi i(\langle \mathbf{e}_1+\vec{\boldsymbol{\alpha}},\mathfrak{u}(\infty)\rangle)}}{\Theta\big(2\mathfrak{u}(\infty)-\mathfrak{u}(a_6)-\mathcal{K}\big)} \frac{\Theta\left(\rho_n\begin{bmatrix}1\\-1\end{bmatrix}+3\mathfrak{u}(\infty)+\mathcal{K}-\frac{1}{2}(\varkappa_2+1)\begin{bmatrix}1\\-1\end{bmatrix}\right)}{\Theta\left(\rho_n\begin{bmatrix}1\\-1\end{bmatrix}+\mathfrak{u}(\infty)+\mathcal{K}-\frac{1}{2}(\varkappa_2+1)\begin{bmatrix}1\\-1\end{bmatrix}\right)}$$

and therefore in (6.5)

$$\big(h_{n-1}^o(x)\big)^{-1} = ie^{-n\ell}\big(C(\infty^+)\big)^{-1}C_0^{-1}e^{2\pi i(\rho_n+\langle \mathbf{e}_1+\vec{\boldsymbol{\alpha}},\mathfrak{u}(\infty)\rangle)}\left\{\frac{T(\rho_n)+\mathcal{O}\left(n^{-1}\right)}{\vartheta^2(\rho_n)}\right\} \tag{6.6}$$

as $n \to \infty$ away from the zeroset $\mathcal{Z}_n$ determined in (4.43). We introduced

$$T(\rho_n) = \frac{\Theta\left(\left(\rho_n-\frac{\varkappa_2+1}{2}\right)\begin{bmatrix}1\\-1\end{bmatrix}+3\mathfrak{u}(\infty)+\mathcal{K}\right)}{\Theta\big(2\mathfrak{u}(\infty)-\mathfrak{u}(a_6)-\mathcal{K}\big)} \tag{6.7}$$

The formula (6.6) is our fundamental pivot to analyze the location of the zeroes of $\widehat{Q}_n(x) = \mathcal{Q}_n(n^{\frac{2}{3}}x)$; indeed we remind the reader that

$$\big(h_{n-1}^o(x)\big)^{-1} = \left(\frac{\widehat{Q}_{n-1}(x)}{\widehat{Q}_n(x)}\right)^2. \tag{6.8}$$

The error term in the numerator of (6.6) prevents us from localizing the zeroes of $\widehat{Q}_{n-1}$; however we can detect those of $\widehat{Q}_n$ because they appear as poles of $h_{n-1}^o(x)$. In particular the poles of $h_{n-1}^o(x)$ must be of second order, which is automatically guaranteed in our approximation (6.6) by the fact that the denominator is a square.

We shall thus verify (Proposition 6.3 below) that the zeros of the leading approximation $T(\rho_n)$ never coincide with the denominator's. Then, using the argument principle on a small circle around a point of $\mathcal{Z}_n$ we shall see that indeed the function $(h_{n-1}^o(x))^{-1}$ has a double pole within the enclosed disk.

Proposition 6.3. *The functions $\vartheta(z), z \in \mathbb{C}$ and $T(z), z \in \mathbb{C}$ have no common roots.*

Proof. The roots of $\vartheta(z)$ are located at $z^* \equiv \frac{1}{2}(1+\varkappa_2) \bmod (\mathbb{Z}+\varkappa_2\mathbb{Z})$, or equivalently (compare Lemma 4.9 and Corollary B.4), we have for some $P_0 \in X$

$$\mathfrak{u}(P_0) \equiv \mathfrak{u}(\infty^+) + \mathcal{K} \mod (\mathbb{Z}^2 + \boldsymbol{\tau}\mathbb{Z}^2).$$

But at the points $z = z^*$ the numerator in (6.7) is proportional to

$$\Theta\big(\mathfrak{u}(P_0)+\mathcal{K}+2\mathfrak{u}(\infty)\big) = \Theta\big(\mathfrak{u}(P_0)+\mathfrak{u}(\infty^+)-\mathfrak{u}(\infty^-)+\mathcal{K}\big)$$

and vanishes precisely if $P_0 = \infty^-$. But then we would have

$$\mathfrak{u}(\infty^-) \equiv \mathfrak{u}(\infty^+) + \mathcal{K} \quad \Leftrightarrow \quad 2\mathfrak{u}(\infty^-) \equiv \mathfrak{u}(a_3)+\mathfrak{u}(a_5) \mod (\mathbb{Z}^2+\boldsymbol{\tau}\mathbb{Z}^2)$$

and in the last equality both sides are equal to the Abel map of a nonspecial divisor of degree 2. However the genus of X is two and the Abel map is one-to-one on the set of nonspecial divisors of degree two, hence both sides cannot be the same. Thus $\vartheta(z)$ cannot be zero at the same time as $T(z)$. ☐

In order to detect poles of $(h_{n-1}^o)^{-1}$ in (6.6) we shall use the argument principle by tracking the increment of the argument as x makes a small loop around a point of the zeroset $\mathcal{Z}_n$ (4.43). There are two salient points worth mentioning here;

(1) the approximation (6.6) is a uniform approximation of the holomorphic function $(h_{n-1}^o)^{-1}(x)$ by a *smooth* function of x;

(2) the circle used in the detection of the poles must not contain any zero of the leading term approximation.

The first point follows from the fact that the conditions (3.36) that determine the branch points of the Riemann surface X are real–analytic constraints. Nonetheless the argument principle can be used because the approximation is uniform.

In regard to the second point, the strategy is as follows; we shall prove that $\rho_n(x)$ given by (4.35) is a locally smooth function from $\mathbb{C} \simeq \mathbb{R}^2$ to $\mathbb{C} \simeq \mathbb{R}^2$. Therefore, if x makes a small loop around a point $x_\star$, then so does $\rho_n(x)$ around $\rho_n(x_\star)$. If the loop is chosen sufficiently small around a point of $\mathcal{Z}_n$ we can exclude the zeros of $T(\rho)$ because by Prop. 6.3 the zeros of $T(\rho)$ and $\vartheta(\rho)$ never coincide and thus the argument of (6.6) has the same increment as the argument of the denominator $\vartheta^2(\rho)$, thus proving that $(h^o_{n-1}(x))^{-1}$ (which is a priori a meromorphic function) must have a double pole within the loop in the x-plane.

We thus now recall that (4.43) holds iff

$$\rho_n = \rho_n(x) = \frac{n}{2\pi i}\left[\oint_{\mathcal{B}_1} \mathrm{d}\phi + \varkappa_2 \oint_{\mathcal{A}_1} \mathrm{d}\phi\right] + \frac{1}{2}\left[\int_{a_1}^0 \frac{\eta_2}{\mathbb{A}_{22}} + \frac{\varkappa_2}{2}\right] \equiv \frac{1}{2}(1+\varkappa_2) \mod (\mathbb{Z} + \varkappa_2\mathbb{Z})$$

in other words iff we choose $x = x_{n,j,k}$ in such a way that

$$\frac{n}{2\pi i}\left[\oint_{\mathcal{B}_1} \mathrm{d}\phi + \varkappa_2 \oint_{\mathcal{A}_1} \mathrm{d}\phi\right] + \frac{1}{2}\left[\int_{a_1}^0 \frac{\eta_2}{\mathbb{A}_{22}} - \frac{\varkappa_2 + 2}{2}\right] = j + \varkappa_2 k, \quad j,k \in \mathbb{Z}.$$

We aim at showing that $\rho_n(x)$ makes a loop around $\rho_n(x_{n,j,k})$ as x makes a loop around $x_{n,j,k}$. For this fix $x \in \mathbb{C} : x - x_{n,j,k} = \frac{\epsilon}{n}, \epsilon \in \mathbb{C}$ with $|\epsilon| > 0$ sufficiently small and consider

$$\Xi = \Xi(x) = \rho_n(x) - \rho_n(x_{n,j,k}) = \frac{n}{2\pi i}\left[\oint_{\mathcal{B}_1} \mathrm{d}\phi + \varkappa_2 \oint_{\mathcal{A}_1} \mathrm{d}\phi\right] + \frac{1}{2}\left[\int_{a_1}^0 \frac{\eta_2}{\mathbb{A}_{22}} - \frac{\varkappa_2 + 2}{2}\right] - j - \varkappa_2 k,$$

i.e. we need to show that Ξ makes a loop around the origin. This will be achieved by evaluating the Jacobian of the mapping $\Xi = \Xi(u,v)$ with $x = u(\Re\epsilon, \Im\epsilon) + iv(\Re\epsilon, \Im\epsilon), u, v \in \mathbb{R}$ at $\epsilon = 0$. Put

$$A(\epsilon) = \frac{1}{2\pi i}\oint_{\mathcal{A}_1} \mathrm{d}\phi, \qquad B(\epsilon) = \frac{1}{2\pi i}\oint_{\mathcal{B}_1} \mathrm{d}\phi$$

and notice that $A, B \in \mathbb{R}$. Now any point in the complex plane can be written as $b + a\varkappa_2, a, b \in \mathbb{R}$, hence

$$\Xi = n\big(B(\epsilon) + \varkappa_2(\epsilon)A(\epsilon)\big) - \left(j + \frac{1}{4} + b(\epsilon)\right) - \left(k + \frac{1}{4} + a(\epsilon)\right)\varkappa_2(\epsilon).$$

We recall (compare Section 3.4) that the differential $\mathrm{d}\phi$ is the unique meromorphic differential on X such that

$$\Re\left(\oint_\gamma \mathrm{d}\phi\right) = 0 \quad \forall \gamma \in H_1(X,\mathbb{Z}); \qquad \mathrm{d}\phi(z) = \pm\frac{1}{2}\left(\frac{1}{z^4} - \frac{x}{z^2} + \mathcal{O}(1)\right)\mathrm{d}z, \quad z \to 0^\pm$$

$$d\phi(z) = \pm\frac{1}{2}\left(z^{-1} + \mathcal{O}\left(z^{-2}\right)\right)\mathrm{d}z, \quad z \to \infty^\pm.$$

Hence, $\partial_u \mathrm{d}\phi$ and $\partial_v \mathrm{d}\phi$ are the unique meromorphic differentials on X with a double pole at $z = 0^\pm$, vanishing residues, purely imaginary periods and behavior $\mathcal{O}\left(z^{-2}\right)$ as $z \to \infty^\pm$. In order to construct them explicitly, we consider (as a function on the universal covering of X)

$$G(z) = \mathbb{A}_{11}\sqrt{R(z)}\frac{\mathrm{d}}{\mathrm{d}z}\ln\vartheta_1\left(\int_0^z \frac{\eta_1}{\mathbb{A}_{11}}\Big|\varkappa_1\right).$$

As z varies on X, notice that

$$z \mapsto z_\gamma \text{ along } \mathcal{A}_1: \ G(z_\gamma) = G(z); \qquad z \mapsto z_\gamma \text{ along } \mathcal{A}_2: \ G(z_\gamma) = G(z);$$

$$z \mapsto z_\gamma \text{ along } \mathcal{B}_1: \ G(z_\gamma) = G(z) - 2\pi i; \qquad z \mapsto z_\gamma \text{ along } \mathcal{B}_2: \ G(z_\gamma) = G(z) - 2\pi i,$$

and thus

$$\partial_u \mathrm{d}\phi = \frac{\mathrm{d}G(z)}{\mathbb{A}_{11}} + 2\pi i\frac{\Im(\mathbb{A}_{11}^{-1})}{\Im\varkappa_1}\frac{\eta_1}{\mathbb{A}_{11}}, \qquad \partial_v \mathrm{d}\phi = \frac{i\mathrm{d}G(z)}{\mathbb{A}_{11}} + 2\pi i\frac{\Re(\mathbb{A}_{11}^{-1})}{\Im\varkappa_1}\frac{\eta_1}{\mathbb{A}_{11}}.$$

We also compute

$$\frac{1}{2\pi i}\oint_{\mathcal{A}_1}\partial_u \mathrm{d}\phi = \frac{\Im(\mathbb{A}_{11}^{-1})}{\Im\varkappa_1} \qquad \frac{1}{2\pi i}\oint_{\mathcal{B}_1}\partial_u \mathrm{d}\phi = -\Re(\mathbb{A}_{11}^{-1}) + \Im(\mathbb{A}_{11}^{-1})\frac{\Re\varkappa_1}{\Im\varkappa_1}$$
$$\frac{1}{2\pi i}\oint_{\mathcal{A}_1}\partial_v \mathrm{d}\phi = \frac{\Re(\mathbb{A}_{11}^{-1})}{\Im\varkappa_1} \qquad \frac{1}{2\pi i}\oint_{\mathcal{B}_1}\partial_v \mathrm{d}\phi = \Im(\mathbb{A}_{11}^{-1}) + \Re(\mathbb{A}_{11}^{-1})\frac{\Re\varkappa_1}{\Im\varkappa_1}$$

and obtain therefore

$$\det\begin{bmatrix}\partial_u A & \partial_u B\\ \partial_v A & \partial_v B\end{bmatrix} = \frac{|\mathbb{A}_{11}^{-1}|^2}{\Im\varkappa_1} > 0.$$

The Jacobian of the mapping

$$\big(\Re\epsilon, \Im\epsilon\big) \mapsto \Big(\Re\big(\Xi(u,v)\big), \Im\big(\Xi(u,v)\big)\Big)$$

equals

$$J(\epsilon) = \frac{1}{n^2}\det\begin{bmatrix}\partial_u\Re\Xi & \partial_v\Re\Xi\\ \partial_u\Im\Xi & \partial_v\Im\Xi\end{bmatrix}.$$

Hence at $\epsilon = 0$,

$$\begin{aligned} J(0) &= \det\left(\begin{bmatrix}B_u + A_u\Re\varkappa_2 & B_v + A_v\Re\varkappa_2\\ A_u\Im\varkappa_2 & A_v\Im\varkappa_2\end{bmatrix} - \frac{1}{n}\begin{bmatrix}b_u + a_u\Re\varkappa_2 & b_v + a_v\Re\varkappa_2\\ a_u\Im\varkappa_2 & a_v\Im\varkappa_2\end{bmatrix}\right)\\ &= \Im\varkappa_2\det\begin{bmatrix}B_u & B_v\\ A_u & A_v\end{bmatrix} + \mathcal{O}\left(n^{-1}\right) = -|\mathbb{A}_{11}^{-1}|^2\frac{\Im\varkappa_2}{\Im\varkappa_1}\left(1 + \mathcal{O}\left(n^{-1}\right)\right)\end{aligned}$$

which shows that we can find a sufficiently small $r_0 > 0$ which is n independent such that the small circle

$$x = x_{n,j,k} + \frac{r_0}{n}e^{i\alpha}, \quad \alpha \in [0, 2\pi)$$

is mapped smoothly onto a curve in the Ξ-plane, around the origin with a diameter that is bounded with respect to n. By choosing r_0 sufficiently small we can thus guarantee that no zeroes of $T(\rho)$ are included. Then the total increment of the argument in the leading approximation (6.6) is solely determined by the denominator $\vartheta^2(\rho)$; this proves that indeed the function $(h^o_{n-1})^{-1}(x)$ has a pole in a $1/n$ neighborhood of the zeroset $\mathcal{Z}_n$ (4.43) and completes the proof of Theorem 1.6.

Appendix A. Airy parametrices

Our constructions in Subsection (4.1) make use of certain piecewise analytic functions which are constructed out of a Wronskian matrix. On the technical level (we use here the identical construction of [2]), introduce

$$A_0(\zeta) = \begin{bmatrix}\frac{\mathrm{d}}{\mathrm{d}\zeta}\mathrm{Ai}(\zeta) & e^{i\frac{\pi}{3}}\frac{\mathrm{d}}{\mathrm{d}\zeta}\mathrm{Ai}\Big(e^{-i\frac{2\pi}{3}}\zeta\Big)\\ \mathrm{Ai}(\zeta) & e^{i\frac{\pi}{3}}\mathrm{Ai}\Big(e^{-i\frac{2\pi}{3}}\zeta\Big)\end{bmatrix}, \qquad \zeta\in\mathbb{C} \tag{A.1}$$

where $\mathrm{Ai}(\zeta)$ the solution to Airy's equation

$$w'' = zw$$

uniquely determined by its asymptotics as $\zeta\to\infty$ and $-\pi < \arg\zeta < \pi$

$$\mathrm{Ai}(\zeta) = \frac{\zeta^{-1/4}}{2\sqrt{\pi}}e^{-\frac{2}{3}\zeta^{3/2}}\left(1 - \frac{5}{48}\zeta^{-3/2} + \frac{385}{4608}\zeta^{-6/2} + O\left(\zeta^{-9/2}\right)\right).$$

Next assemble the model function

$$A^{RH}(\zeta) = \begin{cases} A_0(\zeta), & \arg\zeta\in(0,\frac{2\pi}{3}),\\ A_0(\zeta)\begin{bmatrix}1 & 0\\ -1 & 1\end{bmatrix}, & \arg\zeta\in(\frac{2\pi}{3},\pi),\\ A_0(\zeta)\begin{bmatrix}1 & -1\\ 0 & 1\end{bmatrix}, & \arg\zeta\in(-\frac{2\pi}{3},0),\\ A_0(\zeta)\begin{bmatrix}0 & -1\\ 1 & 1\end{bmatrix}, & \arg\zeta\in(-\pi,-\frac{2\pi}{3}),\end{cases} \tag{A.2}$$

which solves the RHP with jumps for $\arg\zeta = -\pi, -\frac{2\pi}{3}, 0, \frac{2\pi}{3}$ as depicted in Figure 19. Besides the indicated

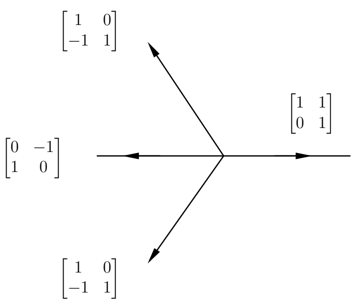

FIGURE 19. A jump behavior which can be modeled explicitly in terms of Airy functions

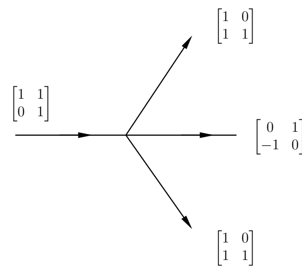

FIGURE 20. Another jump behavior which can be modeled in terms of Airy functions

jump behavior we also have an expansion as $\zeta \to \infty$ which is valid in a full neighborhood of infinity:

$$A^{RH}(\zeta) = \frac{\zeta^{\sigma_3/4}}{2\sqrt{\pi}} \begin{bmatrix}-1 & i\\ 1 & i\end{bmatrix} \left\{ I + \frac{1}{48\zeta^{3/2}} \begin{bmatrix}1 & 6i\\ 6i & -1\end{bmatrix} + \mathcal{O}\left(\zeta^{-6/2}\right) \right\} e^{-\frac{2}{3}\zeta^{3/2}\sigma_3}. \tag{A.3}$$

Next we construct out of (A.1) the function

$$\tilde{A}_0(\zeta) = -\left[\begin{smallmatrix}0 & 1\\ 1 & 0\end{smallmatrix}\right]\sigma_3 A_0\big(e^{-i\pi}\zeta\big)\sigma_3, \qquad \zeta \in \mathbb{C}$$

and then assemble

$$\tilde{A}^{RH}(\zeta) = \begin{cases} \tilde{A}_0(\zeta)\begin{bmatrix}0 & 1\\ -1 & 1\end{bmatrix}, & \arg\zeta \in (0, \frac{\pi}{3}),\\ \tilde{A}_0(\zeta)\begin{bmatrix}1 & 1\\ 0 & 1\end{bmatrix}, & \arg\zeta \in (\frac{\pi}{3}, \pi),\\ \tilde{A}_0(\zeta), & \arg\zeta \in (\pi, \frac{5\pi}{3}),\\ \tilde{A}_0(\zeta)\begin{bmatrix}1 & 0\\ 1 & 1\end{bmatrix}, & \arg\zeta \in (\frac{5\pi}{3}, 2\pi). \end{cases} \tag{A.4}$$

This model function solves again a RHP with jumps on the rays $\arg\zeta = 0, \frac{\pi}{3}, \pi, \frac{5\pi}{3}$ (indicated in Figure 20) and we have the uniform expansion

$$\tilde{A}_{RH}(\zeta) = \frac{\big(e^{-i\pi}\zeta\big)^{-\sigma_3/4}}{2\sqrt{\pi}} \begin{bmatrix}1 & -i\\ 1 & i\end{bmatrix} \left\{ I + \frac{i}{48\zeta^{3/2}} \begin{bmatrix}-1 & 6i\\ 6i & 1\end{bmatrix} + \mathcal{O}\left(\zeta^{-6/2}\right) \right\} e^{-\frac{2}{3}i\zeta^{3/2}\sigma_3}, \quad \zeta \to \infty. \tag{A.5}$$

APPENDIX B. SOME BASIC FACTS ABOUT THETA FUNCTIONS AND DIVISORS

The reference for all the following theorems is [10], we quote here certain results about general Riemann surfaces of the genus $g \in \mathbb{N}$.

The Riemann theta function, associated with a symmetric matrix $\boldsymbol{\tau}$ that has a strictly positive imaginary part, is the function of the vector argument $\vec{z} \in \mathbb{C}^g$ given by

$$\Theta(\vec{z}\,|\boldsymbol{\tau}) = \sum_{\vec{k}\in\mathbb{Z}^g} \exp\left[i\pi\langle\vec{k}\boldsymbol{\tau}, \vec{k}\,\rangle + 2\pi i\langle\vec{k}, \vec{z}\,\rangle\right]. \tag{B.1}$$

Often the dependence on $\boldsymbol{\tau}$ is omitted from the notation.

Proposition B.1. *The theta function has the following properties:*

(1) $\Theta(\vec{z}\,|\boldsymbol{\tau}) = \Theta(-\vec{z}\,|\boldsymbol{\tau})$ *(parity);*

(2) *For any* $\vec{\lambda}, \vec{\mu} \in \mathbb{Z}^g$ *we have*

$$\Theta(\vec{z} + \vec{\mu} + \boldsymbol{\tau}\vec{\lambda} \,|\boldsymbol{\tau}) = \exp\Big[-2\pi i \langle \vec{\lambda}, \vec{z}\,\rangle - i\pi\langle \vec{\lambda}\boldsymbol{\tau}, \vec{\lambda}\,\rangle \Big] \Theta(\vec{z}\,|\boldsymbol{\tau}). \tag{B.2}$$

In addition to (B.1) we also use the theta function with characteristics $\vec{\boldsymbol{\alpha}}, \vec{\boldsymbol{\beta}} \in \mathbb{C}^g$

$$\Theta\begin{bmatrix}\vec{\boldsymbol{\alpha}}\\ \vec{\boldsymbol{\beta}}\end{bmatrix}(\vec{z}\,|\boldsymbol{\tau}) = \exp\left[2\pi i\left(\frac{1}{8}\langle\vec{\boldsymbol{\alpha}}\boldsymbol{\tau}, \vec{\boldsymbol{\alpha}}\,\rangle + \frac{1}{2}\langle\vec{\boldsymbol{\alpha}}, \vec{z}\,\rangle + \frac{1}{4}\langle\vec{\boldsymbol{\alpha}}, \vec{\boldsymbol{\beta}}\,\rangle\right)\right]\Theta\left(\vec{z} + \frac{1}{2}\vec{\boldsymbol{\beta}} + \frac{\boldsymbol{\tau}}{2}\vec{\boldsymbol{\alpha}}\,\middle|\,\boldsymbol{\tau}\right) \tag{B.3}$$

Proposition B.2. *The theta function with characteristics* $\vec{\boldsymbol{\alpha}}, \vec{\boldsymbol{\beta}} \in \mathbb{C}^g$ *has the properties*

$$\Theta\begin{bmatrix}\vec{\boldsymbol{\alpha}}\\ \vec{\boldsymbol{\beta}}\end{bmatrix}(\vec{z} + \vec{\mu} + \boldsymbol{\tau}\vec{\lambda}\,|\boldsymbol{\tau}) = \exp\left[2\pi i\left(\frac{1}{2}\Big(\langle\vec{\boldsymbol{\alpha}}, \vec{\mu}\,\rangle - \langle\vec{\lambda}, \vec{\boldsymbol{\beta}}\,\rangle\Big) - \langle\vec{\lambda}, \vec{z}\,\rangle - \frac{1}{2}\langle\vec{\lambda}\boldsymbol{\tau}, \vec{\lambda}\,\rangle\right)\right]\Theta\begin{bmatrix}\vec{\boldsymbol{\alpha}}\\ \vec{\boldsymbol{\beta}}\end{bmatrix}(\vec{z}\,|\boldsymbol{\tau}), \quad \vec{\mu}, \vec{\lambda} \in \mathbb{Z}^g.$$

$$\Theta\begin{bmatrix}\vec{\boldsymbol{\alpha}} + 2\vec{\mu}\\ \vec{\boldsymbol{\beta}} + 2\vec{\lambda}\end{bmatrix}(\vec{z}\,|\boldsymbol{\tau}) = \exp\Big[i\pi\langle\vec{\boldsymbol{\alpha}}, \vec{\lambda}\rangle\Big]\Theta\begin{bmatrix}\vec{\boldsymbol{\alpha}}\\ \vec{\boldsymbol{\beta}}\end{bmatrix}(\vec{z}\,|\boldsymbol{\tau}), \quad \vec{\mu}, \vec{\lambda} \in \mathbb{Z}^g.$$

For the case of a hyperelliptic Riemann surface X

$$X = \left\{(z, w) :\, w^2 = \prod_{j=1}^{2g+2}(z - a_j)\right\}$$

with fixed homology basis $\{\mathcal{A}_j, \mathcal{B}_j\}_{j=1}^g$, let $\{\omega_j\}_{j=1}^g$ denote the collection of holomorphic one forms on X with standard normalization

$$\oint_{\mathcal{A}_j}\omega_k = \delta_{jk}, \quad j, k = 1, \ldots, g$$

and B-period matrix $\boldsymbol{\tau}$. We denote with $\mathbb{J}_{\boldsymbol{\tau}} = \mathbb{C}^g/(\mathbb{Z}^g + \boldsymbol{\tau}\mathbb{Z}^g)$ the underlying Jacobian variety. If

$$\mathfrak{u}(p) = \int_{a_1}^{p}\vec{\omega}, \qquad \mathfrak{u} : X \to \mathbb{J}_{\boldsymbol{\tau}}$$

is the Abel map extended to the whole Riemann surface then

Theorem B.3 ([10], p. 308)**.** *For* $\mathbf{f} \in \mathbb{C}^g$ *arbitrary, the (multi-valued) function* $\Theta(\mathfrak{u}(z) - \mathbf{f}\,|\boldsymbol{\tau})$ *on the Riemann surface either vanishes identically or it vanishes at* g *points* $p_1, \ldots, p_g$ *(counted with multiplicity). In the latter case we have*

$$\mathbf{f} = \sum_{j=1}^{g}\mathfrak{u}(p_j) + \mathcal{K}. \tag{B.4}$$

where the vector of Riemann constants equals

$$\mathcal{K} = \sum_{j=1}^{g}\mathfrak{u}(a_{2j+1}).$$

An immediate consequence of Theorem B.3 is the following statement.

Corollary B.4. *The function* $\Theta(\mathbf{e}\,|\boldsymbol{\tau})$ *vanishes at* $\mathbf{e} \in \mathbb{J}_{\boldsymbol{\tau}}$ *iff there exist* $g-1$ *points* $p_1, \ldots, p_{g-1}$ *on the Riemann surface such that*

$$\mathbf{e} = \sum_{j=1}^{g-1}\mathfrak{u}(p_j) + \mathcal{K}. \tag{B.5}$$

On a Riemann surface of genus g a divisor is a collection of points (counted with a multiplicity). We are going to consider here only positive divisors, namely, with positive multiplicities.

Definition B.5. *A (positive) divisor of degree* $k \leq g$ *is called special if the vector space of meromorphic functions with poles at the points of order not exceeding the given multiplicities has dimension strictly greater than* 1*. (Note that the constant function is always in this space).*

As the definition suggests, generic divisors of degree $\leq g$ do not admit other than the constant function in the above-mentioned vector space. The other fact that we have used is that a divisor $\mathcal{D} = p_1 + \cdots + p_k$ ($k \leq g$) on the hyperelliptic Riemann surface X is special if and only if at least one pair of points are of the form $(z, \pm w)$ (i.e. the points are on the two sheets and with the same z value).

References

[1] M. Bertola, Boutroux curves with external field: equilibrium measures without a variational problem, *Anal. Math. Phys.* **01** (2011), no. 2-3, 167-211.

[2] P. Bleher, T. Bothner, Exact solution of the six-vertex model with domain wall boundary conditions. Critical line between disordered and antiferroelectric phases, *Random Matrices: Theory Appl.* **01**, 1250012 (2012) DOI: 10.1142/S2010326312500128.

[3] R. Buckingham, P. Miller, Large-degree asymptotics of rational Painlevé-II functions. I., *Nonlinearity* **27** (2014), 2489-2577.

[4] R. Buckingham, P. Miller, Large-degree asymptotics of rational Painlevé-II functions. II., preprint: arXiv:1406.0826.

[5] P. Clarkson, E. Mansfield, The second Painlevé equation, its hierarchy and associated special polynomials, *Nonlinearity* **16** (2003), R1-R26.

[6] P. Deift, *Orthogonal polynomials and random matrices: A Riemann-Hilbert approach*, Courant lecture notes, 1999.

[7] P. Deift, T. Kriecherbauer and K. T-R. McLaughlin, New results on equlibirum measure for logarithmic potentials in the presence of an external field, *J. Approx. Theory* **95** (1998), 388-475.

[8] P. Deift, T. Kriecherbauer, K. T-R. McLaughlin, S. Venakides and X. Zhou, Uniform asymptotics for polynomials orthogonal with respect to varying exponential weights and applications to universality questions in random matrix theory, *Commun. Pure Appl. Math.* **52** (1999), 1335-1425.

[9] P. Deift, X. Zhou, A steepest descent method for oscillatory Riemann-Hilbert problems. Asymptotics for the MKdV equation, *Ann. of Math.*, **137** (1993), 295-368.

[10] H. M. Farkas, I. Kra, *Riemann Surfaces*, Springer-Verlag, New York, 1980.

[11] A. Fokas, A. Its and A. Kitaev, Discrete Painlevé equations and their appearance in quantum gravity, *Comm. Math. Phys.* **142** (2) (1991), 313-344.

[12] J. Jenkins, D. C. Spencer, Hyperelliptic trajectories, *Ann. of Math.* (1951), **53**, 4–35.

[13] K. Kajiwara, Y. Ohta, Determinant structure of the rational solutions for the Painlevé II equation, *Journal of Mathematical Physics* **37** (1996), 4693-4704.

[14] K. Strebel, Quadratic differentials, Ergebnisse der Mathematik und ihrer Grenzgebiete, vol. 5, Berlin 1984.

[15] A. Tovbis, S. Venakides, X. Zhou, Semiclassical focusing nonlinear Schrödinger equation I: inverse scattering map and its evolution for radiative initial data, *Int. Math. Res. Not.*, **22**, (2007), Art. ID rnm094, 54.

[16] A. Vorob'ev, On rational solutions of the second Painlevé equation, *Diff. Eqns* **1** (1965), 58-9 (in Russian).

[17] A. Yablonskii, On rational solutions of the second Painlevé equation, *Vesti Akad. Navuk. BSSR Ser. Fiz. Tkh. Nauk.* **3** (1959), 30-5 (in Russian).

Centre de recherches mathématiques, Université de Montréal, C. P. 6128, succ. centre ville, Montréal, Québec, Canada H3C 3J7 and, Department of Mathematics and Statistics, Concordia University, 1455 de Maisonneuve W., Montréal, Québec, Canada H3G 1M8

E-mail address: bertola@mathstat.concordia.ca

Centre de recherches mathématiques, Université de Montréal, C. P. 6128, succ. centre ville, Montréal, Québec, Canada H3C 3J7 and, Department of Mathematics and Statistics, Concordia University, 1455 de Maisonneuve W., Montréal, Québec, Canada H3G 1M8

E-mail address: bothner@crm.umontreal.ca